High-throughput methods for the analysis of pigments in aquatic sediments

By

Neungrutai Saesaengseerung

A thesis submitted in partial fulfilment of the requirements for the degree of Doctor of Philosophy at the University of York

University of York

Department of Chemistry

January 2013

Abstract

High-throughput methods for the analysis of complex mixtures of sedimentary pigments have been developed by improving the efficiency and speed of pigment extraction and chromatographic analysis. A method for the routine and automated extraction of highly sensitive chlorin pigments from sediments has been developed and compared with the widely used method of sonic extraction. Pigments were identified by high performance liquid chromatography with on-line photodiode array detection and multistage tandem mass spectrometry. The efficacy and integrity of accelerated solvent extraction (ASE) varies for temperatures within the range 20°C to 175°C. The pigment yields and absence of alteration products indicate 70°C to be the optimal temperature for ASE in pigment analysis, yields and distributions of pigments being very similar to those obtained using sonication. Extraction time and solvent consumption are considerably lower than those for sonication, leading to increased efficiency and lower environmental impact and cost. Significant improvements in precision for quantification were achieved by freeze drying and sieving sediments prior to extraction. In addition, an ultra-high performance liquid chromatography (UHPLC) method has been developed for the analysis of complex pigment distributions in natural samples, examining the effects of, and optimising, flow rate, injection volume, column length, mobile phase composition and column temperature. The new chromatographic methods have been demonstrated for the analysis of pigment compositions in an extract from sediment (Priest Pot, Cumbria UK) and a natural water-column filtrand (Little Long Lake). Detection and identification of components was achieved by online UV/Vis detector and multistage tandem mass spectrometry (up to MS^3). The separation, identification and confirmation by MS of photosynthetic pigments from Priest Pot and bacteriophaeophytin *c* and *d* homologues from Little Long Lake is achieved in under 18 min, five times faster than the established HPLC method. The new ASE and UHPLC methods were applied to the study of three sediment cores from Lake Heidi, Lake Nella and Lake 14, Larsemann Hills, Antarctica at high sampling resolution. The methods offer significant savings in time, solvent and sample consumption, have improved limits of detection and generate more reliable data. Hence, the use of the methods will enable the rapid screening of environmental samples and the profiling of sediment cores at high sampling resolutions within reasonable timescales.

Contents

List of tables

List of figures

List of schemes

Acknowledgements

I would like to thank the Ministry of Science and Technology, Department of Science Service and the Royal Thai Government, Thailand for provision of a studentship. I am extremely grateful to my supervisor Professor Brendan Keely for his support, advice, guidance and encouragement throughout my Ph.D. Dr. Dominic Hodgson and The British Antarctic Survey (BAS) are thanked for providing sediment samples. Associate Professor Dr. Tirayut Vilaiva and Assistant Professor Dr. Worawan Bhanthumnavin are thanked for supporting me with reference letters and advice when starting my Ph.D.

I would like to thank all members in the Keely research group past and present; Matt, Chris, Suleman, Haslina, Kim, Angela, Denize, Adam, Scott and Cezary for friendship and support throughout my Ph.D. Special thanks to Matthew Pickering for every answer, helpful idea and laboratory experience, Chris Knappy for a very nice standard pigment, and Trevor Dransfield and Edmund Bergström for training me on the mass spectrometers.

I would like to thank all my Thai colleagues at the Department of Science Service for all their hard work to help me gain a great opportunity to do my Ph.D. Special thanks to Saruta Benjanuvatra for every step when taking me to the department, Pitiwut Teerakittikul for computing help and all my friends; Orachorn, Penchan, Sukonta, Netnapa, Wanida, Salina and Somjit (Pee Yo) for listening, understanding, and accepting in me.

Finally, extremely special thanks go to my Mom and Dad for their eternal love, unconditional support and strong encouragement given to me all the time. I would like to thank my lovely sister; Doungrutai Saesaengseerung and my grandfather for their brave and reasoned suggestions and for not allowing me to turn back.

Author’s declaration

I hereby declare that the work described in this thesis is my own, except where otherwise acknowledged, and has not been submitted previously for a degree at this or any other university.

……..

Neungrutai Saesaengseerung

Chapter 1

Introduction

1.1 Chlorophylls

1.1.1 Structure

There are three basic core structures of chlorophylls, each involving a cyclic tetrapyrrole structure; porphyrin (**1**), chlorin (**2**) and bacteriochlorin (**3**) (Scheer, 1991) (Fig. 1.1). These structures are all aromatic, having an 18 electron π-system. All chlorophylls have an additional five membered isocyclic ring (ring E) joined to ring C (e.g. Fig. 1.2) (Scheer, 1991).

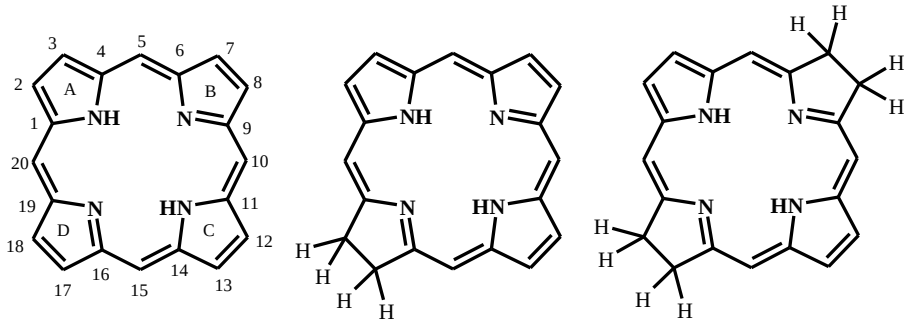

Figure 1.1. The three basic chlorophyll core structures; porphyrin (**1**), chlorin (**2**) and bacteriochlorin (**3**) (adapted from Scheer, 1991).

In nature, a range of different chlorophyll structures exist exhibiting a variety of additional structural elements (Scheer, 1991). The most common chlorophyll structure is chlorophyll *a* (chl *a*, **4**, Fig. 1.2) which has a chlorin macrocycle and the following key structural features; a complexed magnesium atom, (Scheer, 1991) a vinyl group at position C-3, a ketone at C-13^1, a carbomethoxy group at C-13^2, and a phytyl propionate ester at C-17 (Scheer, 1999; see Fig. 1.2 for numbering). In terms of the stereochemistry of chlorophyll *a* (**4**), that at C-17 and C18 is fixed whereas reversible isomerization has been reported at C-13^2 (typically in the *R* form, chl *a*, Fig.1.2) to form a less stable *S* diastereomeric product (Brockmann, 1968; Fleming, 1967).

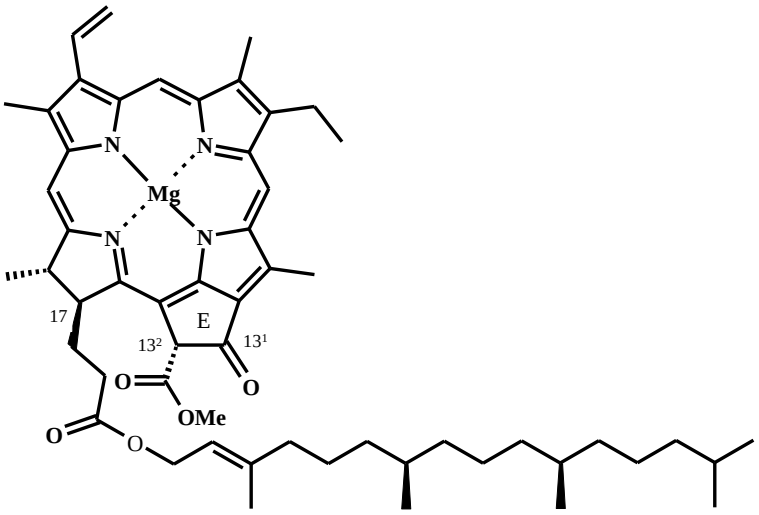

Chlorophyll *a*
(**4**)

Figure 1.2. Structure of chlorophyll *a* (**4**) showing stereochemistry at C-17, C-18 and C-13^2

1.1.2 Occurrence

Photosynthesis is performed by photoautotrophic organisms and is the major method of primary production, the conversion (or 'fixation') of inorganic carbon (e.g. CO_2) into organic materials (Killops and Killops, 2004). Generally, photosynthesis can be divided into two types, oxygenic and anoxygenic photosynthesis. Oxygenic photosynthesis is typically performed by aerobic photoautotrophs and involves the light-driven conversion of carbon dioxide and water into carbohydrates and oxygen according to Equation 1.1 (full example described in Hall and Rao, 1999; Killops and Killops, 2004). Anoxygenic photosynthesis is typically performed by anaerobic photoautotrophs, using hydrogen sulphide (H_2S) as a source of hydrogen instead of water (H_2O) to drive carbohydrate biosynthesis according to Equation 1.2 (Killops and Killops, 2004). Notably, in this case oxygen is not a by-product.

$$6CO_2 + 6H_2O \xrightarrow{\text{light}} C_6H_{12}O_6 + 6O_2 \qquad (1.1)$$

$$CO_2 + 2H_2S \xrightarrow{\text{light}} CH_2O + 2S + H_2O \qquad (1.2)$$

By virtue of their strong light absorption properties, chlorophylls are used as light harvesting pigments by photosynthetic organisms (Renger, 2008). In addition, certain chlorophylls are involved with photosynthetic reaction centres (Scheer, 2008), however, not all chlorophylls perform both functions. Chlorophylls *a* (**4**, Fig. 1.2) and *b* (**5**, Fig. 1.3) occur in oxygenic photosynthetic organisms whereas bacteriochlorophylls *a*-*d* (**6-9**; respectively, Fig. 1.3) occur in anaerobic photoautotrophs (Scheer, 2008). The occurrence of some of the major chlorophyll pigments and their function is summarised in Table 1.1.

Table 1.1. Occurrence, location and function of photosynthetic pigments (chlorophylls and bacteriochlorophylls); LH = Light-harvesting, eT = electron transfer (reaction centre). Adapted from Scheer, (1991) and Scheer, (2008).

Pigment	**Occurrence**	**Location**	**Function**
Chlorophyll *a*	All oxygenic photosynthetic organisms	Antenna, reaction centres	LH+eT
Chlorophyll *b*	Green plants, algae	Peripheral antenna	LH
Chlorophylls *c*	Phaeophyta, Cryptophyta, Pyrrophyta, Chrysophyta, Bacillariophyta	Peripheral antenna	LH
Bacteriochlorophyll *a*	Photosynthetic bacteria	Antenna, reaction centre	LH+eT
Bacteriochlorophyll *b*	Purple bacteria	Antenna, reaction centre	LH+eT
Bacteriochlorophyll *c* and *d*	Chlorobiaceae, Chloroflexaceae	Peripheral antenna (chlorosomes)	LH

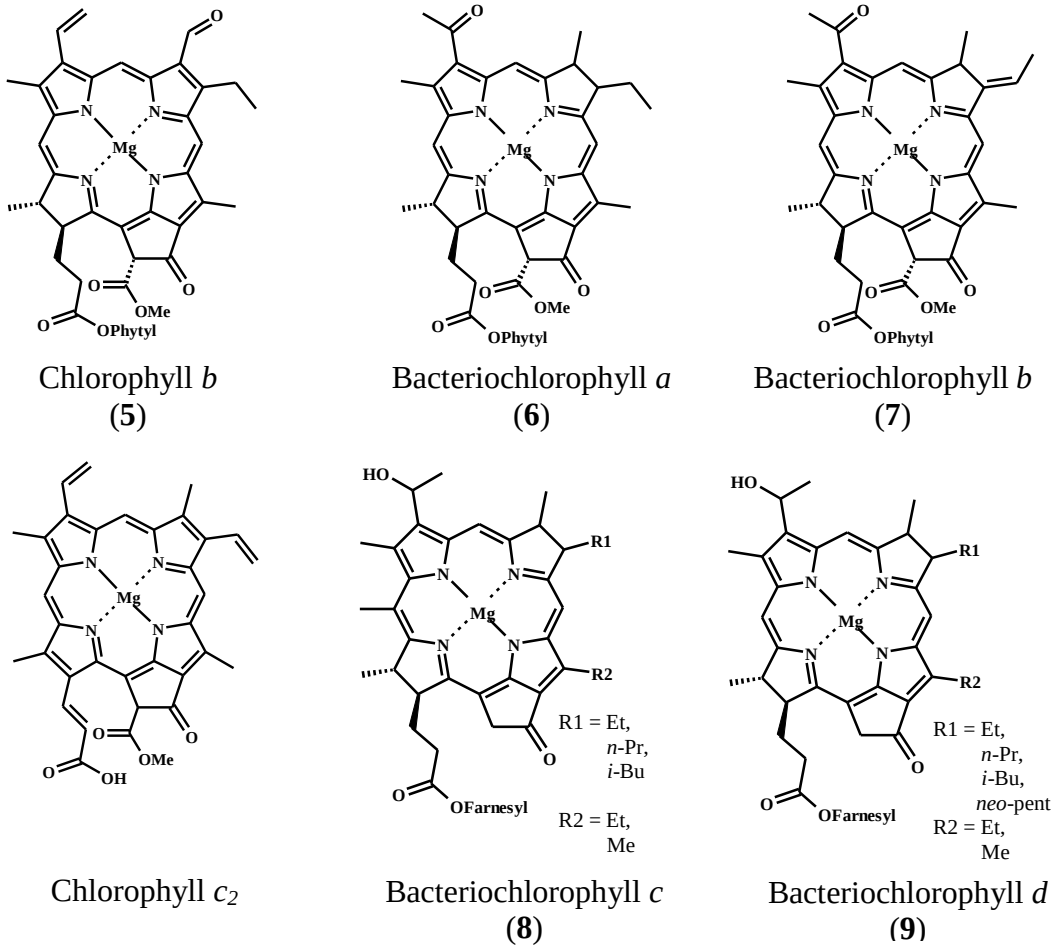

Figure 1.3. Structure of photosynthetic pigments described in Table 1.1

1.1.3 Geochemistry

In the 1930's, the German chemist Alfred Treibs proposed a series of transformations (e.g. Fig. 1.4) that could lead to conversion of chlorophyll *a* into sedimentary porphyrins (e.g. deoxophylloerythroetioporphyrin, DPEP (**10**, Fig. 1.4)) (Treibs, 1936). After this pioneering work, Treibs' hypothesis has been confirmed by isotopic evidence (Hayes et al., 1987; Ocampo et al., 1989) and the isolation and characterisation of the minimum number of intermediates necessary in the conversion pathway of chlorophyll *a* to DPEP (**10**, Fig. 1.4) (Keely et al., 1990). The reactions in the chlorophyll *a* conversion pathway (Fig. 1.4) involve demetallation, deesterification, decarbomethoxylation, vinyl reduction, ketone reduction, aromatisation of the macrocycle and decarboxylation.

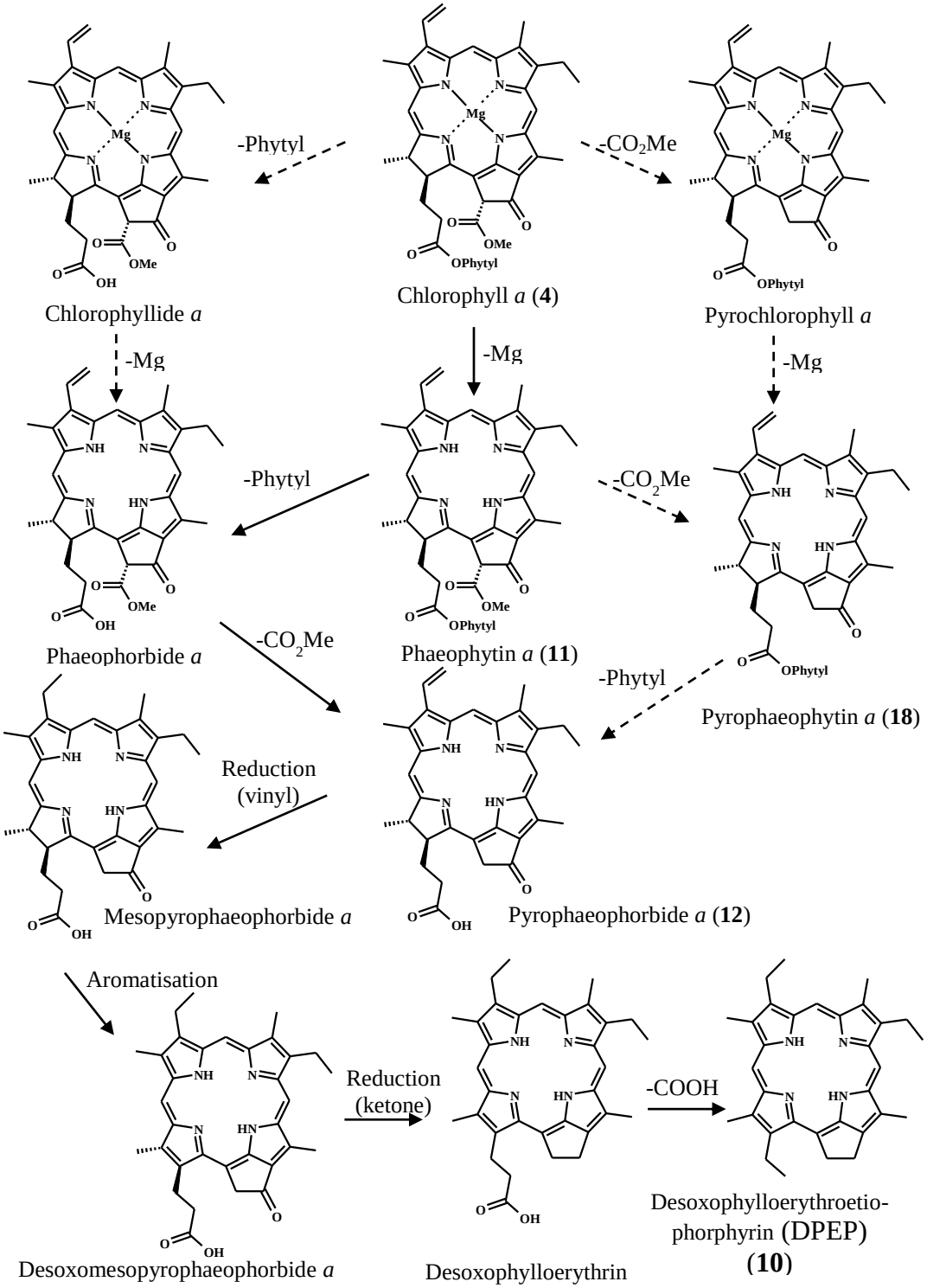

Figure 1.4. Representation of the Treibs Scheme by which chlorophyll *a* (**4**) is converted to DPEP (**10**), adapted from Keely et al, (1990) and Keely (2006). The solid arrows indicate the minimum number of intermediates required for the conversion while dashed arrows indicate variations possible in the reaction order. Note, many other transformations of chlorophylls other than those shown are known.

The Treibs hypothesis, showing the link between a sedimentary compound (porphyrins) and a specific biological precursor (chlorophyll), often termed the biological marker concept, led to the development of the field of organic geochemistry.

Structural correlations between sedimentary porphyrins and their source organisms (e.g. algae and bacteria) have been reported (Callot et al., 1990). Sedimentary chlorophylls can be related back to the source organisms that produced them and indicate the structure and composition of the primary producer community at the time of deposition. For example, the presence of chlorophylls *a* (**4**, Fig. 1.2) and *b* (**5**, Fig. 1.3) signify a contribution from algae, whereas the presence of bacteriochlorophylls *c* (**8**, Fig. 1.3) and *d* (**9**, Fig. 1.3) indicate a contribution from green sulfur bacteria (Keely, 2006). Furthermore the transformation products of chlorophylls can be used as indicators of specific environment conditions (Keely, 2006). The transformation reactions of chlorophyll in the natural environment can be divided into two types: type I reactions which modify the periphery of the molecule while preserving the macrocycle (such as, loss of magnesium, loss of phytol and modification of the side chains), and type II reactions which involve oxidative cleavage of the macrocyclic ring to yield smaller fragments (Hendry et al., 1987). In sunlit, oxic natural environments, type II reactions and destruction of chlorophyll dominate. This involves a photo-oxidation reaction involving the initial attack of oxygen at the C-5 position (Mühlecker et al., 1993) to yield weakly coloured linear tetrapyrroles. In environments where oxygen is low/deficient the products of type I reactions can be observed (Keely, 2006).

The regular type I transformation products of chlorophyll, including phaeophytins, phaeophorbides, and their pyro-derivatives, are formed by simple defunctionalisation around the periphery of the macrocyclic and are shown in Fig. 1.4 (Keely, 2006). They can be produced during the processes of senescence (cell aging and death) or ingestion by herbivores (Shuman and Lorenzen, 1975), and are generally found as the major products in immature sediments (Airs et al., 2001a; Airs and Keely, 2003; Keely et al., 1990; Squier et al., 2002; Squier et al., 2004; Villanueva et al., 1994a; Wilson et al., 2004). Although these transformation products have been found to arise from different algal species under a variety of environmental conditions, the

reactions share common pathways. Demetallation of chlorophyll to form phaeophytin *a* (**11**, structure shown in Fig. 1.4) can be mediated by the enzyme Mg-dechelatase present in algal cells (Hendry et al., 1987; Owens and Falkowski, 1982) or via acid catalysis (Hodgson et al., 1960; Hynninen, 1991). Dephytolisation at C-17^3 is mediated by the enzyme chlorophyllase (Jeffrey and Hallegraeff, 1987). Similarly, pyro-derivatives (e.g. pyrophaeophorbide *a* (**12**, structure shown in Fig. 1.4)) can be formed by enzymatic decarbomethoxylation at C-13^2 (Spooner et al., 1994). The abundance of phaeopigments observed in the faecal pellets of heterotrophic organisms has led to suggestions that they could be used to indicate grazing (Cartaxana et al., 2003; Currie, 1962; Downs and Lorenzen, 1985; Hurley and Armstrong, 1990; Patterson and Parsons, 1963; Shuman and Lorenzen, 1975). However, this interpretation should be treated with caution as phaeopigments are also produced during cell senescence (Spooner et al., 1994).

Other, more reliable, markers for grazing process are steryl chlorin esters (SCEs) (Harradine et al., 1996; King and Repeta, 1991; Pearce et al., 1993). SCEs form in the guts of herbivores by esterification of the pigment with a sterol derived from the algae or grazer (Harradine et al., 1996; Talbot et al., 1999b). In addition, increasing of steryl chlorin esters formation by microorganisms was found under anoxia condition rather than oxic condition (Szymczak-Zyla et al., 2008). The chlorophyll derivative 13^2, 17^3-cyclopheophorbide *a* enol (Fig. 1.5) is produced from algal chlorophyll after ingestion by herbivorous protists and has been suggested as a biomarker for protistan activity (Kashiyama et al., 2012). As chlorophyll *a* can generate harmful singlet oxygen species, the formation of 13^2, 17^3-cyclopheophorbide *a* enol is thought to be a mechanism of detoxifying chlorophyll *a* and protecting the organism from oxidative damage (Kashiyama et al., 2012).

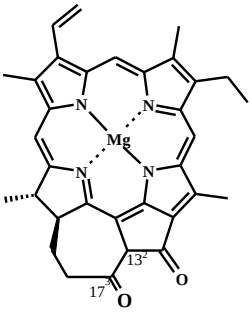

Figure 1.5. 13^2, 17^3-cyclopheophorbide *a* enol.

In addition to the regular type I transformation products discussed above, a range of oxidised transformation products of chlorophyll can form by reaction with molecular oxygen at ring E (Keely, 2006). The mechanisms of reaction for the oxidation have been detailed in previous studies (Hynninen, 1973; Hynninen, 1991; Walker, 2004a; Woolley et al., 1998). The major products of these oxidative transformations are hydroxychlorophyll derivatives, purpurin-7, purpurin-18, and chlorin e_6 (Fig. 1.6) (Louda et al., 2011; Naylor and Keely, 1998; Walker et al., 2002). The presence of oxidised transformation products of chlorophyll has been suggested to indicate the oxicity of the depositional environment (Louda et al., 2000; Squier et al., 2002; Walker et al., 2002). Thus, the nature of sedimentary chlorophylls and their degradation products provide a valuable tool for palaeoenvironmental reconstruction.

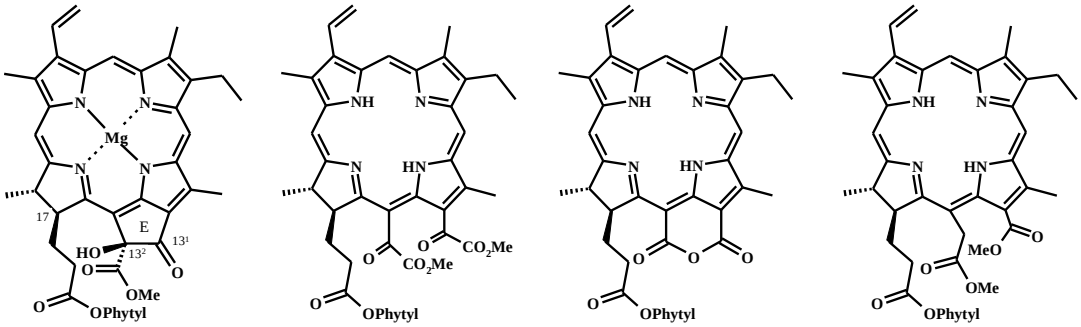

Hydroxychlorophyll *a* (**13**)

Purpurin-7 dimethyl phytyl ester (**14**)

Purpurin-18 phytyl ester (**15**)

Chlorin e_6 dimethyl phytyl ester (**16**)

Figure 1.6. Structure of oxidative transformation products; hydroxychlorophyll *a* (**13**), purpurin-7 dimethyl phytyl ester (**14**), purpurin-18 phytyl ester (**15**) and chlorin e_6 dimethyl phytyl ester (**16)** produced *via* a type I reaction.

1.2 Extraction of chlorophylls from sediments

1.2.1 Sonic extraction

Typically, the extraction of chlorophyll pigments from sediments involves sonication with organic solvent followed by centrifugation and filtering the supernatant through a solvent extracted cotton wool plug. The process is repeated up to 10 times or until the extraction solvent is colourless. The extracts are combined and reduced to dryness by rotary evaporation (Airs et al., 2001a; Squier et al., 2002; Squier et al., 2004; Walker and Keely, 2004b). Several solvent systems such as acetone, acetone/water (9:1 v/v), acetone/methanol (1:1 v/v), methanol, and dichloromethane /methanol (9:1 v/v) were tested for extraction efficiency and absolute acetone was found to be the most efficient solvent for pigment extraction (Keely and Brereton, 1986). In addition, acetone is typically used as the extraction solvent instead of alcoholic solutions as autoxidation (allomerisation) reactions can occur in the latter during extraction (Johnston and Watson, 1956; Woolley et al., 1998). Although the sonication extraction method does not require specialised or expensive equipment, the method is time consuming and involves large volumes of solvent. In addition, the method is not readily amenable to automation, limiting its application for the extraction of large numbers of samples.

1.2.2 Accelerated solvent extraction (ASE)

Accelerated solvent extraction (ASE) is a relatively new extraction technique that is capable of being fully automated (Richter et al., 1996). The technique involves solvent extraction at elevated temperature and pressure to improve solvent penetration into the sample and extraction efficiency (Richter et al., 1996). A high pressure is maintained inside the extraction cell to keep the solvent in its liquid state, allowing extraction temperatures in excess of the boiling point of the solvent to be used (Giergielewicz-Mozajska et al., 2001). The ASE system consists of a set of solvent reservoirs, extraction cell, cell oven, and collection vial (Figure 1.7). Nitrogen gas is used to deliver the solvents and pressurise the cell. Typically, extraction of analytes from a solid sample matrix can be described by three steps;

i) desorption of the analyte from a solid particle, ii) diffusion through the solvent located inside a matrix pore and iii) transfer to the bulk of the flowing fluid (Giergielewicz-Mozajska et al., 2001; Pawliszyn, 1993). At elevated temperature, extraction efficiency is enhanced due to the increasing capacity of the solvent to solubilize analytes and the increase in the rate of diffusion (mass transfer) (Richter et al., 1996). In addition, the efficiency of extraction is increased at greater temperatures by an increasing disruption of surface equilibria; van der Waals forces, hydrogen bonding and dipole attraction between the solutes and active sites on the matrix are disrupted by increased temperature (Richter et al., 1996).

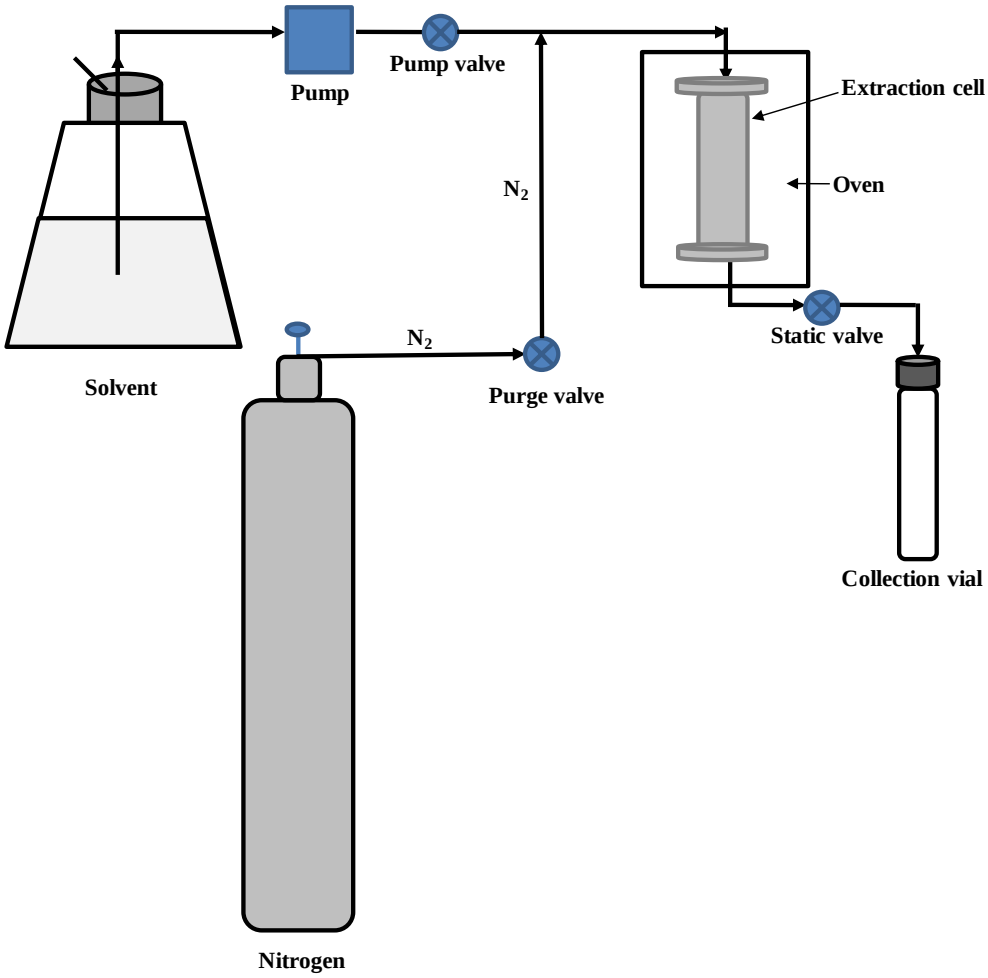

Figure 1.7. Accelerated solvent extraction (ASE) system adapted from Ritcher et al. (1996). Arrow illustrates flow direction of solvent and nitrogen gas.

ASE has been applied to soil and sediment samples for the extraction of a large number of different compounds classes; for example, herbicides present in agricultural soil (Guzzella and Pozzoni, 1999), polychlorinated biphenyls (PCBs) and polycyclic aromatic hydrocarbons (PAHs) from dried compost (Brändli et al., 2006), and phosphorus in lake sediments (Waldebäck et al., 1998). Comparison between ASE extraction and conventional methods; including sonication and Soxhlet extraction, indicate that extraction time and solvent consumption is lower for ASE (Giergielewicz-Mozajska et al., 2001) and that the automation capability of this technique can increase sample throughput, especially if the maximum sample loading (maximum of 24 samples in the carousel at once) is performed (Giergielewicz-Mozajska et al., 2001; Waldebäck et al., 1998). In terms of extraction efficiency, application of the ASE technique to herbicide extraction from soil sample gave the same recovery efficiency as a traditional Soxhlet extraction (Guzzella and Pozzoni, 1999). To date ASE has not been applied to the extraction of sediment. Given the sensitivity of chlorophylls to alteration; for example, loss of the complexed Mg from chlorophyll *a,* any ASE method would first have to be validated in order to demonstrate that it did not alter the distributions of sedimentary pigments during extraction.

1.3 Analysis of chlorophylls

1.3.1 Reversed phase high performance liquid chromatography (RP-HPLC)

High performance liquid chromatography (HPLC) is an analytical technique capable of separating complex mixtures of analytes. It involves a metal column packed with a solid adsorbent (stationary phase) comprising very small particles (typically 3-5 µm diameter). Solvent (the mobile phase) is pumped through the column at high pressure (providing the name of the technique) (Meyer, 1988). The typical components of an HPLC instrument are shown in Scheme 1.1. The most common mode of HPLC is reversed phase high performance liquid chromatography (RP-HPLC) (Krstulović and Brown, 1982) and involves the use of a nonpolar stationary phase (e.g. silica particles coated with C18 chains) and a polar mobile phase. The solvent composition of the mobile phase can be kept the same (isocratic elution) or altered over the course of the analytical run (gradient elution). In the case of RP-

HPLC, gradient elution is usually from a polar starting composition to a less polar one.

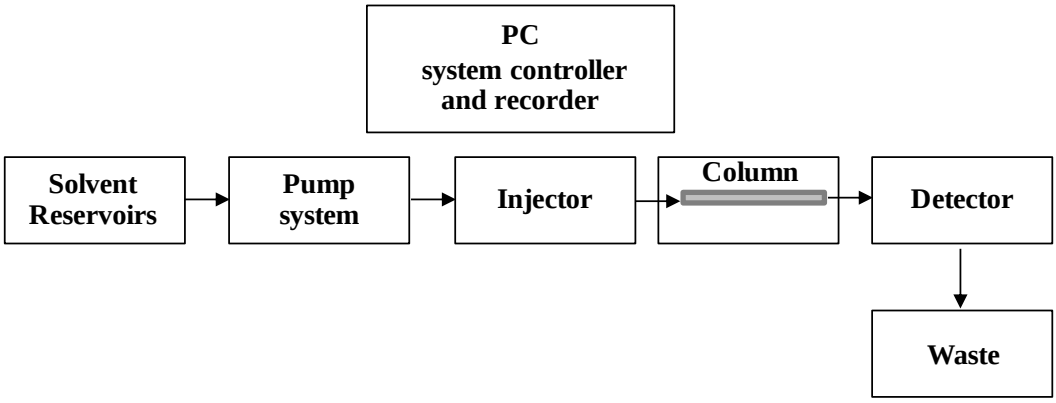

Scheme 1.1. Schematic representation of a typical HPLC system adapted from (Walker, 2004a). Arrow shows the direction of flow of the mobile phase.

The basic theory of the RP-HPLC separation process involves the distribution of analytes between the stationary phase and mobile phase. When an analyte mixture is injected onto the analytical column the analytes are transported along the column at different rates depending on their solubility in the mobile and stationary phases. Thus, separation will occur due to the differences in the distribution constants (*K* in Equation 1.3) of the individual analyte in a sample mixture (Poole and Poole, 1991 and Skoog et al., 1998).

$$K = \frac{c_S}{c_M} \tag{1.3}$$

Where; c_S is the molar concentration of the solute in the stationary phase and c_M is its molar concentration in the mobile phase (Skoog et al., 1998).

There are two terms are widely used for describing of chromatographic column efficiency; i) number of theoretical plates (*N*) and ii) plate height (*H*) according to Equation 1.4 (Skoog et al., 1998).

$$N = \frac{L}{H} \tag{1.4}$$

Where; L is the length of the column packing in centimetres.

The efficiency of chromatographic columns increases with increasing plate count and decreasing plate height. The term plate height (H) can be can be mathematically described by the van Deemter equation; created in the 1950s by Dutch chemical engineers (van Deemter et al., 1956). The equation can be written as Equation 1.5 (Skoog et al., 1998).

$$H = A + B/u + C_m u + C_s u \tag{1.5}$$

Where; H = The theoretical plate height (cm)

u = The linear velocity of the mobile phase (cm s^{-1})

A, B and C = Coefficients related to the multiple flow paths, longitudinal diffusion, and mass transfer between phases, respectively.

The multipath term (A) called "eddy diffusion" describes zone broadening arising due to the multiple pathways by which a molecule can navigate through a packed column. Differences in the length of these pathways causes variation in the residence time on column for molecules of the same species. According to Equation 1.6, this effect is directly proportional to the diameter of the particles making up the column packing (Skoog et al., 1998).

$$A = 2\lambda d_p \tag{1.6}$$

Where; d_p = Diameter of packing particle (cm)

λ = A packing characterization factor (van Deemter et al., 1956)

The longitudinal diffusion term (*B/u*) describes band broadening due to diffusion of solutes from the concentrated peak center to more dilute regions ahead and behind. This diffusion is both towards and opposite to the direction of mobile phase flow rate. According to Equation 1.7, the longitudinal diffusion term (*B/u*) is directly proportional to the mobile-phase diffusion coefficient (D_M) and inversely proportional to the mobile phase velocity (Skoog et al., 1998).

$$B/u = \frac{2\gamma D_M}{u} \tag{1.7}$$

Where; D_M = Diffusion coefficient in mobile phase ($cm^2\ s^{-1}$)

γ = The constant called obstructive factor, which recognizes that longitudinal diffusion is hindered by the packing.

The mass-transfer coefficients (C_S and C_M) of the van Deemter equation (Equation 1.5) are calculated as shown in the Equations 1.8 and 1.9. Band broadening from these effects arise because the equilibrium between the mobile and the stationary phase is established slowly. Consequently, analyte molecules at the front of a band are swept ahead by the mobile phase before they have time to equilibrate with the stationary phase and thus be retained. Also, equilibrium is not reached at the trailing edge of a band, and molecules are left behind in the stationary phase by the fast-moving mobile phase (Skoog et al., 1998).

$$C_m = \frac{f_m(k')d_p^2}{D_m} \tag{1.8}$$

$$C_s = \frac{f_s(k')d_f^2}{D_s} \tag{1.9}$$

Where; d_p = Diameter of packing particle (cm)

D_m = Diffusion coefficient in mobile phase ($cm^2\ s^{-1}$)

D_s = Diffusion coefficient in stationary phase ($cm^2\ s^{-1}$)

k' = Retention factor calculated from the equation; $k' = \frac{t_R - t_M}{t_M}$

$f(x)$ = Function of x

d_f = Thickness of liquid coating on stationary phase (cm)

t_R = Retention time of analyte peak (min)

t_M = Time of the unretained species to reach the detector (min)

Column efficiency is described in terms of the theoretical plate height (*H*) with greater efficiency having a lower *H* and producing less band broadening of the chromatographic peak. In general the greatest column efficiencies are obtained when all of the terms in Equation 1.5 are optimized to obtain the lowest band broadening.

Early RP-HPLC analysis of chloropigments began in the 1970s using isocratic elution. Subsequently a method was developed using gradient elution (Roy, 1987). Early pigments analyses used photodiode array detection coupled with RP-HPLC in order to obtain spectral information on chlorophyll derivatives and carotenoids (Keely, 2006 and references therein). More recently, a powerful RP-HPLC method for the separation of complex sedimentary pigment mixtures was reported by Airs et al. (Method A, 2001a). The method (Airs et al., 2001a), which combines online photodiode array detection and multistage tandem mass spectrometric detection, gives excellent resolution of over 60 components with an analysis time of 115 min. Airs et al (2001a) Method A has been applied to the stratigraphic profiling of chlorophyll pigments in sediment cores; for example, for palaeoenvironmental reconstruction of Kirisjes Pond in the Larsemann Hills, Eastern Antarctica (Squier et al. 2002). The pigment profiling in that study was performed on three sections of the core; the uppermost section (surface-88 cm; *c*. present to 6205 Yrs BP), the middle section (88-94 cm; c. present to 6205-6285 Yrs BP) and the deepest section (112-114 cm; c. present to 6525-11195 Yrs BP) (Squier et al., 2002). The sections studied were divided into 1 cm horizons. The interval represented by each 1 cm horizon (for example in the uppermost section (Squier et al., 2002)), can be calculated at approximately 71 years. Accordingly, the results of pigment analysis on each of those horizons represent an average for the sediment accumulated over that period. In order to obtain a more detailed picture for palaeoenvironmental reconstruction, it is desirable to analyse sediment cores at a much greater temporal resolution (0.5-0.1 cm intervals). The lengthy analysis time and large volumes of solvent associated with

using Airs et al., (2001a) Method A (115 min/sample) makes analysing the large quantity of samples needed for a high resolution pigment profiling study unfeasible.

1.3.2 Ultra high performance liquid chromatography (UHPLC)

In recent years, advances in stationary phase technology have enabled the production of HPLC columns packed with smaller (sub-2 µm) particles. Hence rapid HPLC methods have been developed using shorter columns, smaller particle sizes and higher mobile phase pressures have been employed to separate mixtures of compounds in shorter analysis times (Gilpin and Zhou, 2008; Nguyen et al., 2006; Swartz, 2005). Such rapid HPLC methods have been known by several different names depending on the different instrument manufacturer's trademarks; for example, Ultra Performance Liquid Chromatography™ (UPLC™), Rapid Separation Liquid Chromatography (RSLC) and Ultra-high Performance liquid chromatography (UHPLC) are used by Waters, Dionex and Agilent, respectively. The term UHPLC has become the widely accepted generic term and will be used throughout this thesis to avoid confusion and provide a reminder that the technique is developed with the same basic chromatographic theory as that for HPLC analysis. The decreased particle size of the stationary phase in UHPLC results in a reduction in the theoretical plate high (*H*) by alteration of the *A* term of the van Deemter equation (Equation 1.5). In addition, not only is column efficiency significantly increased but, for particle sizes less than 2.5 µm, greater linear mobile phase flow rates can also be used without compromising separation efficiency (Swartz, 2005). This is illustrated in Fig. 1.8 which shows the relationship between linear velocity and *H* for particle sizes 1.7, 3.5, 5 and 10 µm. Notably, the 1.7 µm particles exhibit the greatest efficiency (lowest *H*) and very little change in *H* over linear velocities between 3 and 7 mm s^{-1}.

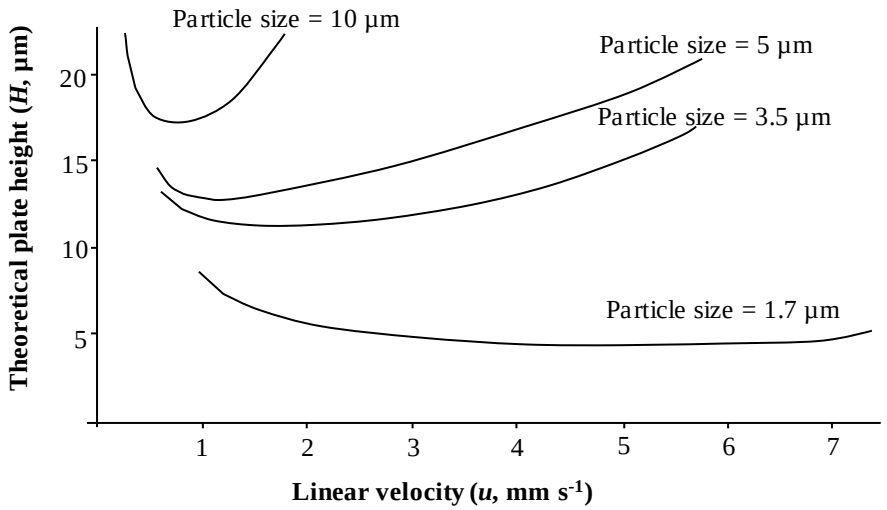

Figure 1.8. Representation of the van Deemter plot, showing the relationship between theoretical plate height (*H*) and the particle size of stationary phase packed in the column; adapted from Swartz, (2005).

One consequence of using small size particles (sub-2 µm) is high column back pressures (> 400 bar) compared with HPLC columns, even when using shorter column lengths (Nguyen et al., 2006). Accordingly, the pump systems of UHPLC instruments need to be capable of delivering solvent at high pressure consistently. In addition, an injector capable of rapidly introducing low volumes of sample, and a rapid highly sensitive detector (which can cope with peak widths at half-height of less than one second) are required (Swartz, 2005 and references therein). Since the launch of the first commercial UHPLC instrument by the Waters company in 2004 (Swartz, 2005), there have been a large number of publications involving UHPLC applications in numerous fields; for example, pharmaceutical analysis; (Chesnut and Salisbury, 2007; Nováková et al., 2006; Swartz, 2005), food analysis (Leandro et al., 2006), beverage analysis (Gruz et al., 2008) and the analysis of polycyclic aromatic hydrocarbons (PAHs) contamination in environment (Purcaro et al., 2012).

Recently, the analysis of pigments in plant extracts using UHPLC has been reported (Bohoyo-Gil et al., 2012; Fu et al., 2012). Bohoyo-Gil et al. (2012) reported the UHPLC separation of a mixture of seven carotenoids extracted from fruit in 10 min. Their method achieves high resolution using a C_{18} column (2.1×50 mm, 1.8 µm particle size) and a mobile phase gradient system. A mixture of carotenoid and

chlorophyll pigments, including chlorophylls *a* (**4**) and *b* (**5**) and their epimers, extracted from microalgae have been analysed in 20 min by UHPLC coupled with UV and a quadrupole time-of-flight hybrid mass spectrometer (Fu et al., 2012). Although these methods gave good resolution and short analysis times, the pigments extracted from plants exhibit relatively simple distributions compared to those which typically occur in sediments.

1.4 Aims of study

The aim of the work described in this thesis was the development and validation of rapid high-throughput methods for the extraction and analysis of complex mixtures of sensitive sedimentary pigments and evaluation of the developed methods by creating profiles of pigments in sediment cores at high temporal resolution. This will enable the rapid processing of environmental samples and a more detailed reconstruction of palaeoenvironmental conditions based on sedimentary pigment biomarkers than previously practical. Specific aims encompassed three main aspects critical for the development of a high throughput capability for sedimentary pigment analysis. These relate specifically to work described in each of Chapters 2, 3, and 4

Chapter 2: To develop and optimise an ASE method for the extraction of chlorin pigments from aquatic sediments and cell cultures.

Chapter 3: Transfer of the Airs HPLC Method A (Airs et al., 2001a) to a UHPLC method and optimisation of the separation conditions (such as gradient composition, separation temperature and mobile phase flow rate) for two types of UHPLC column.

Chapter 4: To evaluate the new ASE and UHPLC methods for suitability in their application to high throughput extraction and analysis of pigments in sediment cores. The efficiency of the methods are discussed both in terms of the total analysis time and the quality of pigment profiles create.

Chapter 2

Accelerated solvent extraction from aquatic sediments

2.1 Introduction

Lake and marine sediments contain valuable palaeoenvironmental records in the inorganic and organic matter accumulated over long periods of time. The organic content, through the presence of specific biological marker compounds (Eglinton and Calvin, 1967), can reflect the environment in which the source organisms lived. Generally, sedimentary organic compounds are solvent extracted before analysis by chromatographic separation coupled to mass spectrometric detection. For examples see review by previous study (Canstaneda and Schouten, 2011).

Chlorophylls, bacteriochlorophylls and their derivatives are especially valuable biological markers, being produced exclusively by photoautotrophic organisms (algae, higher plants and certain types of bacteria) in the capture of energy from sunlight for use in the conversion of inorganic forms of carbon to organic molecules (Hall and Rao, 1999). Specific structures can reveal the composition of the primary producer community. For example, chlorophyll *a* (**4**, Scheme 2.1) and chlorophyll *b* (**5**) and their phaeophytin (phe, **11**, **17**), pyrophaeophytin (pphe **18**, **19**), phaeophorbide (phorb; **20, 21**), pyrophaeophorbide (**22**, **23**), chlorophyllone (**24, 25**, see Appendix of structures), steryl ester (**26-28**) and associated C-13^2 stereoisomer derivatives indicate the presence of oxygenic primary producers. Bacteriochlorophyll *a* (bchl *a*, **6**, Scheme 2.2), its phaeophytin derivatives (bphe *a*, **29** and its epimer, **30**) and pyrobacteriophaeophytin *a* (pbphe *a*, **31**) are markers for anoxygenic phototrophic bacteria (Scheer, 2008). Bacteriochlorophylls *c* (**8**, see Appendix of structures) and *d* (**9**, see Appendix of structures) are markers for green sulfur bacteria, obligate anaerobes whose presence indicates the existence of photic zone anoxia in contemporary and past environments (Squier et al., 2002; Airs and Keely, 2003). The abundances and distributions of chlorophylls can provide information on the intensity of palaeo-production at the time of the deposition (Harris et al., 1996), changes in relative sea level (Squier et al., 2002) and ice cover (Squier et al., 2004) while certain chlorophyll transformation products can infer particular environmental conditions, such as grazing pressure on the phytoplankton community (Shuman and Lorenzen, 1975; Talbot et al., 1999; Walker and Keely, 2004b).

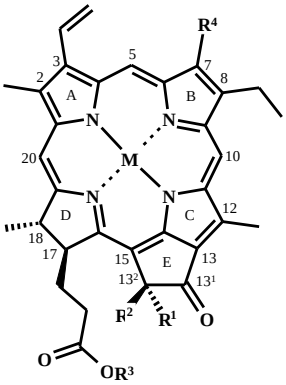

Pigments	Appendix of Structures	M	R^1	R^2	R^3	R^4
chl *a*	**4**	Mg	CO_2CH_3	H	Phytyl	CH_3
chl *b*	**5**	Mg	CO_2CH_3	H	Phytyl	CHO
phe *a*	**11**	2H	CO_2CH_3	H	Phytyl	CH_3
phe *b*	**17**	2H	CO_2CH_3	H	Phytyl	CHO
pphe *a*	**18**	2H	H	H	Phytyl	CH_3
pphe *b*	**19**	2H	H	H	Phytyl	CHO
phorb *a*	**20**	2H	CO_2CH_3	H	Methyl	CH_3
phorb *b*	**21**	2H	CO_2CH_3	H	Methyl	CHO
pphorb *a*	**22**	2H	H	H	Methyl	CH_3
pphorb *b*	**23**	2H	H	H	Methyl	CHO
phorb *a* steryl ester	**26**, **27, 28**	2H	H	H	Steryl	CH_3
phe *a*'	**32**	2H	H	CO_2CH_3	Phytyl	CH_3
phe *b*'	**33**	2H	H	CO_2CH_3	Phytyl	CHO
OH-phe *a*	**34**	2H	CO_2CH_3	OH	Phytyl	CH_3
OH-phe *a*'	**35**	2H	OH	CO_2CH_3	Phytyl	CH_3

Scheme 2.1. Structures of chlorophyll *a* (**4**), chlorophyll *b* (**5**) and closely related derivatives.

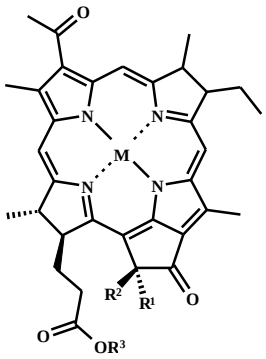

Pigments	Appendix of Structures	M	R^1	R^2	R^3
bchl *a*	**6**	Mg	CO_2CH_3	H	Phytyl
bphe *a*	**29**	2H	CO_2CH_3	H	Phytyl
bphe *a*'	**30**	2H	H	CO_2CH_3	Phytyl
pbphe *a*	**31**	2H	H	H	Phytyl

Scheme 2.2. Structures bacteriochlorophyll *a* (**6**) and closely related derivatives.

Current methods for the analysis of chlorins typically employ extraction by sonication followed by liquid chromatography mass spectrometry (LC-MS) analysis. Sonication may require up to 10 repeats to extract all of the soluble pigment (Airs et al., 2001a; Walker, 2004a; Pickering, 2009), hence the method is not readily amenable to automation. Accelerated solvent extraction (ASE) uses liquid solvents at elevated temperatures and pressures to enhance extraction efficiency and reduce both extraction time and solvent consumption (Richter et al., 1996). Applications of ASE include extraction of natural product molecules from plant matter (Cho et al., 2007), petroleum hydrocarbons, polycyclic aromatic hydrocarbons (PAHs) and polychlorinated biphenyls (PCBs) from soils (Richter et al., 1997; Zuloaga et al., 1998; Wang et al., 2007) and lipid biomarkers (C_{19}-C_{34} *n*-alkanes, *n*-alcohols, *n*-fatty acids, dehydroabietic acid and β-sitosterol) from sandy soils (Jansen et al., 2006). In all cases ASE was more efficient than commonly used extraction techniques such as Soxhlet extraction and microwave extraction. ASE is becoming increasingly used in geochemistry for extraction from ancient sediments (Hinrichs et al., 1999; Schouten et al., 2007; Sluijs et al., 2008). Although the method offers advantages in efficiency and its potential for automation, it has not yet been evaluated for the extraction of highly sensitive chlorophyll pigments. The aim of this study was to develop and optimise an ASE method for the extraction of pigments from aquatic sediments, considering sample preparation procedures in order to control precision in quantification.

2.2 Results and discussion

The reactivity of chlorophyll pigments limits the choice of solvent for extraction. Methanol should be avoided as chlorophylls rapidly form several transformation products *via* oxidation (allomerisation) in solutions containing methanol (Johnston and Watson, 1956; Woolley et al., 1998). Previous studies identified absolute acetone as the most efficient solvent for the extraction of pigments from wet sediments (Keely and Brereton, 1986). Although acetone can promote the oxidation of tetrahydroporphyrin bacteriochlorophylls to form bacterioviridin (**36**), the reaction is considerably slower than the allomerisation reaction of chlorophyll *a* (**4**) in methanol (Woolley et al., 1998). Thus, acetone was selected as the solvent for extraction from sediments.

2.2.1 Lake Reid

Sediment collected and frozen by the British Antarctic Survey (BAS) in 1997 from Lake Reid (Larsemann Hills, Antarctica) was thawed, excess water removed by pipette and homogenised by grinding using a pestle and mortar (for more details see Experimental, Chapter 6, Section 6.3.1.1 and Table 6.1). Aliquots of homogenised sediment from Lake Reid extracted with acetone; by sonication at room temperature and by ASE at each of the following temperatures 20, 50, 75, 100, 125 150 and 175°C; show the presence of essentially the same chlorophylls and derivatives but exhibit differences in the relative abundance of those components (Fig. 2.1). The distribution from sonication (Fig. 2.1a) contains abundant phaeophytin *a* (**11**) accompanied by a range of more polar pigments including chlorophyll *a* (**4**), phaeophorbide *a* methyl ester (**20**) and pyrophaeophorbide *a* methyl ester (pphorb *a*, **22**). Pyrophaeophytin *a* (**18**) occurs in low relative abundance.

Total pigment yields for ASE normalized to the mass of dry extracted sediment generally increased with extraction temperature (20°C: 21.5 nmol g^{-1}; 50°C 55.4 nmol g^{-1}; 75°C: 61.8 nmol g^{-1}; 100°C: 48.4 nmol g^{-1}, Fig. 2.2) to values slightly less than that for sonication (80.8 nmol g^{-1}, Fig. 2.2) at 125°C (75.4 nmol g^{-1}, Fig. 2.2) and 150°C (72.9 nmol g^{-1}), after which it decreased dramatically (175°C: 31.7 nmol g^{-1}, Fig. 2.2) indicating decomposition of pigments at this temperature. The lower

yield at 100°C could result from poor homogenization due to the sandy/silt nature of the sediment. Although the sediment was mixed prior to division into aliquots for extraction, particle sizes > 1.0 mm accounted for 17% (75°C) and 23% (100°C) of sediment mass as revealed by sieving the extracted sediment. Thus, it is likely that non-uniform distribution of the pigment throughout the sediment accounts for the inconsistency in the yield at 100°C.

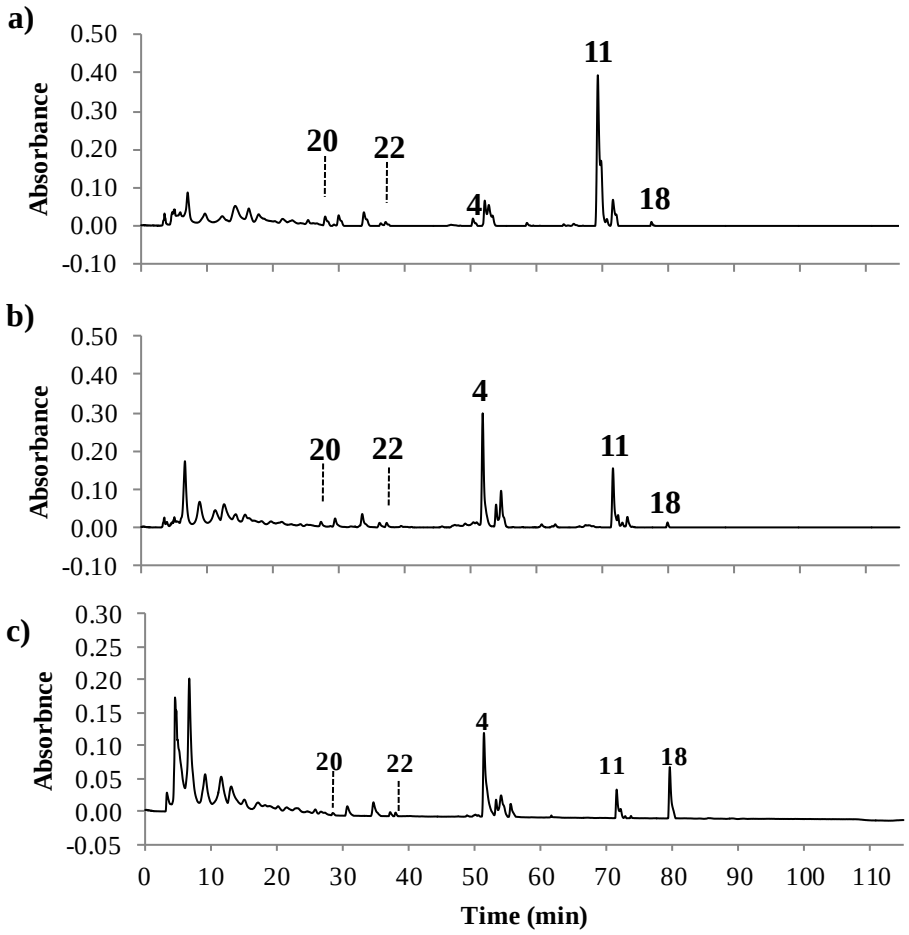

Figure 2.1. HPLC-PDA (350-800 nm) chromatograms of Lake Reid sediment extracted by (a) sonication (b) ASE at 75°C and (c) ASE at 175 °C. Extracts were made up in the same volume of acetone for analysis. Peak assignments are given in Scheme 2.1.

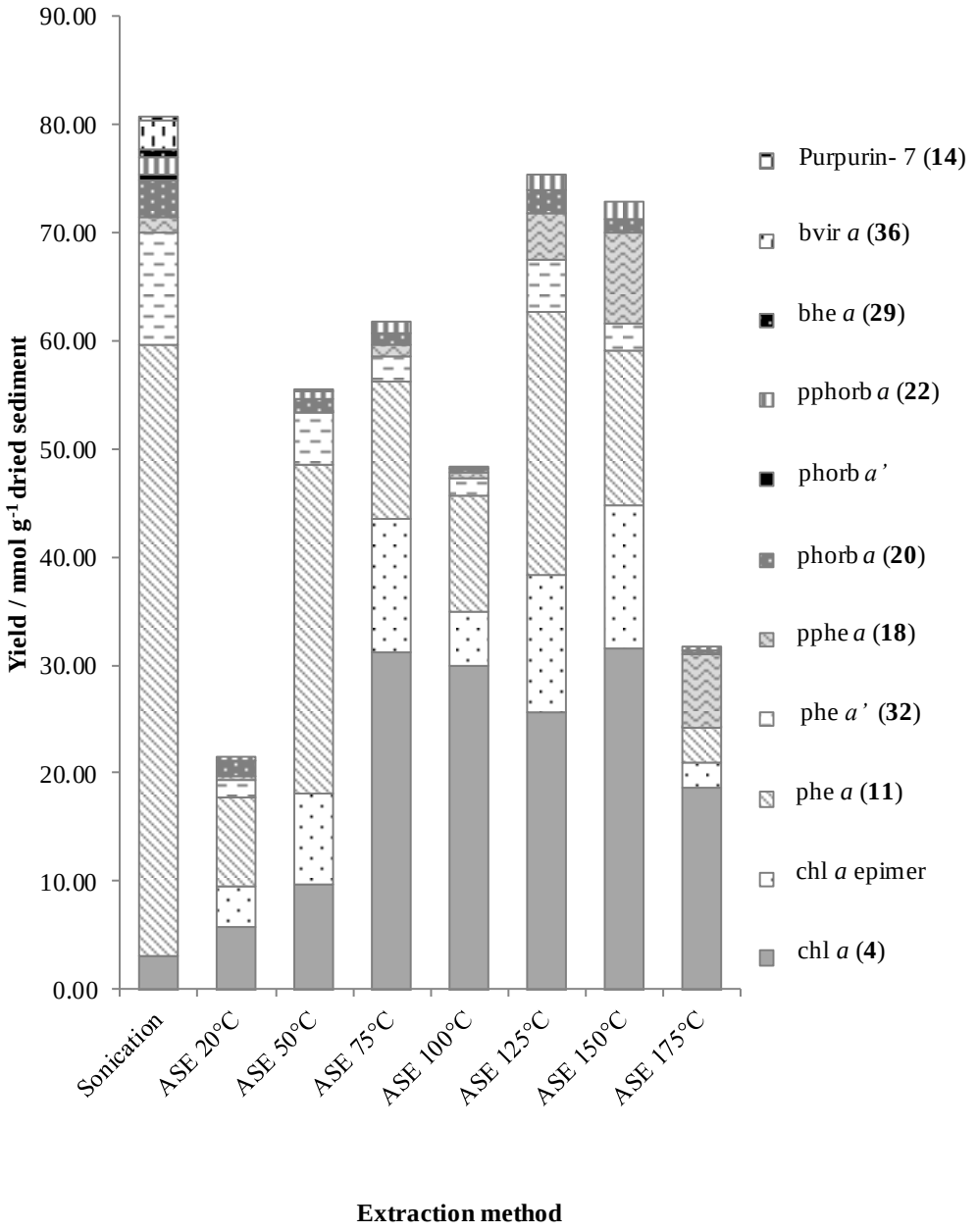

Figure 2.2. Yield of extracted pigments from Lake Reid sediment obtained by the different extraction conditions. The total area of the bar represents the total pigment extracted.

The pigment distribution from ASE at 75°C differs from extracts at lower temperatures and that from sonication: chlorophyll *a* (**4**) dominates the distribution (Fig. 2.1b). The scarcity of chlorophyll *a* (**4**) and higher relative abundance of phaeophytin *a* (**11**) in the extract from sonication could be explained by demetallation of chlorophyll *a* (**4**) during sonication. The Mg-containing counterpart of pyrophaeophorbide *a* (**22**) is not present in this sediment (Airs et al., 2001a). The abundance of pyrophaeophorbide *a* (**22**) relative to phaeophytin *a* (**11**) is lower in the extract from sonication than from ASE (0.03 *vs* 0.08), confirming that phaeophytin *a* (**11**) is formed by demetallation during sonication. The distribution of pigments from extraction at 100°C (Fig. 2.3a) is broadly similar to that at 75°C (Fig. 2.3b), though the pyrophaeophorbide *a* (**22**): phaeophytin *a* (**11**) ratio (0.02) indicates demetallation at the higher temperature.

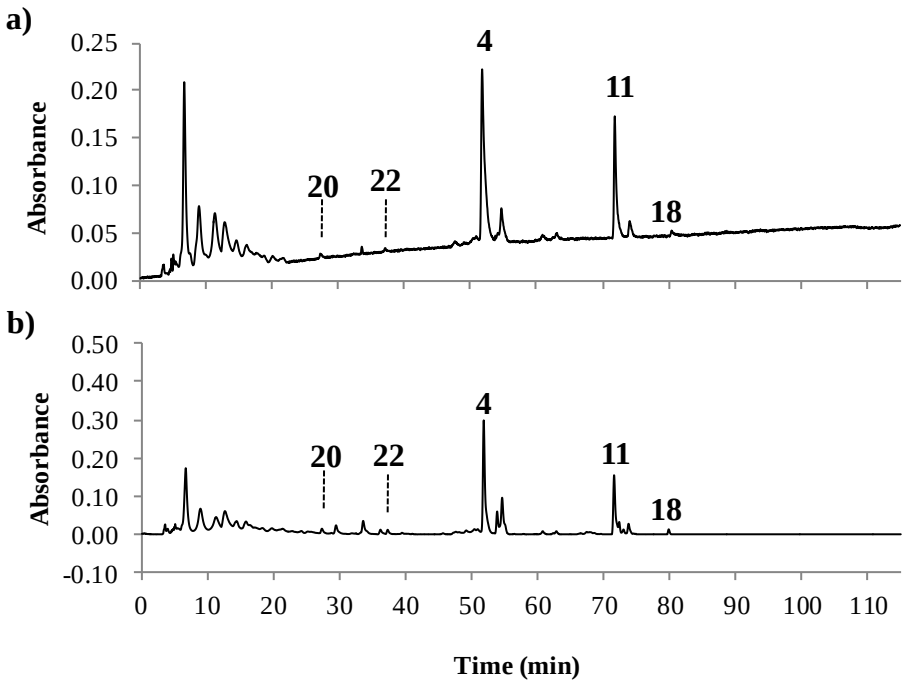

Figure 2.3. HPLC-PDA (350-800 nm) chromatograms of Lake Reid sediment extracted by (a) ASE at 100°C and (b) ASE at 75 °C. Extracts were made up in the same volume of acetone for analysis. Peak assignments are given in Scheme 2.1.

The samples extracted at temperatures above 100°C show higher yields of phaeophytin *a* (**11**) and a systematic decrease in the ratio of pyrophaeophorbide *a* (**22**) to pyrophaeophytin *a* (**18**) (125°C: 0.34; 150°C: 0.19; 175°C: 0.05, Fig. 2.4). Decreases in the ratio from 1.05 at 75°C (Fig. 2.4) indicate an increasing extent of formation of pyrophaeophytin *a* (**18**) *via* thermal alteration of chlorophyll *a* (**4**) and/or phaeophytin *a* (**11**) during extraction, consistent with the known reactivity of the C-13[2] carbomethoxy group in chlorins (Keely et al., 1990) and decarbomethoxylation of chlorophylls during heating at 100°C in degassed pyridine for 24 hours (Hynninen, 1991). The decrease in the abundance of phaeophytin *a* (**11**) at higher temperatures (e.g. 175°C Fig. 2.1c) suggests it to be the major source of pyrophaeophytin *a* (**18**), confirming its origins from transformation during the extraction and not from differences in extraction efficiency. Thus, the ASE 75°C extract (Fig. 2.1b) more accurately represents the pigment distribution in the sediment and the results indicate that ASE at 100°C and above is not suitable for the extraction of sedimentary pigments. The limited amount of Lake Reid sediment available precluded repeat extractions. Thus, in order to determine the optimal temperature, further experiments employed other sediments.

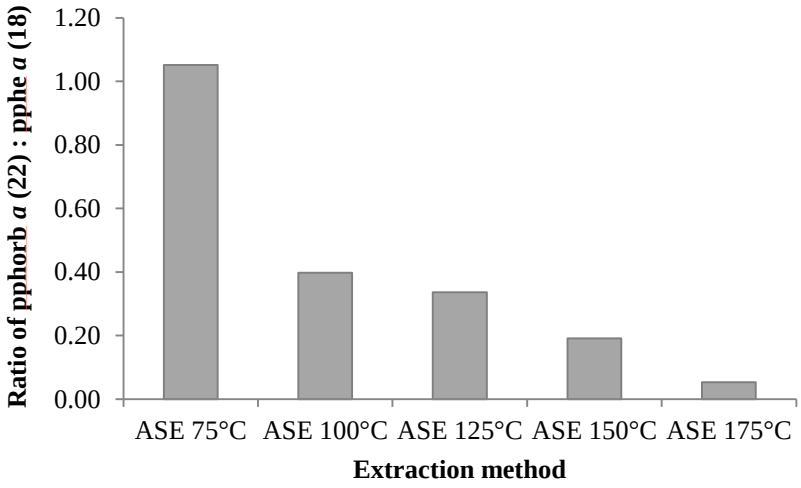

Figure 2.4. Histograms showing the ratio of pyrophaeophorbide *a* (**22**) to pyrophaeophytin *a* (**18**) for Lake Reid sediment extracted by ASE at 75, 100, 125, 150 and 175°C.

2.2.2 Priest Pot

The Priest Pot sediment collected by Brendan J. Keely in 1985 from Cumbria, UK was thawed and excess water removed by pipette. The fine black moist sediment was homogenized by grinding using a pestle and mortar. The Priest Pot sediment extract showed an absence of chlorophyll *a* (**4**). Thus, to examine the stabilities of chlorophylls as a function of ASE temperature the sediment was spiked with known concentrations of chlorophyll *a* (**4**) and chlorophyll *b* (**5**) (see Experimental, Chapter 6, Sections 6.2.2.1 and 6.3.1.2). The spiked sediment, extracted in triplicate by sonication at room temperature and by ASE at intervals over the range 50 to 175°C (Table 2.1), gave similar distributions with phaeophytin *a* (**11**) as the dominant component (Fig. 2.5, Table 2.1).

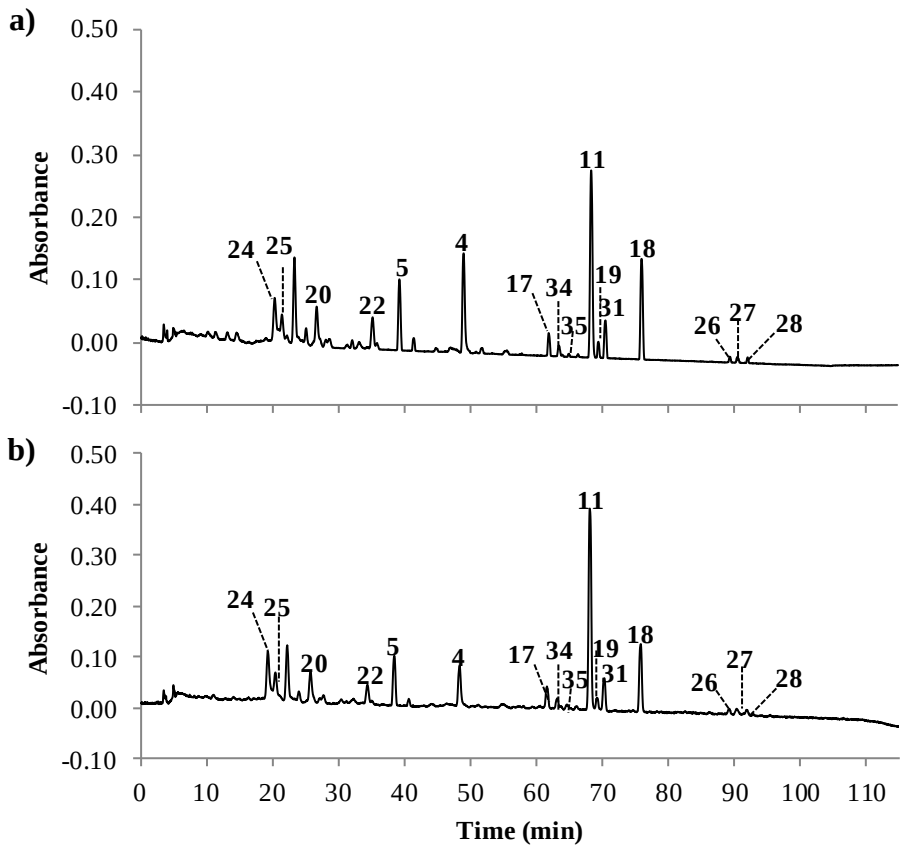

Figure 2.5. HPLC-PDA (350-800 nm) chromatogram of spiked Priest Pot sediment extracted by (a) sonication and (b) ASE at 75°C. Both samples were dissolved in the same volume of acetone for analysis. Peak assignments are given in Scheme 2.1 and Table 2.1.

Total chlorin yields were calculated from the summed abundances of chlorophyll *a* (**4**), phaeophytin *a* (**11**), pyrophaeophytin *a* (**18**), phaeophorbide *a* methyl ester (**20**), pyrophaeophorbide *a* methyl ester (**22**), phaeophytin *a* epimer (**31**), hydroxyphaeophytin *a* (**34**), chlorophyllone diastereomers (**24** and **25**), chlorophyll *b* (**5**), phaeophytin *b* (**17**) and pyrophaeophytin *b* (**19**) (Table 2.1). Components close to the limit of detection (hydroxyphaeophytin *a* epimer, **35,** and pyrophaeophorbide *a* steryl esters, **26**, **27** and **28**, Table 2.1) were not included. The replicates of total pigment yields from sonication and ASE between 50 and 175°C showed normal distributions (Shapiro-Wilk, $p > 0.05$, Table 2.2) and the entire data set showed homogeneity of variance (Levene statistic test, $F(9, 20) = 1.982$, $p = 0.097$). As a result, a one-way ANOVA test was applied and revealed a significant difference (one-way ANOVA, $F(9, 20) = 3.175$, $p = 0.015$). A post-hoc least significant difference (LSD) test revealed that the data from sonication (376.8 ± 74.6 nmol g^{-1} of dried sediment) are not significantly different to ASE from 50°C (306.8 ± 37.8 nmol g^{-1} of dried sediment, $p = 0.069$) to 150°C (342.2 ± 28.5 nmol g^{-1} of dried sediment, $p = 0.354$) but are significantly different to ASE at 175°C (285.7 ± 69.1 nmol g^{-1} of dried sediment, $p = 0.021$) (Table 2.3). The highest values were obtained between 85 and 125°C (Fig. 2.6 and Table 2.1).

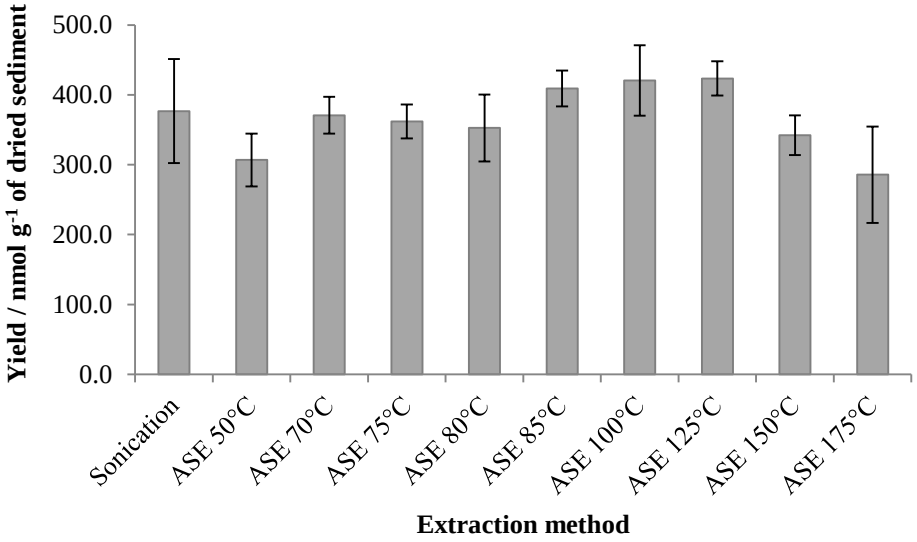

Figure 2.6. Total pigment extract yields for spiked Priest Pot sediment (error bars represent ± 1 standard deviation, $n = 3$).

Table 2.1 Assignments and yields of the major chlorin pigments (mean ± 1 s.d.; *n* = 3) in spiked Priest Pot sediment (continued over).

Assignments	**Main UV/vis $\lambda_{max.}$ (nm)**	**$[M+H]^+$ (*m/z*)[a]**	**Prominent Product ions in MS^n (*m/z*)**	**Esterifying alcohol**	**Yield (nmol g^{-1} of sediment)[c]**				
					Sonication (ºC)	**ASE (ºC)**			
					20	50	70	75	80
Chlorophyll *a* (**4**)	431, 665	871	615, 555	phytol	23.4 ± 5.2	14.7 ± 0.9	13.4 ± 2.9	16.0 ± 3.3	10.8 ± 3.9
Chlorophyll *b* (**5**)	467, 649	907	-	phytol	10.5 ± 2.7	8.9 ± 0.9	8.4 ± 1.5	9.7 ± 1.3	8.3 ± 2.8
Phaeophytin *a* (**11**)	408, 665	871	593, 533	phytol	39.2 ± 5.8	41.7 ± 2.3	47.9 ± 2.6	46.8 ± 4.3	46.0 ± 4.6
Phaeophytin *b* (**17**)	436, 651	885	607, 547	phytol	3.5 ± 1.3	4.5 ± 0.5	5.7 ± 0.1	4.2 ± 0.6	4.4 ± 0.6
Pyrophaeophytin *a* (**18**)	410, 665	813	535, 507	phytol	20.6 ± 3.6	12.6 ± 4.0	17.7 ± 2.1	17.8 ± 2.2	16.0 ± 1.5
Pyrophaeophytin *b* (**19**)	437, 650	827	549	phytol	2.6 ± 1.1	1.4 ± 1.1	2.3 ± 0.5	2.5 ± 0.4	2.1 ± 0.6
Phaeophorbide *a* (**20**)	408, 665	607	547, 461	methanol	7.9 ± 1.6	5.4 ± 2.4	8.4 ± 1.1	6.5 ± 1.6	8.9 ± 0.8
Pyrophaeophorbide *a* methyl ester (**22**)	408, 668	549	521, 435	methanol	5.5 ± 1.6	0.9 ± 1.5	2.4 ± 2.1	2.2 ± 2.5	3.5 ± 1.5
Chlorophyllone (**24**)	410, 665	533	515, 505, 500		9.6 ± 0.6	9.1 ± 1.1	13.3 ± 0.3	12.0 ± 1.5	13.2 ± 1.1
Chlorophyllone (**25**)	407, 670	533	515, 505, 500		6.2 ± 1.2	3.8 ± 0.6	5.8 ± 0.5	5.4 ± 0.6	6.3 ± 1.3
Pyrophaeophorbide *a* steryl ester (**26**)	410, 667	903	-	C_{27} sterol[b]	-	-	-	-	-
Pyrophaeophorbide *a* steryl ester (**27**)	410, 670	929	-	C_{29} sterol[b]	-	-	-	-	-
Pyrophaeophorbide *a* steryl ester (**28**)	409, 663	931	-	C_{29} sterol[b]	-	-	-	-	-
Phaeophytin *a* epimer (**32**)	409, 666	871	593, 533	phytol	7.5 ± 1.1	7.7 ± 0.5	8.8 ± 0.5	7.9 ± 0.6	7.7 ± 0.7
Hydroxyphaeophytin *a* (3**4**)	406, 664	887	609, 591	phytol	1.5 ± 1.5	1.7 ± 1.5	3.2 ± 0.8	1.6 ± 1.4	2.0 ± 0.6
Hydroxyphaeophytin *a* epimer (**35**)	404, 661	887	609, 591	phytol	-	-	-	-	-
Total pigment yields (nmol)					137.9 ± 24.9	112.4 ± 12.5	137.2 ± 9.7	132.7 ± 10.1	129.1 ± 14.4
Total pigment yields (nmol g^{-1} of dry sediment)					376.8 ± 74.6	306.8 ± 37.8	370.8 ± 26.2	361.8 ± 24.3	352.6 ± 48.0
Chlorophyll *a* recovery (%)					63.9 ± 14.3	40.0 ± 2.4	36.5 ± 7.9	43.5 ± 9.0	29.5 ± 10.5
Chlorophyll *b* recovery (%)					73.5 ± 18.6	62.4 ± 6.6	58.8 ± 10.6	67.9 ± 8.8	57.8 ± 19.3
Ratio of pphorb *a* (**22**): phe *a* (**11**)					0.14	0.02	0.05	0.05	0.08

Assignments	**Main UV/vis $\lambda_{max.}$ (nm)**	**$[M+H]^+$ (*m/z*)[a]**	**Prominent Product ions in MS^n (*m/z*)**	**Esterifying alcohol**	**Yield (nmol g^{-1} of sediment)[c]**				
					ASE (ºC)				
					85	100	125	150	175
Chlorophyll *a* (**4**)	431, 665	871	615, 555	phytol	8.9 ± 1.7	5.6 ± 1.3	0	0	0
Chlorophyll *b* (**5**)	467, 649	907	-	phytol	10.1 ± 1.2	7.7 ± 1.2	8.2 ± 0.8	3.1 ± 0.5	3.9 ± 2.3
Phaeophytin *a* (**11**)	408, 665	871	593, 533	phytol	57.6 ± 4.2	62.7 ± 2.7	69.6 ± 2.2	56.8 ± 2.1	48.5 ± 17.2
Phaeophytin *b* (**17**)	436, 651	885	607, 547	phytol	4.8 ± 0.9	5.3 ± 1.3	5.9 ± 0.5	7.6 ± 1.8	4.2 ± 1.6
Pyrophaeophytin *a* (**18**)	410, 665	813	535, 507	phytol	16.8 ± 1.9	17.1 ± 2.1	17.9 ± 1.2	15.5 ± 1.0	14.8 ± 3.6
Pyrophaeophytin *b* (**19**)	437, 650	827	549	phytol	2.3 ± 0.7	1.8 ± 0.6	2.7 ± 0.2	3.5 ± 1.1	2.8 ± 1.8
Phaeophorbide *a* (**20**)	408, 665	607	547, 461	methanol	8.1 ± 1.0	9.2 ± 0.6	7.3 ± 1.1	4.0 ± 0.3	0
Pyrophaeophorbide *a* methyl ester (**22**)	408, 668	549	521, 435	methanol	3.9 ± 1.0	4.7 ± 1.8	5.2 ± 1.0	3.3 ± 1.0	0
Chlorophyllone (**24**)	410, 665	533	515, 505, 500		16.4 ± 4.1	17.5 ± 3.8	17.4 ± 2.8	12.7 ± 1.1	8.0 ± 3.6
Chlorophyllone (**25**)	407, 670	533	515, 505, 500		9.5 ± 1.4	9.5 ± 1.5	7.5 ± 1.7	3.7 ± 1.3	2.1 ± 2.7
Pyrophaeophorbide *a* steryl ester (**26**)	410, 667	903	-	C_{27} sterol[b]	-	-	-	-	-
Pyrophaeophorbide *a* steryl ester (**27**)	410, 670	929	-	C_{29} sterol[b]	-	-	-	-	-
Pyrophaeophorbide *a* steryl ester (**28**)	409, 663	931	-	C_{29} sterol[b]	-	-	-	-	-
Phaeophytin *a* epimer (**32**)	409, 666	871	593, 533	phytol	7.6 ± 1.1	7.4 ± 2.5	9.8 ± 0.8	5.7 ± 3.4	14.2 ± 12.9
Hydroxyphaeophytin *a* (3**4**)	406, 664	887	609, 591	phytol	2.5 ± 0.2	2.7 ± 1.4	3.7 ± 0.3	4.9 ± 0.5	1.0 ± 1.8
Hydroxyphaeophytin *a* epimer (**35**)	404, 661	887	609, 591	phytol	-	-	-	-	-
Total pigment yields (nmol)					148.5 ± 8.0	151.2 ± 15.4	155.2 ± 7.9	120.9 ± 9.5	99.7± 21.8
Total pigment yields (nmol g^{-1} of dry sediment)					409.1 ± 25.6	420.6 ± 50.3	423.5 ± 24.5	342.2 ± 28.5	285.7± 69.1
Chlorophyll *a* recovery (%)					24.3 ± 4.7	15.3 ± 3.5	0	0	0
Chlorophyll *b* recovery (%)					70.5 ± 8.2	54.0 ± 8.2	57.7 ± 5.6	22.0 ± 3.6	27.6 ± 15.7
Ratio of pphorb *a* (**22**): phe *a* (**11**)					0.07	0.07	0.08	0.06	-

[a] All metallated pigments appear in MS as their demetallated counterparts due to post column demetallation prior to MS (Airs and Keely, 2000).

[b] Tentative assignment.

[c] Moist sediment spiked with known concentrations of chlorophylls *a* (**4**) and *b* (**5**) were extracted and wet yield was calculated in nmol g^{-1} of dry sediment after extraction.

Table 2.2 Output from the Shapiro-Wilk test (test of normality at 95% confidence) for total pigment yields from Priest Pot sediment extracted by sonication and ASE at 50-175°C.

Extraction method	Test of Normality		
	Shapiro-Wilk		
	Statistic	df[a]	Sig. (*p*)[b]
Sonication	0.800	3	0.114
ASE 50°C	0.985	3	0.766
ASE 70°C	0.996	3	0.873
ASE 75°C	0.989	3	0.797
ASE 80°C	0.852	3	0.246
ASE 85°C	0.795	3	0.101
ASE 100°C	0.965	3	0.640
ASE 125°C	0.814	3	0.149
ASE 150°C	0.904	3	0.398
ASE 175°C	0.930	3	0.488

[a] df = degrees of freedom

[b] Data is normal distributed at *p*-values > 0.05.

Table 2.3 Output from one-way ANOVA post hoc least significant difference test for total pigment yields from Priest Pot sediment extracted by sonication compared to ASE at 50-175°C.

Method	Mean of total yield (n = 3) (nmol g^{-1} of dried sediment)	s.d.[a]	Mean Difference (I-J)	Std. Error[b]	Sig.
Sonication (I)	376.8106	74.55790	-	-	-
ASE 50°C (J)	306.7613	37.84315	70.04927	36.46548	0.069
ASE 70°C (J)	370.8418	26.20702	5.96877	36.46548	0.872
ASE 75°C (J)	361.8078	24.28340	15.00280	36.46548	0.685
ASE 80°C (J)	352.6245	47.97114	24.18610	36.46548	0.515
ASE 85°C (J)	409.0873	25.63769	-32.27670	36.46548	0.387
ASE 100°C (J)	420.6344	50.33954	-43.82383	36.46548	0.243
ASE 125°C (J)	423.4763	24.54718	-46.66573	36.46548	0.215
ASE 150°C (J)	342.2363	28.48102	34.57433	36.46548	0.354
ASE 175°C (J)	285.6542	69.08089	91.15643*	36.46548	0.021

*The mean difference is significant at the level 0.05 (95% confidence).

[a] Standard deviation was obtained from mean of total yields (n = 3).

[b] Std. Error was obtained from post hoc least significant difference test.

The yield from sonic extraction of spiked sediment (376.8 ± 74.6 nmol g^{-1} extracted sediment) showed low repeatability (± 19.8%), most likely due to extraction being performed on moist sediment. Residual water marginally increases the polarity of the solvent in the first extraction, a feature exploited to maximise extraction efficiency for the more polar chlorophyll transformation products (Keely and Brereton, 1986). McClymont et al., (2007) demonstrated similar yields for acetone extraction of moist sediment and extraction of freeze dried sediments using acetone:water (95:5 v/v), the former being *c* 12% higher. To examine the approach further, Priest Pot sediment was freeze dried, homogenised and sieved (to ≤ 400 μm). Extraction by ASE at 75°C with acetone and with acetone:water (95:5 v/v) gave mean (n = 3) total pigment yields and relative abundances of individual pigments within experimental error (± 8.4%). Accordingly, extraction with acetone was employed in all subsequent experiments. Sonication and ASE at 75°C gave similar yields for freeze-dried sediments (386.5 ± 16.3 nmol g^{-1} extracted sediment and 343.4 ± 31.5 nmol g^{-1} sediment, respectively), with repeatability (± 4.2 and 9.2% of total yield, respectively) being considerably better than with moist sediment. Nevertheless, the yields and repeatability suggest that previous comparisons based on the moist samples, though less precise, are valid.

The recoveries and relative abundances of chlorophyll *b* (**5**), phaeophytin *b* (**17**) and pyrophaeophytin *b* (**19**) are similar for sonication and ASE over the range 50-125°C (Table 2.1). A dramatic decrease in recovery of chlorophyll *b* (**5**) is evident at 150°C and above (Fig. 2.7a), accompanied by decreased abundance relative to phaeophytin *b* (**17**) and pyrophaeophytin *b* (**19**) (Table 2.1). This behaviour contrasts with the recovery of chlorophyll *a* (**4**), where alteration begins to impact recovery at lower extraction temperatures (Fig. 2.7a), and is consistent with the greater chemical stability of chlorophyll *b* (**5**) (Mackinney and Joslyn, 1940; Schanderl et al., 1962). Thus, evaluation of the stability of sensitive pigments only need consider the yield of chlorophyll *a* (**4**).

By contrast with Lake Reid, the extract from sonication gave a higher yield of chlorophyll *a* (**4**) (23.4 ± 5.2 nmol g^{-1}) than from ASE at any temperature (Table 2.1). Either chlorophyll *a* (**4**) spiked into the sediment is more easily extracted than

that present naturally or it is less stable during ASE. Chlorophylls present naturally could be retained by association with mineral or organic matrices of the sediment. For example, porphyrins adsorb to clays, as either anions or cations, in a pH dependent process (Kosiur, 1977). The yield of chlorophyll *a* (**4**) decreased with ASE temperatures above 85°C, reaching zero at 125°C and above (Fig. 2.7b The replicates yields of phaeophytin *a* (**11**) from Priest Pot sediment extracted by sonication and ASE at temperatures from 50 to 175°C were normally distributed except for phaeophytin *a* (**11**) from ASE at 85°C which was significantly different (Shapiro-Wilk, df = 3, $p = 0.024$). The yields obtained from sonication and ASE at temperatures between 50-175°C showed no homogeneity of variance (Levene statistic test, $F(9, 20) = 3.727$, $p = 0.007$). As a result, the Kruskal-Wallis test which was appropriate for non-parametric data was applied. The yield of phaeophytin *a* (**11**) from sonication and ASE between 50 and 175°C showed significant differences (Kruskal-Wallis: $H(9) = 22.488$, $p = 0.007$). In addition, the Mann-Whitney *U* test (Table 2.4) revealed significant differences between the yields of phaeophytin *a* (**11**) from extraction of Priest Pot by sonication and ASE at 50-80 and 175°C versus ASE over the temperature range 85-125°C, the former set of extraction condition having significantly lower yield than the latter (Fig. 2.7b).

The lower pyrophaeophorbide *a* (**22**): phaeophytin *a* (**11**) ratios for ASE than for sonication (Table 2.1) reflect increased phaeophytin *a* (**11**) in ASE extracts, indicating demetallation of chlorophyll *a* (**4**) during the extraction, the skewness of the distribution supporting this suggestion. The similar total pigment yields over the range 70-125°C (Table 2.1) indicates that, although chlorophyll *a* (**4**) is altered, the macrocycle is not destroyed. The best recoveries of chlorophyll *a* (**4**) (40-44%; Table 2.1) were at ASE temperatures 75°C and below. Hence, the optimal temperature for ASE lies between 50 and 75°C, consistent with the findings for Lake Reid sediment (ASE 75°C).

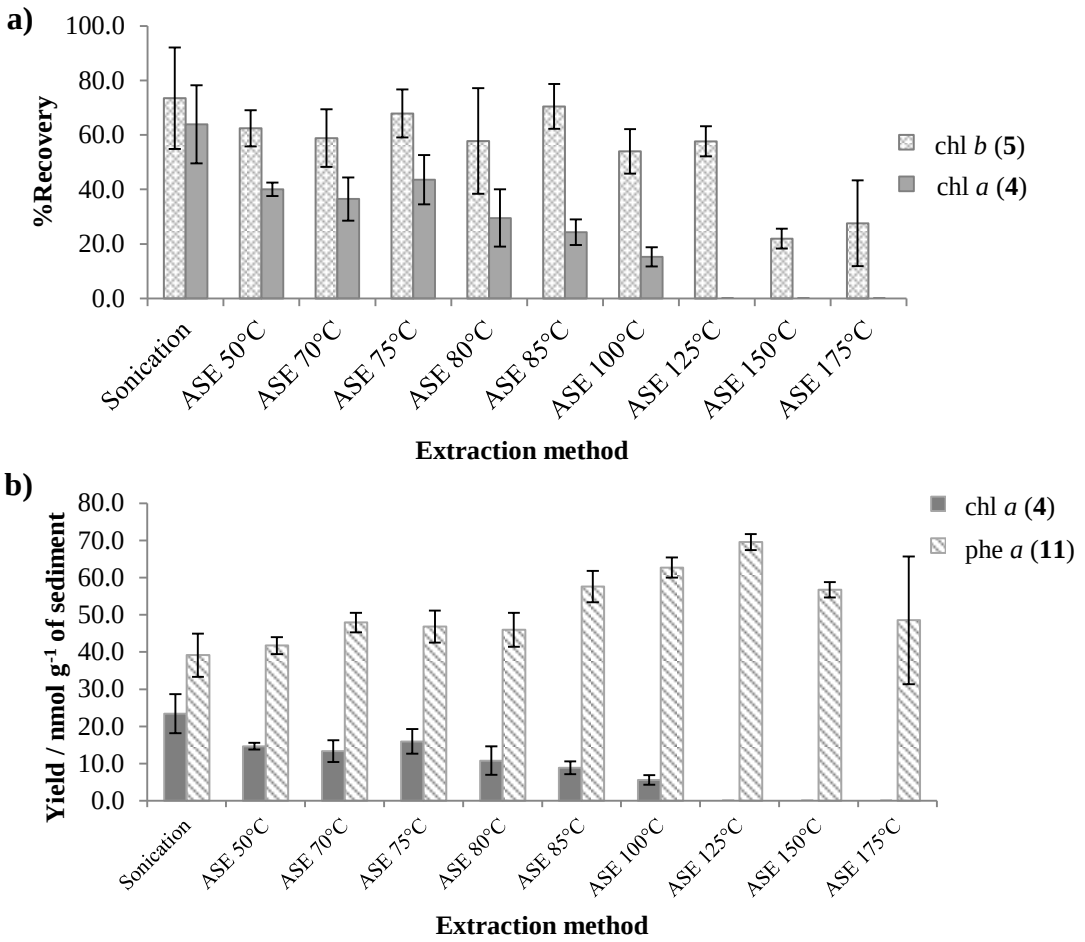

Figure 2.7. Histograms for spiked Priest Pot sediment extraction showing (a) recovery of chlorophylls *a* (**4**) and *b* (**5**) and (b) yield of chlorophyll *a* (**4**) and phaeophytin *a* (**11**) (error bars represent ± 1 standard deviation, $n = 3$).

Table 2.4 Summary of output from the Mann-Whitney test (at 95% confidence) for the yield of phaeophytin *a* (**11**) from Priest Pot sediment extracted by sonication compared to ASE at 50-175°C. *Indicates data are significantly different.

Extraction method		Test statistics		
		Mann-Whitney *U*	Z	Asymp. Sig. (2-tailed)
Sonication	ASE 50°C	3.000	-.655	0.513
	ASE 70°C	1.000	-1.528	0.127
	ASE 75°C	1.000	-1.528	0.127
	ASE 80°C	2.000	-1.091	0.275
	ASE 85°C	0.000	-1.964	0.050*
	ASE 100°C	0.000	-1.964	0.050*
	ASE 125°C	0.000	-1.964	0.050*
	ASE 150°C	0.000	-1.964	0.050*
	ASE 175°C	3.000	-.655	0.513

2.2.3 Loch Ness

Drawing on the results from Lake Reid and Priest Pot sediments, a smaller temperature range for ASE (50, 60, 65, 70, 75 and 80°C) was employed to determine the optimal temperature for pigment extraction from Loch Ness sediment. Loch Ness sediment (Scotland) was collected by Bracewell (1993). The frozen sediment was freeze-dried overnight and subsequently homogenized by grinding using a pestle and mortar. Extraction of the sediment, which naturally contains chlorophyll *a* (**4**), by sonication and ASE at 75°C gave very similar distributions with little difference between them (Fig. 2.8 Table 2.5). The replicates of total pigment yields from Loch Ness sediment extracted by sonication and ASE between 50 and 80°C showed normal distributions (Shapiro-Wilk, $p > 0.05$, Table 2.6) and the entire data set showed homogeneity of variance (Levene statistic test, $F(6, 14) = 2.637$, $p = 0.063$). As a result, a one-way ANOVA test was applied and revealed no significant difference (one-way ANOVA, $F(6, 14) = 2.062$, $p = 0.124$) (Fig. 2.9a and Table 2.2). Notably, unlike the spiked Priest Pot sediment, the abundances of chlorophyll *a* (**4**) and its transformation products show little difference between the two extraction methods (Fig. 2.9b). The improved recovery of chlorophyll *a* (**4**) by comparison with Priest Pot further suggests that spiking of chlorophyll into the sediment is not an ideal approach for testing its stability during extraction. The lower susceptibility to alteration of chlorophyll *a* (**4**) in Loch Ness sediment than when spiked into Priest Pot sediment suggests that it is afforded protection in Loch Ness sediment by intrinsic association with components of the matrix, most likely the organic matter content. By contrast, the adsorption to mineral surfaces that will result from spiking appears to make chlorophyll *a* (**4**) more susceptible to demetallation during ASE extraction, possibly *via* reactions mediated by clay minerals. The slightly lower yields of chlorophyll *a* (**4**) and phaeophytin *a* (**11**) from ASE of Loch Ness sediment below 65°C (Table 2.5) indicates that the total pigment yields were smaller because of lower extraction efficiency rather than demetallation of chlorophyll *a* (**4**) to form phaeophytin *a* (**11**).

The yields of chlorophyll *b* (**5**) from ASE are similar to that obtained for sonication (0.6 ± 0.03 nmol g^{-1} sediment, Table 2.5). Thus, for Loch Ness sediment optimal

total pigment yield and integrity of chlorophyll *a* (**4**) and chlorophyll *b* (**5**) is obtained over the range 65-80°C.

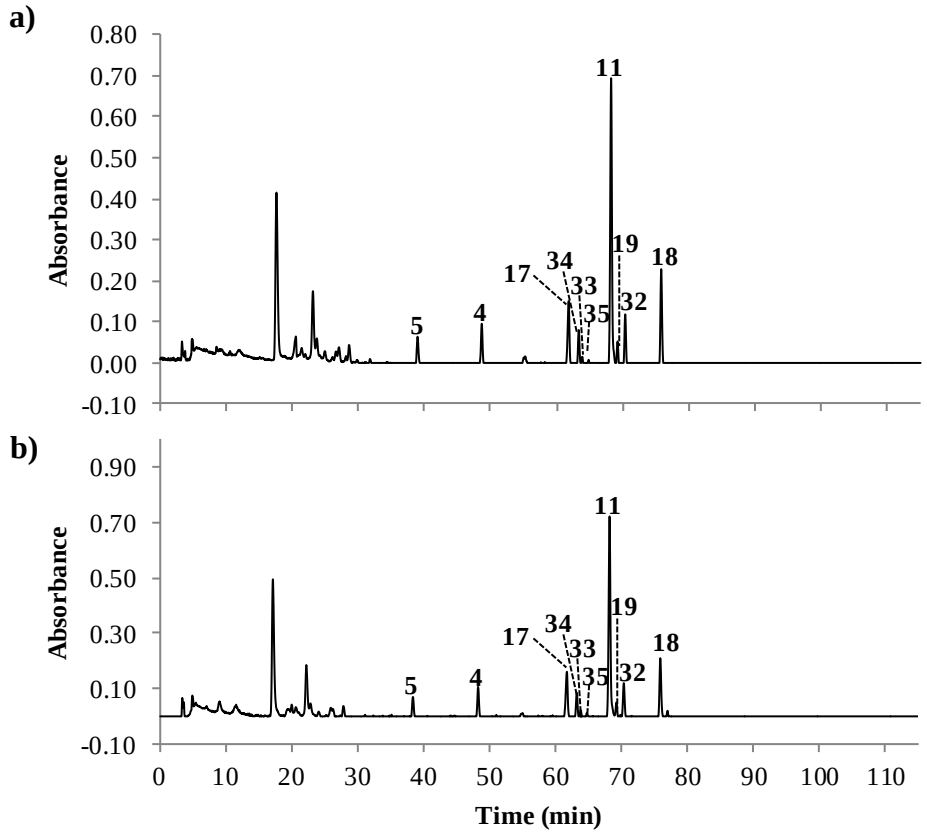

Figure 2.8. HPLC-PDA (350-800 nm) chromatogram of Loch Ness sediment extracted by (a) sonication and (b) ASE at 75°C. Both samples were dissolved in the same volume of acetone for analysis. Peak assignments are given in Scheme 2.1 and Table 2.5.

Table 2.5. Assignments and yields of the major chlorin pigments (mean ± 1 s.d.; *n* = 3) in Loch Ness sediment.

Assignments	**Main UV/vis $\lambda_{max.}$ (nm)**	**$[M+H]^+$ (*m/z*)[a]**	**Prominent Product ions in MS^n (*m/z*)**	**Esterifying alcohol**	**Yield (nmol g^{-1} of dried sediment)**						
					Sonication (ºC)	**ASE (ºC)**					
					20	50	60	65	70	75	80
Chlorophyll *a* (**4**)	432, 665	871	-	phytol	1.1 ± 0.1	1.1 ± 0.1	1.0 ± 0.1	1.3 ± 0.1	1.2 ± 0.01	1.2 ± 0.1	1.1 ± 0.1
Chlorophyll *b* (**5**)	467, 644	885	-	phytol	0.6 ± 0.03	0.5 ± 0.08	0.4 ± 0.03	0.7 ± 0.06	0.55 ± 0.04	0.6 ± 0.06	0.5 ± 0.01
Phaeophytin *a* (**11**)	408, 665	871	593, 533	phytol	6.9 ± 0.3	6.9 ± 0.5	6.7 ± 0.1	7.6 ± 0.4	6.6 ± 0.1	7.0 ± 0.3	6.9 ± 0.6
Phaeophytin *b* (**17**)	436, 647	885	-	phytol	1.1 ± 0.1	1.2 ± 0.1	1.1± 0.01	1.3 ± 0.1	1.1 ± 0.3	1.2 ± 0.1	1.1 ± 0.1
Pyrophaeophytin *a* (**18**)	410, 665	813	535, 507	phytol	2.2 ± 0.1	2.1 ± 0.2	2.2 ± 0.1	2.4 ± 0.2	1.9 ± 0.2	2.1 ± 0.1	2.2 ± 0.3
Pyrophaeophytin *b* (**19**)	437, 650	827	549	phytol	0.38 ± 0.08	0.40 ± 0.07	0.41 ± 0.03	0.48 ± 0.03	0.33 ± 0.08	0.36 ± 0.02	0.40 ± 0.08
Phaeophytin *a* epimer (**32**)	408, 665	871	593, 533	phytol	1.1 ± 0.2	1.2 ± 0.1	1.1 ± 0.1	1.3 ± 0.02	1.1 ± 0.2	1.1 ± 0.1	1.2 ± 0.1
Phaeophytin *b* epimer (**33**)	437, 645	885	-	phytol	0.15 ± 0.01	0.17 ± 0.03	0.15 ± 0.02	0.20 ± 0.02	0.14 ± 0.02	0.16 ± 0.03	0.14 ± 0.2
Hydroxyphaeophytin *a* (**34**)	408, 668	887	-	phytol	0.7 ± 0.1	0.8 ± 0.1	0.8 ± 0.04	0.8 ± 0.04	0.8 ± 0.03	0.8 ± 0.1	0.8 ± 0.1
Hydroxyphaeophytin *a* epimer (**35**)	407, 665	887	-	phytol	-	-	-	-	-	-	-
Total pigment yields (nmol g^{-1} of dried sediment)[b]					14.3 ± 0.7	14.2 ± 1.2	14.0 ± 0.1	16.0 ± 0.9	13.7 ± 0.7	14.5 ± 0.8	14.3 ± 1.5

[a] All metallated pigments appear in MS as their demetallated counterparts due to post column demetallation prior to MS (Airs and Keely, 2000).

[b] Sum of all components except OH-phe *a*' (**35**) which occurs at levels less than the signal to noise ratio (S/N = 3).

Table 2.6 Output from the Shapiro-Wilk test (test of normality at 95% confidence) for total pigment yields from Loch Ness sediment extracted by sonication and ASE at 50-80°C.

Extraction method	Test of Normality		
	Shapiro-Wilk		
	Statistic	df[a]	Sig. (*p*)[b]
Sonication	0.778	3	0.063
ASE 50°C	0.881	3	0.328
ASE 60°C	0.985	3	0.763
ASE 65°C	0.876	3	0.312
ASE 70°C	0.940	3	0.526
ASE 75°C	0.831	3	0.190
ASE 80°C	0.905	3	0.403

[a] df = degrees of freedom

[b] Data is normal distributed at *p*-values > 0.05.

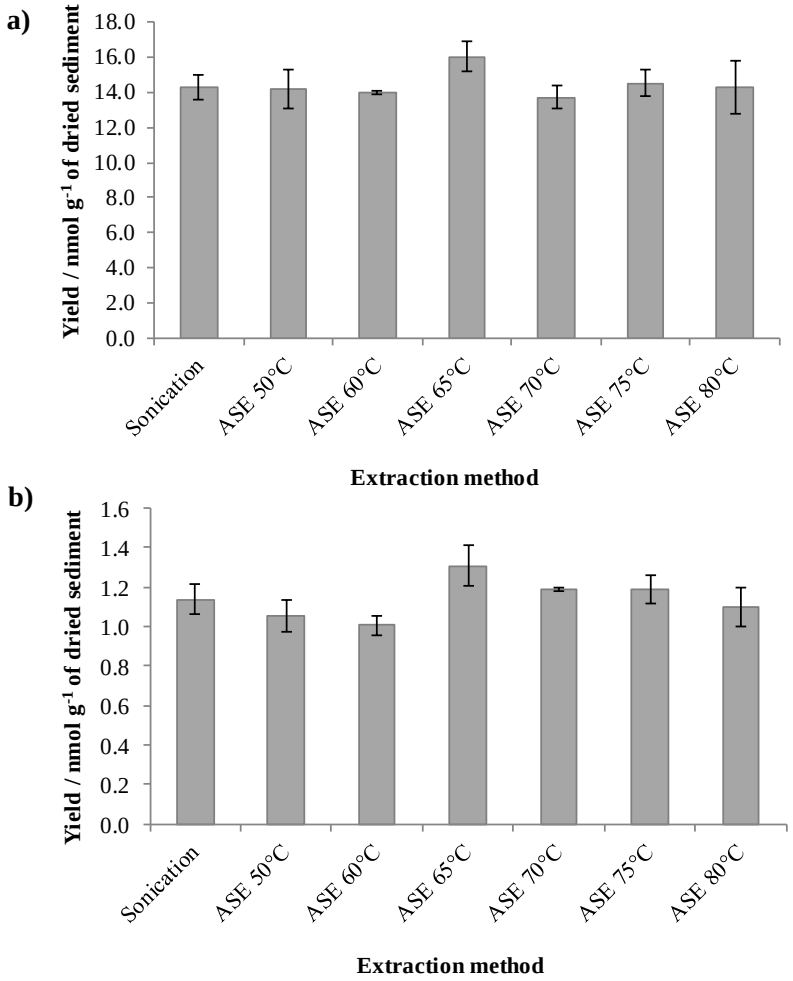

Figure 2.9. Histograms for Loch Ness sediment extraction showing (a) yield of total pigments and (b) yield of chlorophyll *a* (**4**) (error bars represent ± 1 standard deviation, $n = 3$).

2.2.4 Chiprana

Sediment from lake Chiprana, Spain, contains tetrahydroporphyrin (bacteriochlorophyll *a*-derived) pigments in addition to pigments of eukaryotic origin, allowing examination of the extraction efficiency and stability of these highly reactive tetrapyrroles. The frozen sediment was freeze-dried overnight and subsequently homogenized by grinding using a pestle and mortar (see Experimental, Chapter 6, Section 6.3.1.4) before sonic and ASE extraction. The pigment distributions from sonication at room temperature and ASE at temperatures of 50, 60, 65, 70, 75, 80, 85 and 90°C were broadly similar, e.g. Fig. 2.10. Phaeophytin *a* (**11**) and bacteriophaeophytin *a* (**29**, Scheme 2.2) are the dominant tetrapyrroles (Fig. 2.10) with chlorophyll *a* (**4**) and pyrophaeophytin *a* (**18**) also being present in high relative abundance. Total pigment yields were taken as the sum of these four major chlorins (Fig. 2.11 and Table 2.7). The replicates of total pigment yields from Chiprana sediment extracted by sonication and ASE at temperatures from 50 to 90°C were normally distributed (Shapiro-Wilk, $p > 0.05$, Table 2.8), but the homogeneity of variances was significantly different (Levene statistic test, $F(8, 18) = 2.651$, $p = 0.041$). As a result, the Kruskal-Wallis test was applied. Comparison of the total pigment yields for the Chiprana sediments extracted by sonication and by ASE shows no significant difference between the two methods (Kruskal-Wallis: $H(8) = 8.265$, $p = 0.408$). Extracts from both techniques gave similar proportion of chlorophyll *a* (**4**) and phaeophytin *a* (**11**) (Fig. 2.11b) indicating that demetallation of chlorophyll did not occur. The slightly lower amount of chlorophyll *a* extracted by ASE at the lower temperatures reflects lower extraction efficiency rather than loss *via* alteration to phaeophytin *a* (**11**) because the relative abundance of phaeophytin *a* (**11**) was the same as that obtained by sonication (Fig. 2.11b).

Bacteriophaeophytin *a* (**29**) is more sensitive to alteration than chlorins due to the susceptibility of the C7-C8 bond to oxidation with formation of a double bond *via* dehydrogenation (Wilson et al., 2004; Keely, 2006). The oxidation product (**36**) was not formed during extraction. The replicates of yield of bacteriophaeophytin *a* (**29**) from Chiprana sediment extracted by sonication and ASE at temperatures from 50 to 90°C were normally distributed (Shapiro-Wilk, $p > 0.05$, Table 2.9), but the homogeneity of variances was significantly difference (Levene statistic test, $F(8, 18)$

= 2.618 , p = 0.043). As a result, the Kruskal-Wallis test was applied and the yield of bacteriophaeophytin *a* (**29**) was not significantly different between sonication and ASE at temperature from 50-90°C (Kruskal-Wallis: $H(8)$ = 10.508, p = 0.231). In addition, loss of the carbomethoxy at the $C13^2$ position of bacteriophaeophytin *a* (**29**) to form pyrobacteriophaeophytin *a* (**31**) did not occur over the temperature range examined. To validate this point, sediment from lake Estanya, Spain, which also contains chlorins and bacteriochlorophyll-derived compounds including pyrobacteriophaeophytin *a* (**31**), was examined.

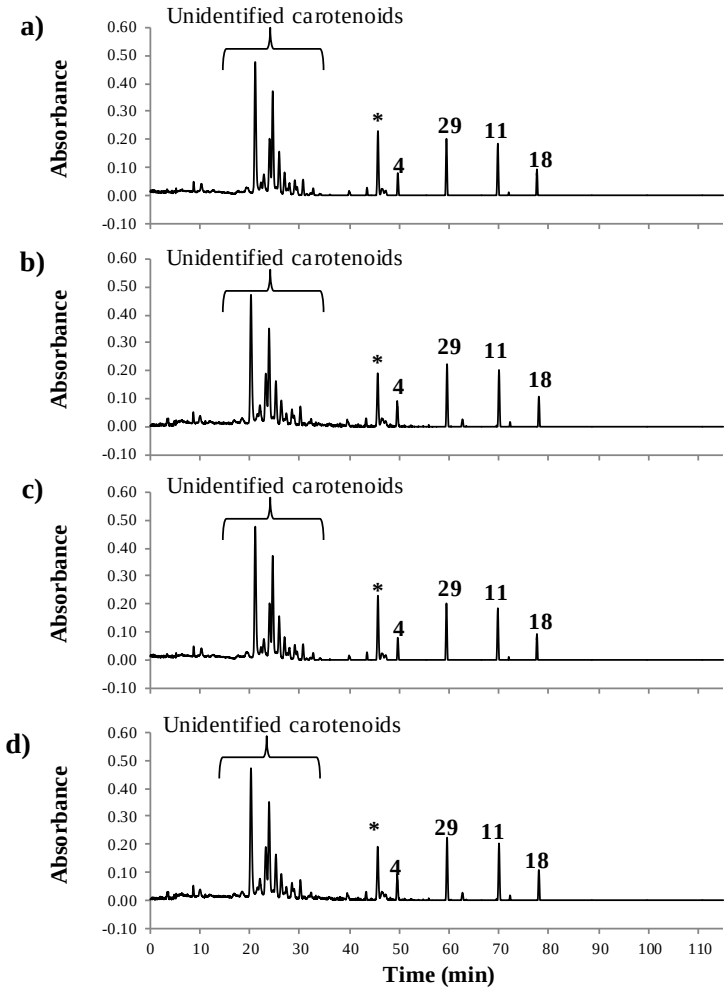

Figure 2.10. HPLC-PDA (350-800 nm) chromatogram of Chiprana sediment extracted by (a) sonication and (b) ASE at 50°C, (C) ASE at 75°C and (d) ASE at 90°C. All samples were dissolved in the same volume of acetone for analysis. Peak assignments of the major chlorins are given in Scheme 2.1, 2.2 and Table 2.7. *Not chlorins.

Table 2.7. Assignments and yields of the major chlorin pigments (mean ± 1 s.d.; *n* = 3) in Chiprana sediment.

Assignments	**Main UV/vis $\lambda_{max.}$ (nm)**	**$[M+H]^+$ (*m/z*)[a]**	**Prominent Product ions in MS^n (*m/z*)**	**Esterifying alcohol**	**Yield (nmol g^{-1} of dried sediment)**								
					Sonication (ºC)	**ASE (ºC)**							
					20	50	60	65	70	75	80	85	90
chl *a* (**4**)	431, 666	871	-	phytol	19.1 ± 1.4	16.1 ± 1.2	18.2 ± 0.6	20.5 ± 0.3	19.7 ± 0.9	21.4 ± 3.1	15.5 ± 2.1	19.5 ± 1.8	19.6 ± 0.4
phe *a* (**11**)	408, 665	871	593, 533	phytol	36.4 ± 3.2	35.4 ± 3.1	33.1 ± 2.2	34.2 ± 7.7	37.7 ± 5.5	38.2 ± 1.7	27.4 ± 6.2	33.4 ± 4.1	33.8 ± 2.1
pphe *a* (**18**)	410, 665	813	535, 507	phytol	20.0 ± 2.6	17.0 ± 3.4	17.6 ± 2.7	18.7 ± 5.9	21.0 ± 3.5	20.1 ± 0.4	15.4 ± 3.1	18.3 ± 3.2	18.4 ± 2.9
bphe *a* (**29**)	357, 527, 746	889	611	phytol	34.2 ± 5.2	35.4 ± 0.8	36.6 ± 2.1	39.9 ± 4.1	39.7 ± 5.1	39.4 ± 1.3	32.5 ± 4.8	36.0 ± 3.4	39.1 ± 2.4
	Total pigment yields (nmol $g^{-1}$of dried sediment)				109.8 ± 12.0	103.9 ± 4.3	105.6 ± 5.8	113.3 ± 17.1	118.1 ± 14.9	119.1± 3.1	90.9 ± 15.2	107.2 ± 10.6	110.8 ± 7.6

[a] All metallated pigments appear in MS as their demetallated counterparts due to post column demetallation prior to MS (Airs and Keely, 2000).

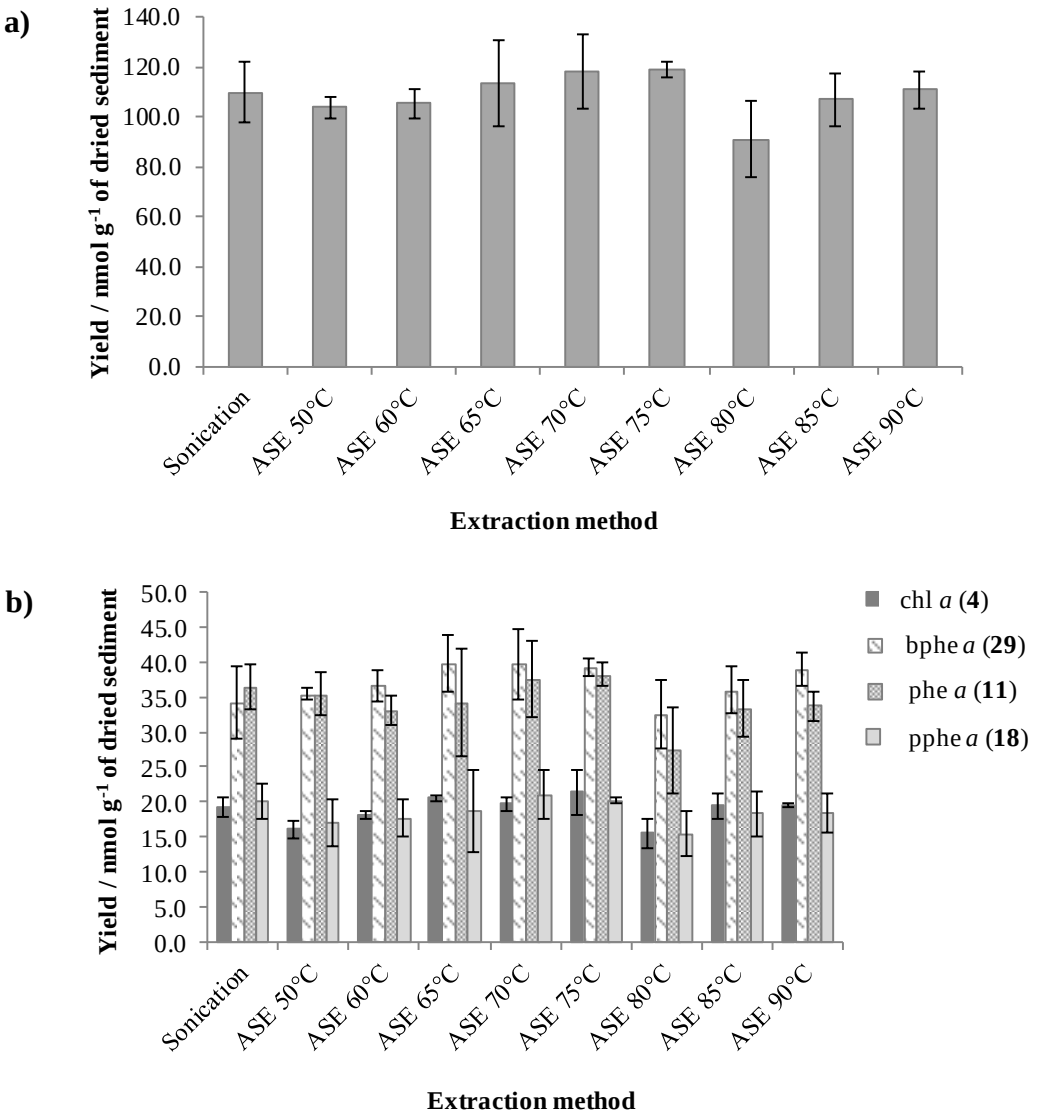

Figure 2.11. Histograms for Chiprana sediment extraction showing (a) yield of total pigments and (b) yield of chlorophyll *a* (**4**), bacteriophaeophytin *a* (**29**), phaeophytin *a* (**11**) and pyrophaeophytin *a* (**18**) (error bars represent ± 1 standard deviation, *n* = 3).

Table 2.8 Output from the Shapiro-Wilk test (test of normality at 95% confidence) for total pigment yields from Chiprana sediment extracted by sonication and ASE at 50-90°C.

Extraction method	Test of Normality		
	Shapiro-Wilk		
	Statistic	df[a]	Sig. (*p*)[b]
Sonication	0.960	3	0.613
ASE 50°C	0.984	3	0.761
ASE 60°C	0.859	3	0.264
ASE 65°C	0.776	3	0.058
ASE 70°C	0.837	3	0.205
ASE 75°C	0.994	3	0.849
ASE 80°C	0.920	3	0.452
ASE 85°C	0.874	3	0.307
ASE 90°C	0.774	3	0.054

[a] df = degrees of freedom

[b] Data is normal distributed at *p*-values > 0.05.

Table 2.9 Output from the Shapiro-Wilk test (test of normality at 95% confidence) for yields of bacteriophaeophytin *a* (**29**) from Chiprana sediment extracted by sonication and ASE at 50-90°C.

Extraction method	Test of Normality		
	Shapiro-Wilk		
	Statistic	df[a]	Sig. (*p*)[b]
Sonication	0.829	3	0.187
ASE 50°C	0.970	3	0.668
ASE 60°C	0.960	3	0.617
ASE 65°C	0.934	3	0.504
ASE 70°C	0.815	3	0.150
ASE 75°C	0.874	3	0.306
ASE 80°C	0.876	3	0.314
ASE 85°C	0.973	3	0.682
ASE 90°C	0.944	3	0.542

[a] df = degrees of freedom

[b] Data is normal distributed at *p*-values > 0.05.

2.2.5 Estanya

Sediment from Estanya (Spain), collected by Professor Brendan J. Keely in 1996, was prepared by freeze-drying, grinding and sieving before extraction (see Experimental, Chapter 6, Section 6.3.1.5). The Estanya extracts from sonication at room temperature and ASE over the range 50-90°C show broadly similar pigment distributions in which bacteriophaeophytin *a* (**29**) dominates (Fig. 2.12, identifications given in Table 2.10). The HPLC chromatogram from sonication (Fig. 2.12a) was essentially identical to the HPLC chromatogram from ASE at 75°C (Fig. 2.12c). The total pigment yields (Fig. 2.13 and Table 2.10) were calculated from the sum of the major chlorins labelled in Fig. 2.12. The replicates of total pigment yields from sonication and ASE between 50 and 90°C showed normal distributions (Shapiro-Wilk, $p > 0.05$, Table 2.11) and the entire data set showed homogeneity of variances (Levene statistic test, $F(8, 18) = 2.134$, $p = 0.087$). Thus, a one-way ANOVA test was applied and revealed a significant difference (one-way ANOVA, $F(8, 18) = 7.886$, $p = 0.000$). A post-hoc least significant difference (LSD) test revealed that the total yields from sonication (101.4 ± 7.1 nmol g^{-1} of dried sediment, Fig. 2.13 and Table 2.10) were not significantly different ASE at 50°C (112.3 ± 13.3 nmol g^{-1} of dried sediment, $p = 0.070$), but it was lower significantly different than ASE from 60°C (126.5 ± 5.0 nmol g^{-1} of dried sediment, $p = 0.000$) to 90°C (129.8 ± 2.1 nmol g^{-1} of dried sediment, $p = 0.000$). In addition, the greatest yield extracted by ASE at 80°C (136.5 ± 2.8 nmol g^{-1} of dried sediment) was not significantly different from ASE at temperatures 70, 75, 85 and 90°C (Fig. 2.13 and Table 2.12). As a result, the maximum total pigment yield of extraction from Estanya sediment lies within ASE temperatures from 70 up to 90°C.

The high degree of reproducibility in the extractions, as shown by the narrow standard deviations (Fig. 2.13 and Table 2.10), can be attributed both to the high pigment content of the sediment and to the homogeneity of the sediment sample as a result of it being sieved prior to extraction. Extraction at 75-80°C does not adversely affect either of the tetrahydroporphyrin components, bacteriophaeophytin *a* (**29**) and pyrobacteriophaeophytin *a* (**31**) (Table 2.10). Sonication gave the lowest bacteriophaeophytin *a* (**29**) yield (43.9 ± 2.9 nmol g^{-1} of dried sediment, Table 2.10)

indicating that ASE is a better extraction method with respect to bacteriophaeophytin *a* (**29**). In terms of chlorophyll *a* (**4**) yield, ASE at 75-80°C gave the highest yields around 8 nmol g^{-1} of dried sediment, while sonication gave around 5 nmol g^{-1} of dried sediment. The lower yield of chlorophyll *a* from sonication appears mainly to be due to extraction efficiency, rather than demetallation of Mg, as the yield of phaeophytin *a* (**11**) (26.1 ± 1.7 nmol g^{-1} of dried sediment) was lower than that for ASE at 75 (32.9 ± 0.3 nmol g^{-1} of dried sediment) and 80°C (32.1 ± 2.3 nmol g^{-1} of dried sediment, Table 2.10). Accordingly, the optimal extraction conditions for the Estanya sediment are ASE at 75 or 80°C.

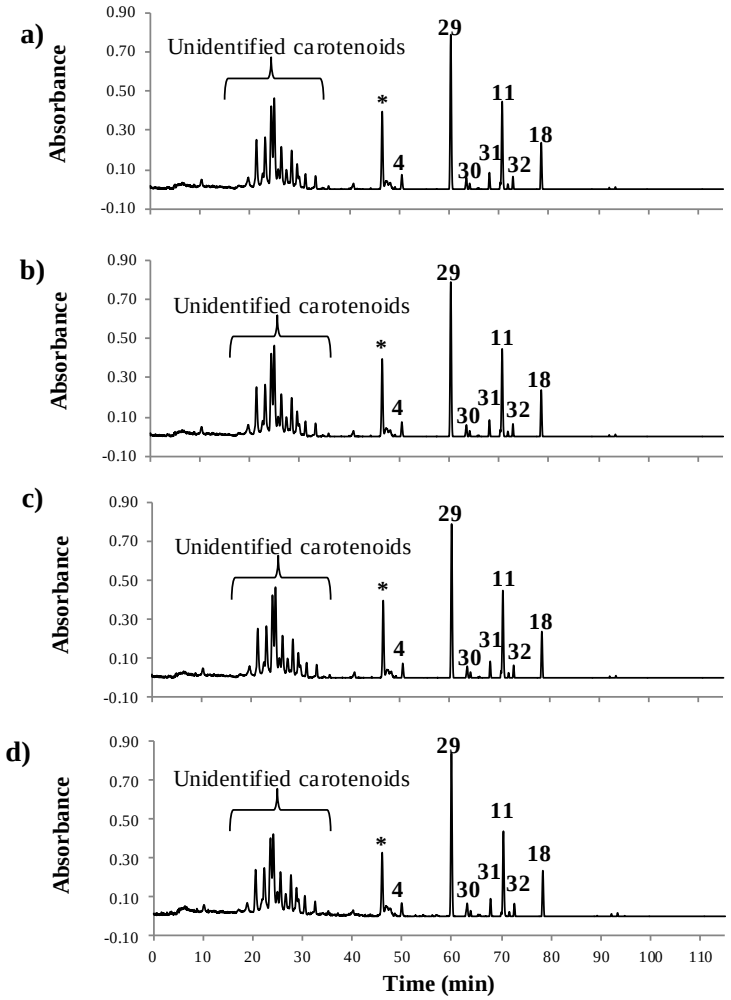

Figure 2.12. HPLC-PDA (350-800 nm) chromatogram of Estanya sediment extracted by (a) sonication and (b) ASE at 50°C, (C) ASE at 75°C and (d) ASE at 90°C. All samples were dissolved in the same volume of acetone for analysis. Peak assignments of the major chlorins are given in Scheme 2.1, 2.2 and Table 2.10. *Not pigment.

Table 2.10. Assignments and yields of the major chlorin pigments (mean ± 1 s.d.; *n* = 3) in Estanya sediment.

Assignments	**Main UV/vis $\lambda_{max.}$ (nm)**	**$[M+H]^+$ (*m/z*)[a]**	**Prominent Product ions in MS^n (*m/z*)**	**Esterifying alcohol**	**Yield (nmol g^{-1} of dried sediment)**								
					Sonication (ºC)	**ASE (ºC)**							
					20	50	60	65	70	75	80	85	90
chl *a* (**4**)	431, 666	871	-	phytol	5.0 ± 0.3	6.8 ± 1.3	7.0 ± 1.6	6.9 ± 1.3	6.0 ± 1.1	8.4 ± 0.1	8.1 ± 0.4	6.0 ± 0.7	6.5 ± 0.5
phe *a* (**11**)	408, 665	871	593, 533	phytol	26.1 ± 1.7	29.4 ± 4.5	32.4 ± 1.7	28.5 ± 5.9	31.0 ± 0.8	32.9 ± 0.3	32.1 ± 2.3	30.8 ± 2.0	30.5 ± 1.0
phe *a'* (**32**)	408, 665	871	593, 533	phytol	3.3 ± 1.4	3.5 ± 1.5	5.0 ± 1.0	3.5 ± 3.0	3.6 ± 0.7	5.5 ± 0.1	5.5 ± 0.5	4.5 ± 0.4	4.6 ± 0.5
pphe *a* (**18**)	410, 665	813	535, 507	phytol	13.2 ± 1.8	13.8 ± 2.7	15.9 ± 1.3	13.2 ± 4.2	14.8 ± 1.2	17.3 ± 0.2	17.6 ± 0.3	15.7 ± 0.5	16.3 ± 0.4
bphe *a* (**29**)	357, 527, 746	889	611	phytol	43.9 ± 2.9	50.4 ± 1.3	54.8 ± 0.4	56.2 ± 6.9	57.9 ± 2.0	59.0 ± 1.5	60.1 ± 1.4	58.0 ± 1.5	59.5 ± 0.7
bphe *a'* (**30**)	357, 528, 747	889	611	phytol	5.4 ± 1.1	3.4 ± 1.7	5.6 ± 0.4	4.8 ± 1.3	5.9 ± 1.1	5.5 ± 0.1	6.3 ± 0.5	6.2 ± 1.2	6,1 ± 0.2
pbphe *a* (**29**)	357, 529, 747	831	552, 523	phytol	4.5 ± 0.6	4.9 ± 1.4	5.9 ± 0.2	5.5 ± 1.1	5.9 ± 0.6	6.5 ± 0.3	6.7 ± 0.5	6.1 ± 0.7	6.3 ± 0.1
	Total pigment yields (nmol g^{-1} of dried sediment)				101.4 ± 7.1	112.3 ± 13.3	126.5 ± 5.0	118.5 ± 10.6	125.1 ± 4.3	135.1 ± 1.7	136.5 ± 2.8	127.3 ± 5.8	129.8 ± 2.1

[a] All metallated pigments appear in MS as their demetallated counterparts due to post column demetallation prior to MS (Airs and Keely, 2000).

Table 2.11. Output from the Shapiro-Wilk test (test of normality at 95% confidence) for total pigment yields from Estanya sediment extracted by sonication and ASE at 50-90°C.

Extraction method	Test of Normality		
	Shapiro-Wilk		
	Statistic	df[a]	Sig. (*p*)[b]
Sonication	0.972	3	0.678
ASE 50°C	0.985	3	0.766
ASE 60°C	0.937	3	0.516
ASE 65°C	0.958	3	0.604
ASE 70°C	0.980	3	0.729
ASE 75°C	0.926	3	0.474
ASE 80°C	0.990	3	0.808
ASE 85°C	0.997	3	0.904
ASE 90°C	0.792	3	0.096

[a] df = degrees of freedom

[b] Data is normal distributed at *p*-values > 0.05.

Table 2.12. Output from one-way ANOVA post hoc least significant difference test for total pigment yields from Estanya sediment extracted by ASE at 80°C compared to sonication and ASE at 50-90°C.

Method	Mean of total yield (n = 3) (nmol g^{-1} of dried sediment)	s.d.[a]	Mean Difference (I-J)	Std. Error[b]	Sig.
ASE 80°C (I)	136.5499	2.78417	-	-	-
Sonication (J)	101.3843	7.11109	35.16567*	5.65801	0.000
ASE 50°C (J)	112.2782	13.29696	24.27170*	5.65801	0.000
ASE 60°C (J)	126.5249	4.99521	10.02500	5.65801	0.093
ASE 65°C (J)	118.5462	10.59037	18.00370*	5.65801	0.005
ASE 70°C (J)	125.1023	4.34890	11.44767	5.65801	0.058
ASE 75°C (J)	135.0952	1.73211	1.45477	5.65801	0.800
ASE 85°C (J)	127.3234	5.78519	9.22657	5.65801	0.120
ASE 90°C (J)	129.7725	2.13499	6.77747	5.65801	0.247

*The mean difference is significant at the level 0.05 (95% confidence).

[a] Standard deviation was obtained from mean of total yields (n = 3).

[b] Std. Error was obtained from post hoc least significant difference test.

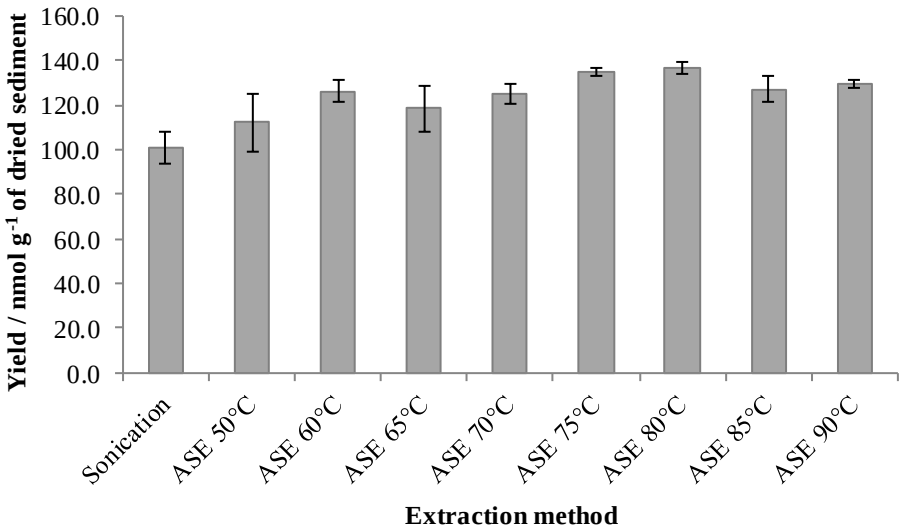

Figure 2.13. Total pigment yields extracted from Estanya sediment by sonication and ASE at a range of temperatures (error bars represent ± 1 standard deviation, n = 3).

2.2.6 *Allochromatium vinosum* bacterium cell paste

Frozen *Allochromatium vinosum* bacterium cell paste (supplied by Sigma Aldrich in 1984, strain not declared) was thawed, homogenised and divided into 2 g portions (see Experimental, Chapter 6, Section 6.3.1.6). Prepared *Allochromatium vinosum* bacterium cell paste was extracted by sonication at room temperature (20°C) and ASE at 50, 65, 70, 75 and 80°C. Three replicates were performed per extraction method before analysis by HPLC using Airs Method A (Airs et al., 2001a) to examine the stability/alteration of bacteriochlorophyll *a* (**6**), which was absent from the sediments examined but, like chlorophyll *a* (**4**), is susceptible to demetallation to form bacteriophaeophytin *a* (**29**). Sonication and ASE at 50 to 70°C gave similar distributions dominated by bacteriochlorophyll *a* (**6**; Fig. 2.14a, b). Although the ratio of **6**:**29** from sonication (Fig. 2.14a) is similar to that for ASE at 70°C (Fig. 2.6b), poor repeatability from sonication is evident from the greater error (Fig. 2.15). The yields of bacteriochlorophyll *a* (**6**) and bacteriophaeophytin *a* (**29**) increased with ASE temperature up to 70°C, with maxima at 3.2 and 1.3 µmol g^{-1} of dried cell paste, respectively. The yields are very similar to those from sonication (3.2 and 1.2 µmol g^{-1} of dried cell paste, respectively; Fig. 2.15). At temperatures ≥ 75°C, alteration of bacteriochlorophyll *a* (**6**) led to an increase in the relative abundance of

bacteriophaeophytin *a* (**29;** Fig. 2.14c). In addition, the diastereomer of bacteriophaeophytin *a* (**30**) is apparent in the extract from ASE at 75°C (Fig. 2.14c), being formed during extraction. As a result, 70°C is the optimal ASE temperature for extraction of bacteriochlorophyll *a* (**6**).

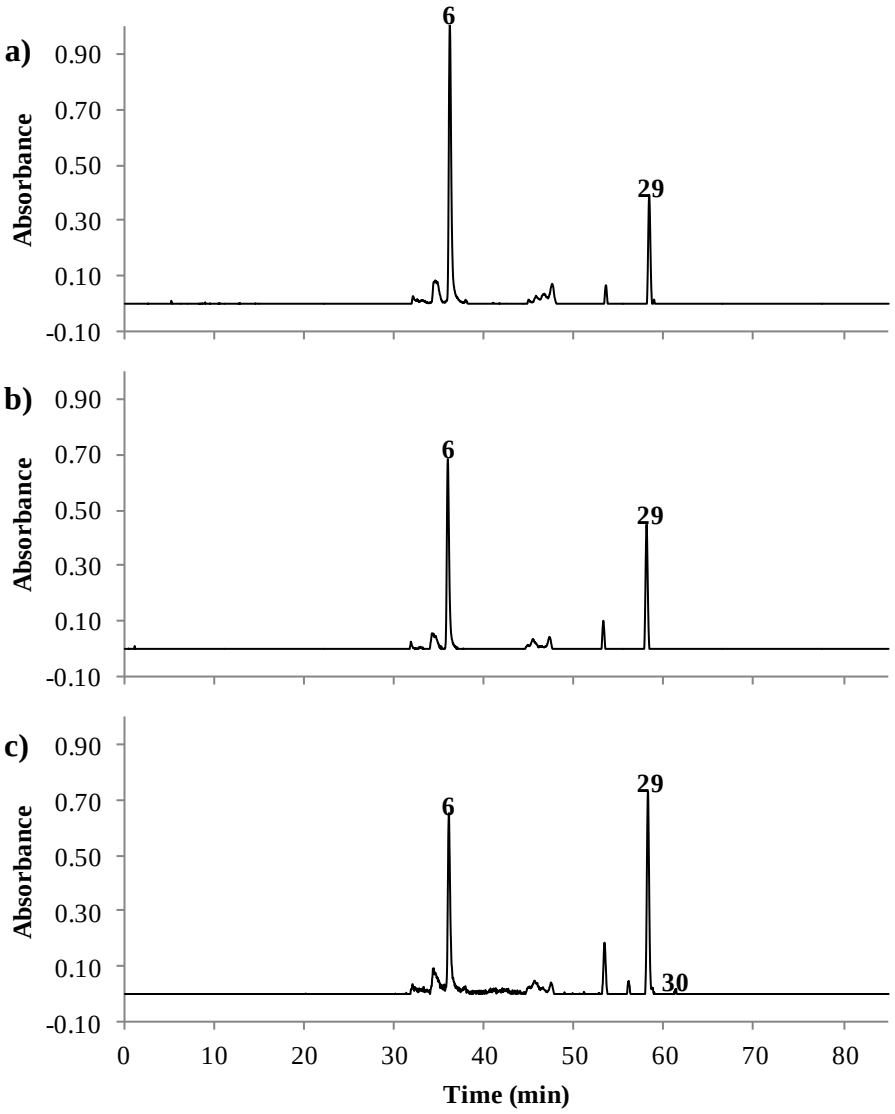

Figure 2.14. HPLC-PDA (350-800 nm) chromatograms of *Allochromatium vinosum* extracted by (a) sonication and (b) ASE at 70°C and c) ASE at 75°C. All samples were dissolved in the same volume of acetone. Peak assignments are given in Scheme 2.2.

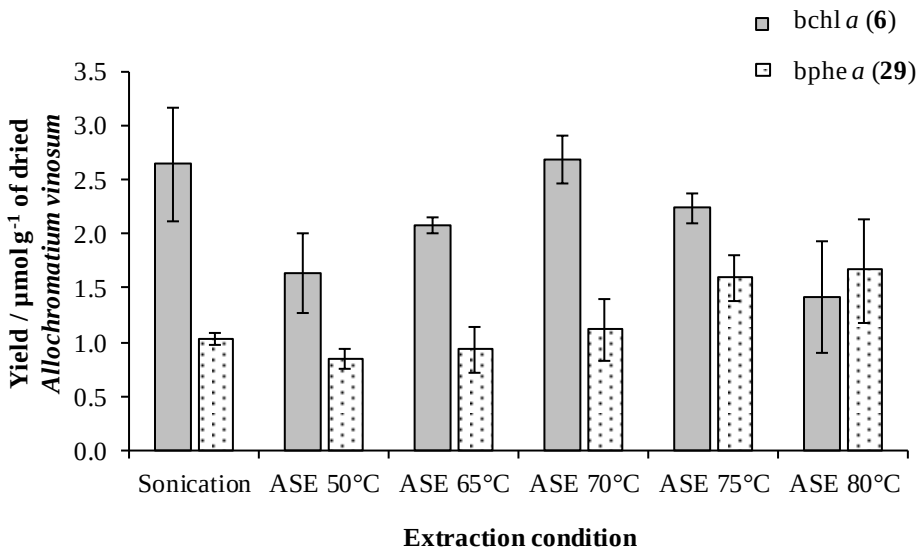

Figure 2.15. Yields of bacteriochlorophyll *a* (**6**) and bacteriophaeophytin *a* (**29**) for *Allochromatium vinosum* extraction, n = 3 (error bars represent ± 1 standard deviation).

2.3 Conclusions

A method for ASE of chlorin pigments from sediments and bacterial cell material has been developed. Sensitive pigments representative of oxygenic primary producers (chlorophylls and their derivatives) and anoxygenic primary producers (bacteriochlorophyll *a* and derivatives) were extracted efficiently and without alteration of bacteriophaeophytin *a* (**29**) to form bacterioviridin (**36**). The study confirms the suitability of freeze-drying in the preparation of sediments for extraction of pigments (McClymont et al., 2007) and illustrates the importance of homogenisation (by grinding and sieving) for achieving high repeatability in yields. Spiking the sediment with target analytes, an approach that is used to test extraction efficacy in a wide range of applications, including many outside geochemistry, gave poor repeatability for chlorophyll *a* (**4**) and chlorophyll *b* (**5**) as a result of their alteration via demetallation. The alteration of the spiked components under conditions in which their sedimentary counterparts are stable indicates that caution should be exercised when assuming identical behaviour for components that are integrated with a matrix and those that are introduced during laboratory manipulation. Temperatures of 75°C and above caused alteration of some of the

pigments and temperatures below 60°C resulted in a reduction in pigment yields and repeatability. Thus, we recommend the use of ASE with acetone at 70°C to provide a rapid, high throughput alternative to sonication for the extraction of chlorophyll pigments from sediments.

Chapter 3

Development of UHPLC methods for separation of photosynthetic pigments

3.1 Introduction

Photosynthetic pigments and their degradation products are important environmental biomarkers in water-columns (Repeta et al., 1989; Villanueva et al., 1994b) and sediments (Reuss et al., 2005; Szymczak-Zyla et al., 2011). The presence and distribution of these compounds is influenced by environmental conditions at the time of deposition. For example, the abundance of chlorins, has been used to estimate primary productivity (Harris et al., 1996). The pigment distributions from Kirisjes Pond in the Larsemann Hills, eastern Antarctica, contain pigments from both eukaryotic and prokaryotic photoautotrophs, revealing a stratified photic zone with the development of a community of anoxygenic primary producers at c. 6285-6525 corr. Yrs BP (Squier et al., 2002). Generally, analysis of photosynthetic pigments and derivatives involves solvent extraction followed by chromatographic separation and detection (Hodgson et al., 1998; Shankle et al., 2002; Yacobi et al., 1991). Various high performance liquid chromatographic methods exist for the analysis of chlorophyll pigments, variously utilising normal-phase, reversed-phase and ion-pair column chemistries (Roy, 1987). These methods have been applied in the analysis of chlorophyll pigments from a diverse range of sources including plants, phyto- and bacterio-plankton, sediments and natural water bodies (Braumann and Grimme, 1981; Daemen, 1986; Eskins et al., 1977; Falkowski and Sucher, 1981; Mantoura and Llewellyn, 1983; Wright et al., 1991; Zapata et al., 1987). Typically, pigment identifications are based on analysis of their retention times and online UV/Vis spectra (Roy, 1987). While methods exist for the separation of simple pigment distributions in plant extracts in analysis times of as little as 21 min (Huang et al., 2008; Kao et al., 2011) they are not adequate for separation of the complex distributions typically encountered in sediments and cultures of certain phototrophic prokaryotes. Advances in mass spectrometry and its coupling to HPLC have led to its increased use for pigment identification in such studies (Harris et al., 1995; Keely and Maxwell, 1990). Airs et al. published a method (Method A) capable of analysing complex pigment mixtures extracted from sediments and cells harvested from cultures (Airs et al., 2001a). The method is based on reversed-phase high performance liquid chromatography (RP-HPLC) on C_{18} columns and was developed to enable liquid chromatography mass spectrometry (LC-MS) with automated acquisition of tandem mass spectra of pigments (Airs et al., 2001a). Although

Method A is capable of resolving highly complex distributions, for example chlorophyll *a* (**4**), and bacteriochlorophylls *a* (**6**), *c* (**8**), *d* (**9**), and their derivatives in a microbial mat extract, (Airs and Keely, 2003) the method is lengthy (115 min). Furthermore, solvent consumption is appreciable, making its routine use in high resolution sample profiling somewhat impractical.

Recently, advances in stationary phase manufacturing coupled with improvements in pump technology, specifically the capabilities to work with high back-pressure, enabled the realisation of ultra-high performance liquid chromatography (UHPLC) utilising stationary phases with small particle dimensions (Nguyen et al., 2006; Swartz, 2005). The van Deemter equation (van Deemter et al., 1956) reveals that stationary phase particle sizes of less than 2.5 μm offer significant gains in efficiency that are relatively insensitive to small changes in flow rate or linear velocity (Leandro et al., 2006; Swartz, 2005) . Thus, UHPLC offers advantages of decreased analysis times and solvent consumption; for example, a study of pesticides in baby food (Leandro et al., 2006) demonstrated separations that were 2.5 times faster than by HPLC. Although UHPLC methods have been developed for applications in many fields, such as food (Leandro et al., 2006) and pharmaceutical analysis, (Nováková et al., 2006) no methods have been reported for the analysis of complex mixtures of sedimentary pigments.

The aim of this work was to develop a UHPLC method for the separation of complex distributions of photosynthetic pigments by adapting the Method A (Airs et al., 2001a) to utilize columns with a smaller particle size.

3.2 Results and discussion

3.2.1 Method transfer from HPLC to UHPLC

The HPLC Method A (Airs et al., 2001a) was the starting point for the development of a UHPLC method for the separation of complex mixtures of photosynthetic pigments in environmental samples. The method employs two Waters Spherisorb ODS2 3 µm cartridge columns (150 mm × 4.6 mm i.d.) coupled in series. This octadecylsilyl stationary phase gives good peak shape and resolution across a broad range in of pigment polarity. Two Acclaim® RSLC 120 C_{18} (Dionex Corporation, USA) were selected for the UHPLC separation, the smaller particle size (2.2 µm), length and column diameter (100 mm × 2.1 mm i.d.) being designed for such separations. The HPLC method parameters were recalculated for UHPLC using a Method Speed-up Calculator Programme (Version 1.14i, Dionex Corporation, USA). The algorithm utilises fundamental chromatographic equations to calculate the theoretical equivalent injection volume, flow rate and solvent gradient for UHPLC based on the template HPLC method and the characteristics of the new column. It targets sufficient resolution in the shortest possible time (Dionex, 2009) The calculator also utilises a boost factor (B.F.), a multiplier applied to a pre-determined flow rate, in order to explore the compromise between the speed of the analysis and resolution.

A sediment extract from Priest Pot, used previously in the development of the HPLC separation Method A (Airs et al., 2001a) contains chlorin pigments that elute throughout the entire analytical run (Fig. 3.1a). Polar regions (I and II, Fig. 3.1a) and apolar regions (III and IV, Fig. 3.1a) of the chromatogram both exhibit areas of limiting resolution. Accordingly, the Method Speed-up Calculator was used without utilising the resolution factor setting; a single region of limiting resolution could not be selected. The resultant chromatogram obtained by UHPLC shows a broadly similar distribution to the HPLC method but with the retention time of each analyte being substantially reduced (UHPLC BF = 1, Table 3.1, Fig. 3.1b). Overall, resolution is similar, though the UHPLC method resolves polar components (e.g. labelled peaks in regions I and II, Fig. 3.1b) slightly better than Method A (Fig. 3.1a) and apolar compounds in region III slightly less well, e.g. the absence of a

pyrophaeophytin *a* (**18**) peak in Fig. 3.1b. Analysis time (56.2 min) and flow rate (0.2 mL min^{-1}) are much lower than for Method A (Airs et al., 2001a) and the injection volume decreased from 20 to 3 µL. Although the response for the different injection volumes cannot be compared directly, the concentrations of the samples analysed by HPLC and UHPLC being slightly different, it is evident that the response and signal-to-noise (S/N) for the two analyses are similar (Fig. 3.1a and b). Thus, the UHPLC method offers a significant advantage by way of a >6-fold reduction in the sample size required for analysis. The back-pressure (200 bar, Table 3.1) is relatively low for UHPLC, indicating a capacity to further speed up the method using the BF. Different BFs do not change the proportions of the mobile phase components, rather they alter the time of the inflection points in the gradient. Values of 1.5 and 2 for the BF gave total analysis times of 37.5 and 28.1 min, respectively (Table 3.1 and Fig. 3.1c). Increasing the BF did not affect chromatographic performance: peak distributions and resolution were comparable with those for BF = 1 (Fig. 3.1b). Although with BF = 2 the back-pressure was higher (450 bar, Table 3.1), it is not close to the limit of the instrument (800 bar). Hence, the method has capacity for further development.

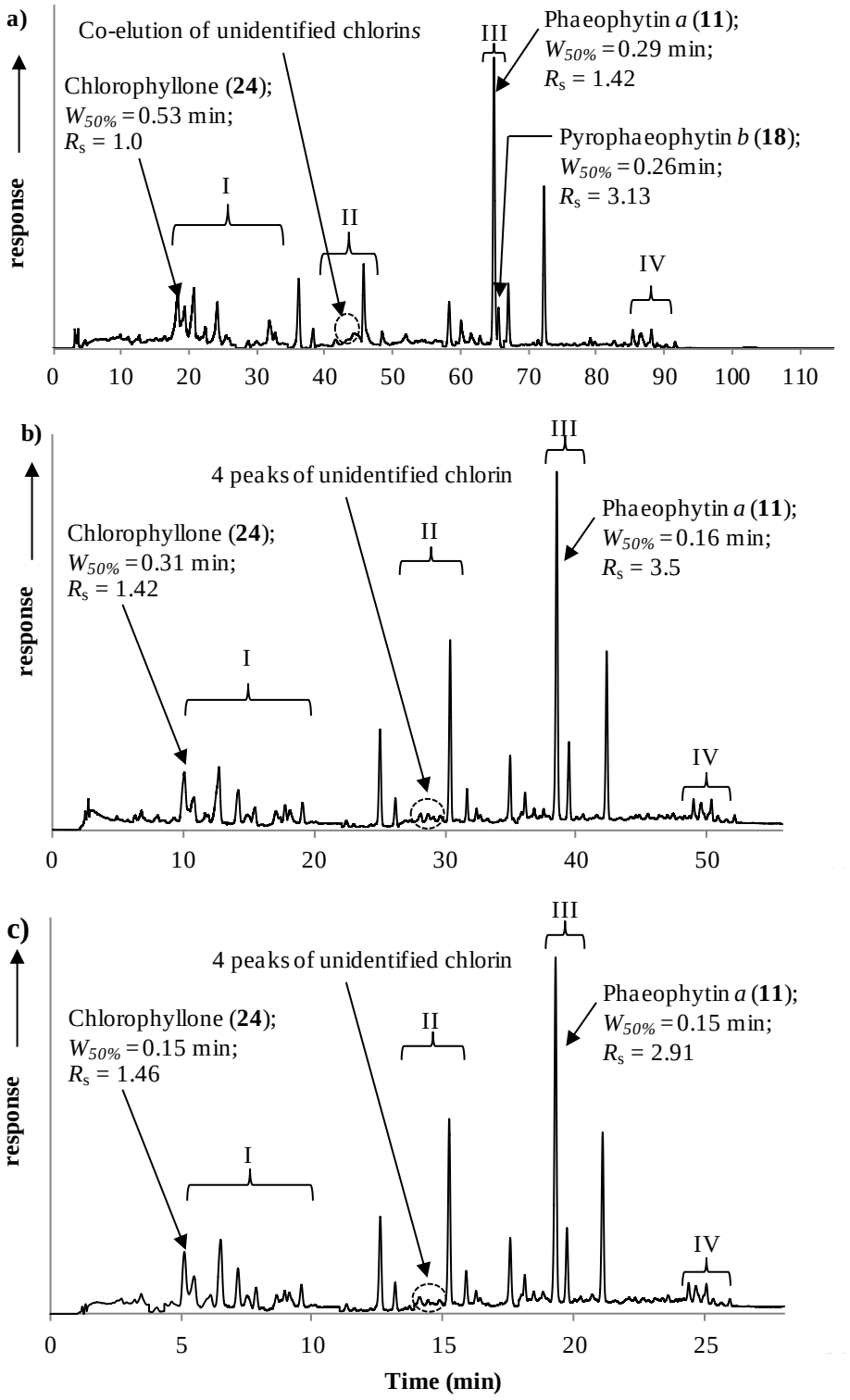

Figure 3.1. LC-PDA (300-800 nm) chromatogram of the sediment extract from Priest Pot obtained using: (a) Method A (Airs et al., 2001a), (b) UHPLC method 1A and (c) UHPLC method 1C (Table 3.1). Injection volumes for the HPLC and UHPLC methods were 20 and 3 µL, respectively.

Table 3.1. Mobile phase gradient programmes of HPLC Airs Method A and UHPLC Method from Dionex Method Speed-up Calculator.

Method	Time (min)			Methanol (%)	Ethyl acetate (%)	Ammonium acetate (0.01 *M*) (%)	Acetonitrile (%)	Injection volume (µL)	Pressure [d] (bar)		
	A	B	C						A	B	C
Airs Method [a]	0			80	0	5	15	20	≈118		
	5			80	0	5	15				
	100			20	65	0	15				
	105			1	98	0	1				
	110			1	98	0	1				
	115			80	0	5	15				
UHPLC Method 1[b]	(B.F. = 1)	(B.F.= 1.5)	(B.F.= 2) (L = 200 mm)					3	≈200	≈350	≈450
	0	0	0	80	0	5	15				
	2.4	1.6	1.2	80	0	5	15				
	48.9	32.6	24.4	20	65	0	15				
	51.3	34.2	25.7	1	98	0	1				
	53.8	35.9	26.9	1	98	0	1				
	56.2	37.5	28.1	80	0	5	15				
UHPLC Method 2[c]	(L = 100 mm)	(L = 300 mm)	-					2	≈201	≈530	-
	0	0		80	0	5	15				
	0.61	2.4		80	0	5	15				
	12.2	48.9		20	65	0	15				
	12.8	51.3		1	98	0	1				
	13.4	53.8		1	98	0	1				
	14.1	56.2		80	0	5	15				

[a] Flow rate = 0.7 mL min^{-1} (Airs et al., 2001a). [b] Flow rate of UHPLC Method 1A = 0.2, B = 0.3 and C = 0.4 mL min^{-1}, respectively.

[c] Flow rate of UHPLC Method 2A = 0.4 and 2B = 0.3 mL min^{-1}. [d] The maximum pressure observed during analysis.

Column temperature of all methods was maintained at 25°C.

3.2.2 Manipulation of flow rate, injection volume and column length for UHPLC

The UHPLC method parameters mobile phase flow rate, column length and injection volume were targeted for optimisation. Firstly, the effect of increasing the flow rate was examined, there being scope to increase the back-pressure further. The influence of flow rate was examined at 0.45 and 0.50 mL min^{-1}. Increasing flow rate over the range 0.40 to 0.50 mL min^{-1} led to faster elution of components, e.g. chlorophyllone (**24**) in polar region I (Fig. 3.1c) eluted 0.5 min and 1.0 min faster when the flow rate was increased to 0.45 and 0.50 mL min^{-1}, respectively. Importantly, the pigment distributions, peak shapes and resolution at the three flow rates were broadly similar, though maximum back-pressure increased to 510 (flow rate 0.45 mL min^{-1}) and 580 bar (flow rate 0.50 mL min^{-1}). Thus, attempting to increase efficiency of the separation by increasing the mobile phase flow rate was not deemed to be a good strategy at this stage. Reduction of the injection volume from 3 µL for Method 1C (Table 3.1) to 2 µL resulted in a reduction in peak width at half-height ($W_{50\%}$) to about 0.01-0.1 min, e.g. chlorophyllone (**24**, peak no.1) and phaeophytin *a* (**11**, peak no.18) given in Fig. 3.2, with consequent improvement in efficiency. Thus, an injection volume of 2 µL was used for later experiments.

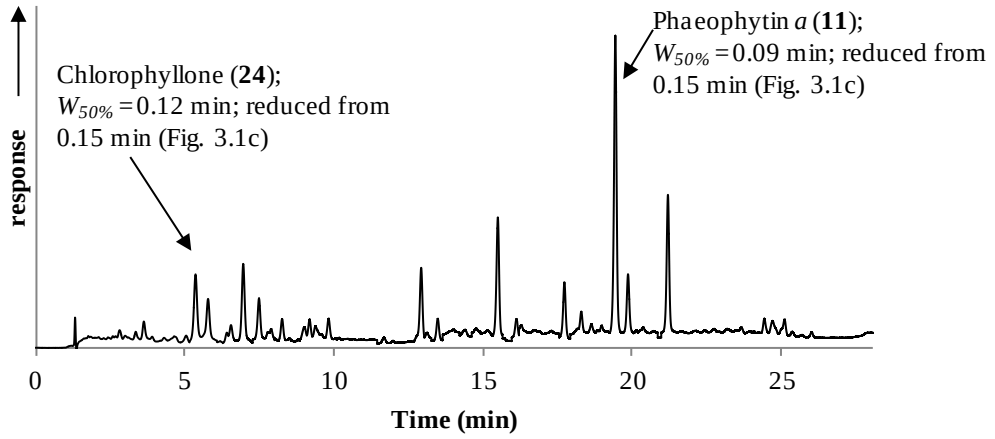

Figure 3.2. UHPLC-PDA (300-800 nm) chromatogram of the sediment extract from Priest Pot obtained using UHPLC method 1C (Table 3.1). Injection volume was 2 µL.

The effect of changing column length (L, Table 3.1) was assessed by varying the number of Acclaim 120 C_{18} 2.2 µm columns (100 mm × 2.1 mm i.d.) coupled in series. The Method Speed-up Calculator generated Methods 2A (L=100) and 2B (L=300; Table 3.1). Owing to high back-pressure, a lower mobile phase flow rate was used for method 2B (0.3 mL min^{-1}) than for Methods 2A and 1C (0.4 mL/min). Consequently, Methods 2A and 1C gave similar $W_{50\%}$ values (Figs. 3.3a and 3.3b), smaller than those for Method 2B (Fig. 3.3c). The lower $W_{50\%}$ at the lower flow rate is attributable to increased longitudinal diffusion, a key band broadening factor in the van Deemter equation (van Deemter et al., 1956). Although the resolution (R_s) of phaeophytin *a* (**11**) and its epimer obtained with Method 2B is greater than for Methods 2A (R_s = 1.49, Fig. 3.3a) and 1C (R_s = 2.82, Fig. 3.3b), the analysis time (56.2 min, Table 3.1) is four times greater than that of Method 2A (14.1 min) and twice that of Method 1C (28.1 min). In view of the relatively long analysis time and high back pressure (530 bar, Table 3.1), the 300 mm column length was discounted. The lower resolution capability of Method 2A suggests that L = 100 mm provides insufficient column length to enable development of a UHPLC method for complex distributions of sedimentary pigments. Alteration of the flow rate, mobile phase composition and temperature of analysis were considered more likely to be effective in increasing resolution. Thus, Method 1C (L = 200 mm, Table 3.1) was selected for further development.

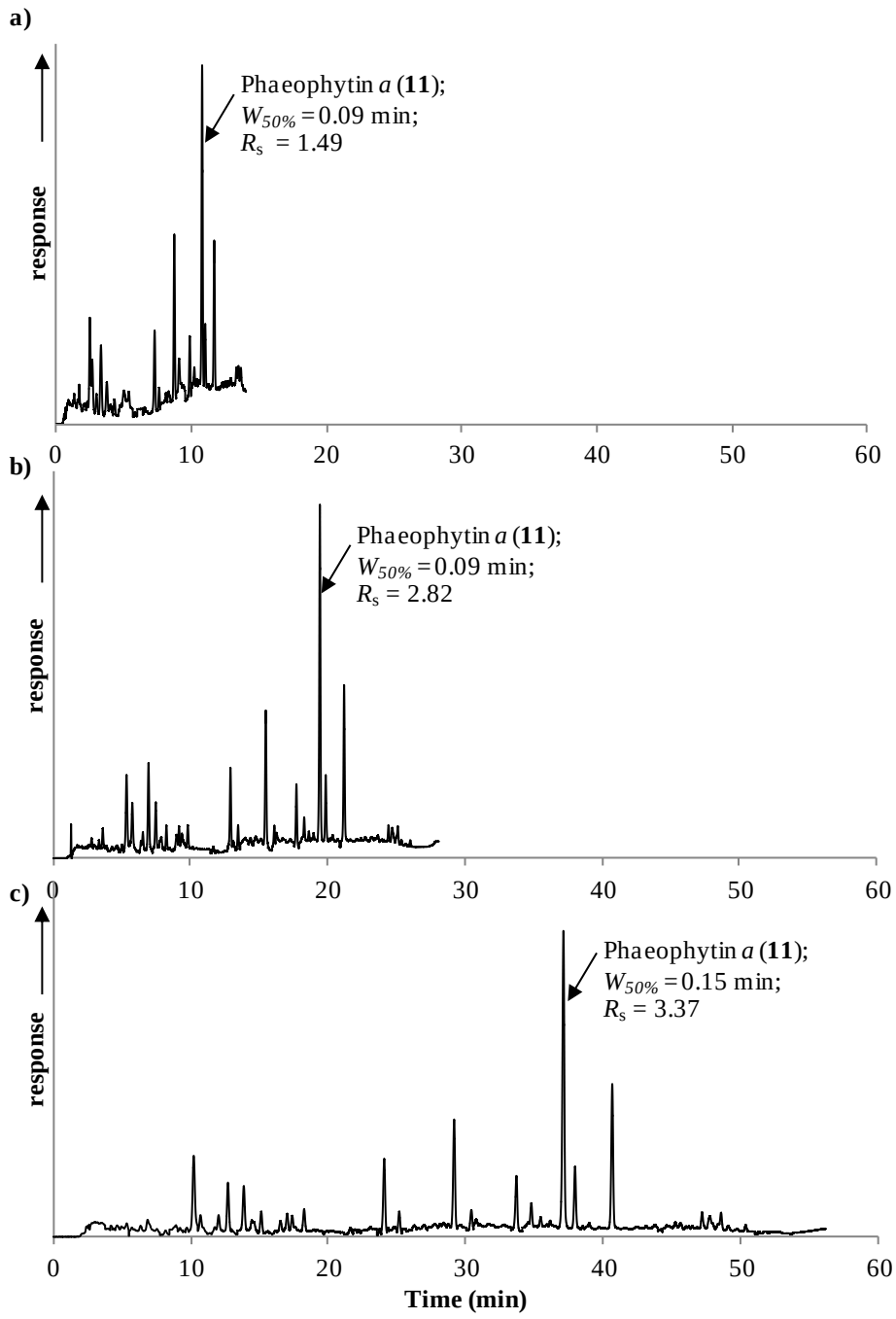

Figure 3.3. UHPLC-PDA (300-800 nm) chromatogram of the sediment extract from Priest Pot obtained using UHPLC method: (a) 2A (column length; L = 100 mm), (b) 1C (L = 200 mm and injection volume = 2 µL) and (c) 2B (L = 300 mm) (Table 3.1).

3.2.3 Modification of the mobile phase gradient

In order to further reduce the analysis time the mobile phase composition and gradient were modified. Method 3A (Table 3.2) was generated by creating a steeper and shorter initial gradient, beginning at 1.2 min and ending at 17 min. The proportion of methanol at the end of the gradient was reduced from 39.1% (Method 1C, Table 3.1) to 10% and balanced by an increase in the ethyl acetate from 44.3% (Method 1C, Table 3.1) to 75%. All of the analytes in the Priest Pot extract eluted within 20 min (the most retained component eluting at 18.6 min; Fig. 3.4a and Table 3.3). The dramatic reduction in polarity at 17 min resulted in much co-elution and a decrease in resolution. For example, phaeophytin *a* and its epimer (peaks 18 and 19, Fig. 3.4a) obtained from Method 3A gave R_s = 1.77 while phaeophytin *a* and its epimer (peaks 18 and 19, Fig. 3.4b) obtained from Method 1C gave R_s = 2.82. Shallower gradients created by increasing the polarity of the mobile phase at 17 min to values closer to that used in Method 1C (Methods 3B and 3C, Table 3.2) increased retention of components beyond the end of the analysis (20 min, Table 3.3). Extending the analysis time to 23 min (Method 4A, Table 3.2) allowed elution of all of the pigments in the extract within 22 min, about 3.3 min faster than with Method 1C (Table 3.3). Steeper gradients for the decrease in methanol and increase in ethyl acetate were employed in Methods 4B and 4C (Table 3.2), reducing the end point in slope from 17 min in Method 4A to 16 min, while maintaining the mobile phase composition. This resulted in faster elution of peaks 10-23, the last eluting at 21.3 min for Method 4B. The retention times of the last 4 peaks (Table 3.3) was even shorter for method 4C.

Reducing the ammonium acetate content of the initial composition from 5% to 3.3%, balanced by an increase in the proportion of methanol (Method 5A), marginally reduced the total analysis time and resulted in earlier elution (by *c.* 1 min) of compounds in the polar and early apolar regions of the chromatogram (peak nos. 1 – 14 in Table 3.3). Reducing the acetonitrile content from 15% to 10% (Method 5B, Table 3.2), compensated for by an increase in methanol, further reduced the total analysis time. The resulting decrease in back-pressure to 500 bar allowed for an increase in flow rate to 0.47 mL min^{-1} (Method 5C, Table 3.2), leading to elution of

peak 23 in 19.5 min (Fig. 3.4c and Table 3.3) and an R_s value for phaeophytin *a* and its epimer of 2.02, less than that for Method 1C (Table 3.1 and Fig 3.4b).

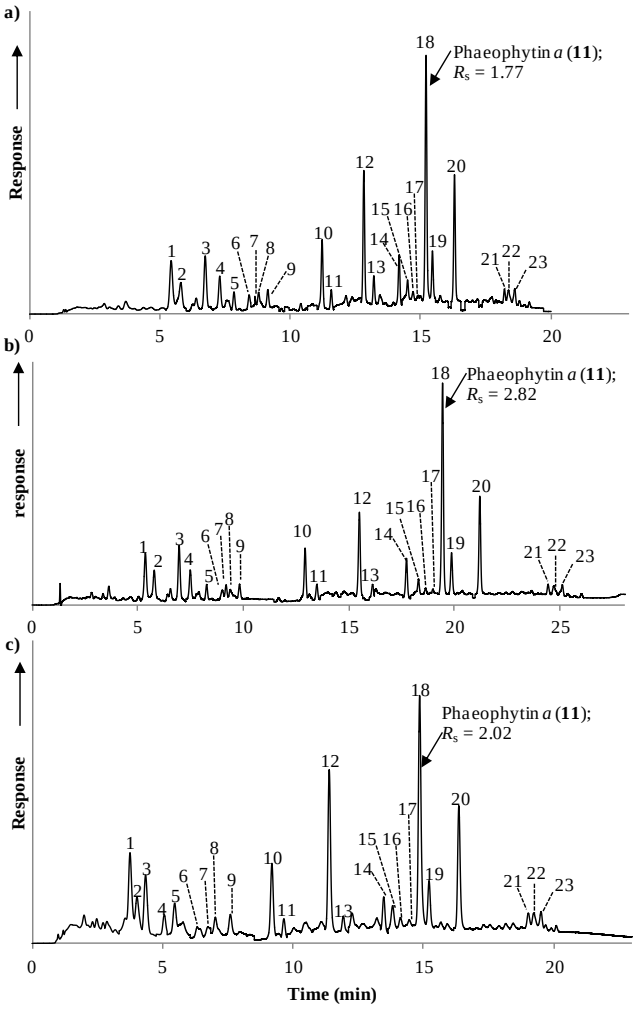

Figure 3.4. UHPLC-PDA (300-800 nm) chromatogram of the sediment extract from Priest Pot obtained using (a) the UHPLC method 3A (Table 3.2), (b) the UHPLC method 1C (Table 3.1) and (c) the UHPLC method 5C (Table 3.2). Retention times of each peak are reported in Table 3.3.

Table 3.2. Mobile phase composition of the UHPLC methods

UHPLC	Time (min)				Methanol (%)				Ethyl acetate (%)				Ammonium acetate (0.01 *M*) (%)				Acetonitrile (%)				Flow rate (mL min^{-1})			
Method 3	**A**	**B**	**C**		**A**	**B**	**C**		**A**	**B**	**C**		**A**	**B**	**C**		**A**	**B**	**C**					
	0	0	0		80	80	80		0	0	0		5	5	5		15	5	5		0.40			
	1.2	1.2	1.2		80	80	80		0	0	0		5	5	5		15	5	5		0.40			
	17	17	17		10	38	35		75	47	50		0	0	0		15	0	0		0.40			
	18	18	18		1	1	1		98	98	98		0	0	0		1	0	0		0.40			
	19	19	19		1	1	1		98	98	98		0	0	0		1	0	0		0.40			
	20	20	20		80	80	80		0	0	0		5	5	5		15	5	5		0.40			
Method 4	**A**	**B**	**C**	**D**	**A**	**B**	**C**	**D**	**A**	**B**	**C**	**D**	**A**	**B**	**C**	**D**	**A**	**B**	**C**	**D**	**A**	**B**	**C**	**D**
	0	0	0	0	80	80	80	80	0	0	0	0	5	5	5	5	15	15	15	15	0.40	0.40	0.40	0.40
	1.2	1.2	1.2	1.2	80	80	80	80	0	0	0	0	5	5	5	5	15	15	15	15	0.40	0.40	0.40	0.40
	17	16	16	16	35	35	35	35	50	50	50	50	0	0	0	0	15	15	15	15	0.40	0.40	0.40	0.45
	20	20	21	21	1	1	1	1	98	98	98	98	0	0	0	0	1	1	1	1	0.40	0.40	0.40	0.50
	22	22	22.5	22.5	1	1	1	1	98	98	98	98	0	0	0	0	1	1	1	1	0.40	0.40	0.40	0.50
	23	23	23	23	80	80	80	80	0	0	0	0	5	5	5	5	15	15	15	15	0.40	0.40	0.40	0.40
Method 5	**A**	**B**	**C**	**D**	**A**	**B**	**C**	**D**	**A**	**B**	**C**	**D**	**A**	**B**	**C**	**D**	**A**	**B**	**C**	**D**	**A**	**B**	**C**	**D**
	0	0	0	0	81.7	86.7	86.7	81.5	0	0	0	0	3.3	3.3	3.3	8.5	15	10	10	10	0.40	0.40	0.47	0.47
	1.2	1.2	1.2	1.2	81.7	86.7	86.7	81.5	0	0	0	0	3.3	3.3	3.3	8.5	15	10	10	10	0.40	0.40	0.47	0.47
	16	16	16	16	35	37	37	37	50	53	53	53	0	0	0	0	15	10	10	10	0.45	0.45	0.47	0.47
	21	21	21	21	1	1	1	1	98	98	98	98	0	0	0	0	1	1	1	1	0.50	0.50	0.47	0.47
	22.5	22.5	22.5	22.5	1	1	1	1	98	98	98	98	0	0	0	0	1	1	1	1	0.50	0.50	0.47	0.47
	23	23	23	23	81.7	86.7	86.7	81.5	0	0	0	0	3.3	3.3	3.3	8.5	15	10	10	10	0.40	0.40	0.47	0.47

Column temperature of all methods was maintained at 25°C, except the method 5C, for which the temperature was set to 25, 35, 45, 55 and 65°C in experiment for the effect of column temperature and method 5D was maintained at 45°C.

Table 3.3. Retention times of the major chromatographic peaks in the sediment extract from Priest Pot obtained by the different UHPLC methods

UHPLC method		1C	3A	3B	3C	4A	4B	4C	4D	5A	5B	5C	1C	3A	3B	3C	4A	4B	4C	4D	5A	5B	5C
Peak number[a]	**Peak name**	**Retention time (min)**											**Peak width at 50% of peak height (min)**										
1	Chlorophyllone (**24**)	5.37	5.44	5.19	5.18	5.20	5.28	5.34	5.17	4.09	4.31	3.76	0.12	0.13	0.13	0.13	0.13	0.12	0.13	-	0.11	0.13	0.14
2	Chlorophyllone (**25**)	5.79	5.81	5.58	5.56	5.57	5.65	5.70	5.53	4.34	4.62	4.02	0.12	0.15	0.16	0.16	0.15	0.14	0.13	0.12	0.11	0.14	0.15
3	Unidentified carotenoid	6.97	6.75	6.65	6.61	6.60	6.69	6.62	6.52	4.67	4.98	4.35	0.11	0.11	0.12	0.12	0.11	0.11	0.11	0.11	0.11	0.16	0.14
4	Phaeophorbide *a* (**20**)	7.50	7.30	7.26	7.22	7.19	6.86	7.24	7.06	5.86	6.20	5.47	0.11	0.09	0.11	0.11	0.11	-	0.10	0.10	0.10	0.12	0.12
5	Unidentified carotenoid	8.27	7.57	7.95	7.89	7.86	7.90	7.83	7.73	6.56	7.07	5.78	0.10	0.17	0.10	0.10	0.09	0.09	0.09	0.11	0.12	-	0.12
6	Unidentified carotenoid	8.81	7.85	8.68	8.61	8.57	8.40	8.51	8.33	6.69	7.51	6.33	n.a.	0.08	0.09	0.10	0.09	0.07	0.13	0.09	-	-	0.10
7	Unidentified chlorin	9.02	8.43	8.93	8.86	8.81	8.57	8.64	8.48	6.96	7.81	6.74	0.17	0.04	0.13	0.08	0.08	0.09	-	-	0.13	0.10	-
8	Unidentified chlorin	9.20	8.79	9.11	9.03	8.99	8.80	8.80	8.72	7.28	7.95	7.03	0.12	0.08	0.12	0.10	0.10	0.08	0.11	0.08	0.16	0.10	0.12
9	Pphorb *a* methyl ester (**22**)	9.83	9.15	9.54	9.45	9.40	9.37	9.38	9.10	8.61	8.40	7.60	0.11	0.08	0.09	0.10	0.09	0.09	0.11	0.09	0.11	0.12	0.12
10	Chlorophyll *b* (**5**)	12.94	11.23	12.23	12.07	12.03	11.86	11.79	11.47	9.77	9.96	9.19	0.10	0.07	0.09	0.09	0.09	0.09	0.09	0.08	0.11	0.11	0.12
11	Chlorophyll *b'* (**37**)	13.50	11.58	12.73	12.55	12.51	12.30	12.23	11.89	10.25	10.41	9.65	0.09	0.07	0.21	0.30	0.23	0.08	0.08	0.08	0.10	0.10	0.11
12	Chlorophyll *a* (**4**)	15.51	12.83	14.52	14.27	14.22	13.91	13.83	13.42	12.05	12.09	11.39	0.10	0.07	0.09	0.08	0.08	0.08	0.08	0.08	0.10	0.11	0.11
13	Chlorophyll *a'* (**38**)	16.14	13.21	15.08	14.81	14.75	14.40	14.33	13.89	12.61	12.61	11.93	0.09	0.07	0.08	0.08	0.08	0.08	0.09	0.07	0.09	0.11	0.10
14	Phaeophytin *b* (**17**)	17.74	14.18	16.60	16.25	16.19	15.74	15.68	15.17	14.16	14.08	13.48	0.09	0.07	0.10	0.09	0.10	0.08	0.09	0.08	0.09	0.10	0.10
15	Hydroxyphaeophytin *a* (**34**)	18.31	14.50	17.04	16.67	16.60	16.14	16.08	15.49	14.59	14.41	13.82	0.09	0.08	0.09	0.09	0.10	0.09	0.12	0.08	0.10	0.12	0.14
16	Hydroxyphaeophytin *a'* (**35**)	18.65	14.71	17.34	16.96	16.89	16.41	16.35	15.79	14.88	14.69	14.12	0.10	0.10	0.08	0.08	0.09	0.08	0.19	0.08	0.09	0.12	0.13
17	Unidentified chlorin	18.99	14.90	17.63	17.24	17.17	16.66	16.61	16.05	15.15	15.02	14.46	0.09	-	0.10	0.10	0.12	0.09	0.24	0.09	0.10	0.08	0.15
18	Phaeophytin *a* (**11**)	19.45	15.21	18.08	17.67	17.60	17.07	17.01	16.43	15.57	15.40	14.86	0.09	0.07	0.09	0.09	0.09	0.08	0.08	0.08	0.09	0.10	0.11
19	Phaeophytin *a'* (**32**)	19.88	15.46	18.45	18.01	17.95	17.39	17.34	16.74	15.94	15.74	15.22	0.09	0.07	0.08	0.06	0.08	0.07	-	0.07	0.09	0.10	0.10
20	Pyrophaeophytin *a* (**18**)	21.22	16.30	19.67	19.19	19.11	18.50	18.44	17.76	17.15	16.83	16.36	0.09	0.07	0.08	0.08	0.08	0.08	0.08	0.07	0.10	0.10	0.11
21	Pphorb *a* steryl ester (**26**)	24.45	18.21	-	-	21.51	20.99	20.72	19.90	19.69	19.27	19.02	0.09	0.09	-	-	0.07	0.07	0.09	0.06	0.07	0.12	0.10
22	Pphorb *a* steryl ester (**27**)	24.73	18.37	-	-	21.64	21.12	20.86	20.03	19.84	19.46	19.23	0.15	0.15	-	-	0.11	0.11	0.14	0.09	0.09	0.15	0.12
23	Pphorb *a* steryl ester (**28**)	25.13	18.61	-	-	21.82	21.30	21.08	20.22	20.06	19.70	19.51	0.10	0.10	-	-	0.07	0.07	0.09	0.07	0.07	0.10	0.09

[a] Peak number refers to the peak labels in Fig. 3.4.

3.2.4 Effect of column temperature

The temperature of the column was increased to reduce the viscosity of the mobile phase and hence lower the back-pressure. In the case of pigment analysis an important consideration is that increasing the column temperature could lead to structural alteration of these sensitive components. For example, loss of the central Mg^{2+} complexed in chlorophyll *a* and bacteriochlorophyll *a* (**6**) occurs readily under mild conditions, forming phaeophytin *a* (**11**) and bacteriophaeophytin *a* (**29**), respectively. A sediment extract from Estanya, containing chlorophyll *a* (**4**), phaeophytin *a* (**11**) and bacteriophaeophytin *a* (**29**), was spiked with bacteriochlorophyll *a* (**6**), one of the least stable pigments. UHPLC analysis of the spiked extract at 10°C intervals over the range 25 - 65°C, the maximum temperature being selected so as not to exceed the temperature limits of either the column (80°C) or the Dionex RSLC system (70°C), showed consistency in the peak area ratios of the metallated pigments (chlorophyll *a* (**4**) and bacteriochlorophyll *a* (**6**)) and their demetallated counterparts (phaeophytin *a* (**11**) and bacteriophaeophytin *a* (**29**) (Fig. 3.5). Thus, column temperatures up to 65°C may be used without risk of alteration of the sensitive pigments (Van Heukelem and Thomas, 2001). The maximum back-pressure during analysis was inversely proportional to column temperature, decreasing by 40-80 bar for every 10ºC increase. Although the column temperature of 65ºC did not cause alteration of the sensitive pigment components and gave the lowest pressure (350 bar) the resolution in the polar region was severely compromised, e.g. unidentified carotenoids shown in Fig. 3.6. Consequently, the mid temperature of the range tested (45°C) was selected for further method development.

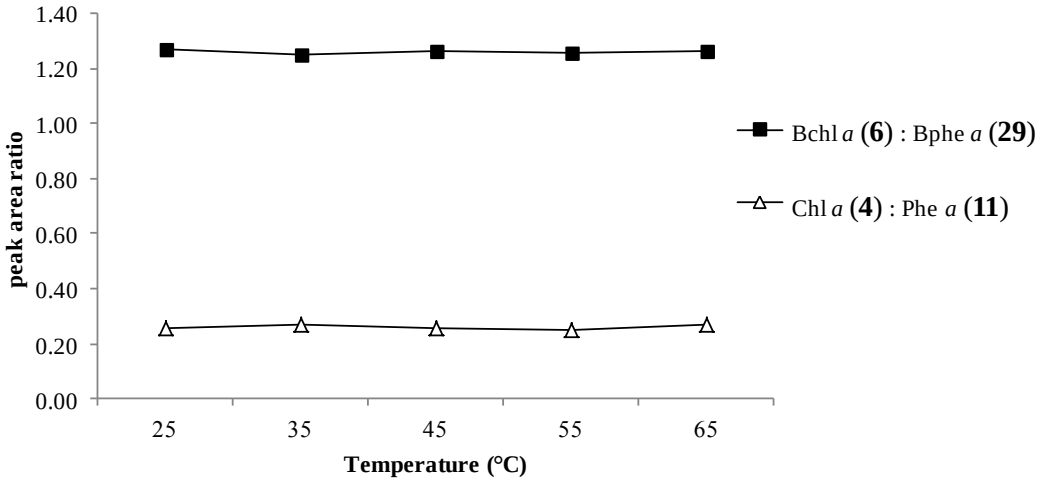

Figure 3.5. Ratio of the peak areas of the sensitive pigments (bacteriochlorophyll *a* (**6**) and chlorophyll *a* (**4**)) to their demetallated derivatives obtained from Estanya sediment spiked with bacteriochlorophyll *a* (**6**) and analysed by Method 5C (Table 3.2) at column temperature increments of 10°C from 25 - 65°C.

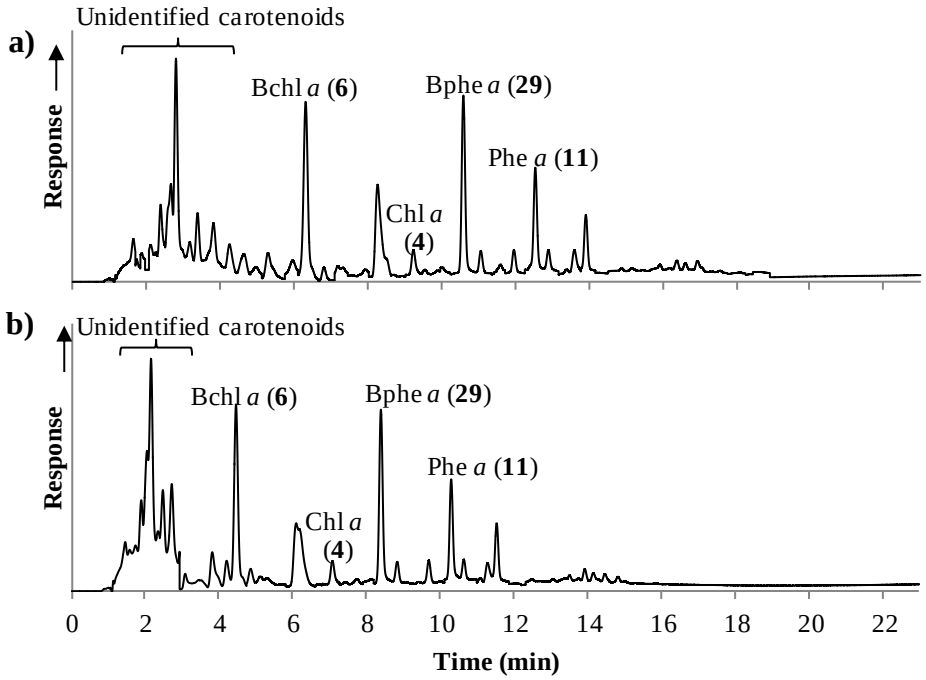

Figure 3.6. UHPLC-PDA (300-800 nm) chromatogram of the extract from Estanya sediment spiked with bacteriochlorophyll *a* (**6**) analysed using UHPLC method 5C (Table 3.2) with column temperature maintained at (a) 45°C and (b) 65 °C.

Co-elution of peaks 1 and 2 and peaks 3 and 4 is clearly evident at 45°C (Fig. 3.7a) compared to 25°C (Fig. 3.4c), and peak 18 (phaeophytin *a* (**11**), Fig. 3.7a) exhibits a different UV/Vis spectrum at the leading edge (λ_{max} = 437, 665) and at the peak centre (λ_{max} = 407, 665), indicating a co-elution. The polarity of the initial mobile phase was raised by increasing the ammonium acetate content to 8.5% (Method 5D, Table 3.2). The increase in ammonium acetate altered the gradient of the mobile phase and gave good resolution of peaks 3 and 4 (Method 5D at 45°C, Fig. 3.7b). Peaks 1 and 2 and peak 18′ (pyrophaeophytin *b* (**19**)) and phaeophytin *a* (**11**; peak 18, Fig. 3.7b) were resolved, though resolution of peaks 3 and 4 was not significantly altered (Fig. 3.7b). Insertion of an additional line at 2.5 min creating Method 6 (Table 3.4) improved resolution of peaks 1 - 4 while still separating peaks 18′ and 18 (Fig. 3.7c), resulting in the optimal method for the separation of sedimentary pigments using the Acclaim columns. The purpose the additional line at 2.5 min (Method 6, Table 3.4) was to create a more gradual ammonium acetate gradient than that of method 5D.

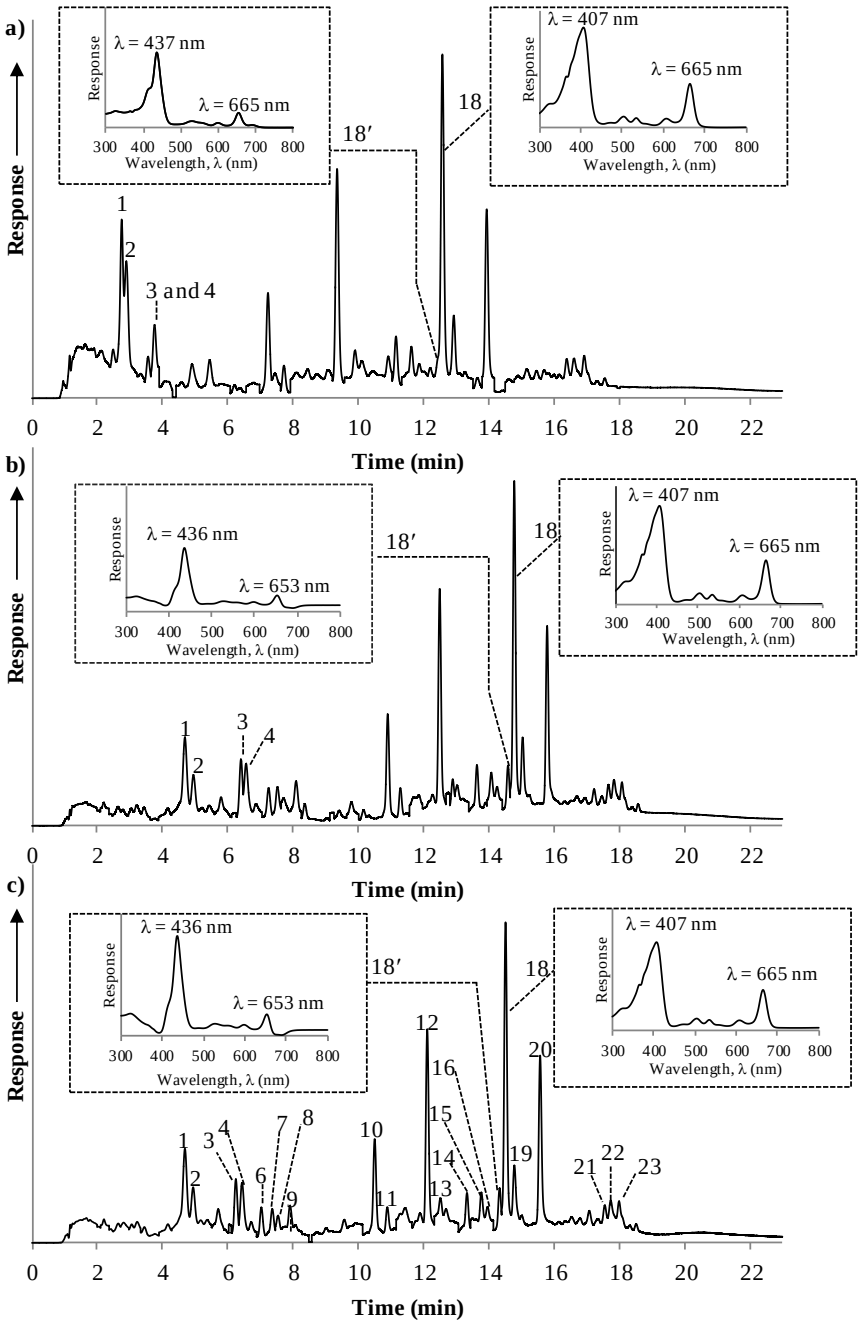

Figure 3.7. UHPLC-PDA (300-800 nm) chromatogram of the sediment extract from Priest Pot obtained using (a) the UHPLC Method 5C (at 45°C), (b) the UHPLC Method 5D (at 45°C) and (c) the UHPLC Method 6 at 45°C (the optimal condition for two Acclaim 120 C_{18} 2.2 µm columns (100 mm × 2.1 mm i.d.), Table 3.4 and pigments identification shown in Table 3.7).

Table 3.4. Optimal UHPLC method for two Acclaim 120 C_{18} 2.2 µm columns (100 mm × 2.1 mm i.d.).

Method	Time (min)	Methanol (%)	Ethyl acetate (%)	Ammonium acetate (0.01 *M*) (%)	Acetonitrile (%)
UHPLC Method 6	0	81.5	0	8.5	10
	1.2	81.5	0	8.5	10
	2.5	78.5	4.7	6.8	10
	16	37	53	0	10
	21	1	98	0	1
	22.5	1	98	0	1
	23	81.5	0	8.5	10

Injection volume was 2 µL. Separation was performed at 45°C with a flow rate of 0.47 mL min^{-1}.

3.2.5 UHPLC Method development for an Acquity UPLC BEH C_{18} column

An Acquity UPLC BEH C_{18} (1.7 µm, 150 mm x 3 mm i.d) (Waters, Ireland) column was evaluated using the optimal method above. In addition to the differences in L, differences in manufacturing and particle size of the two C_{18} stationary phases can be expected to cause differences in separation efficiency. The shorter overall column length and larger column diameter, compared to the two Acclaim® RSLC 120 C_{18} (100 mm × 2.1 mm i.d.), resulted in a shorter analysis time and lower back pressure (345 bar) but with lower resolution of peaks 1 and 2 in polar region I (Fig. 3.8a). Increasing the proportion of ammonium acetate affected the retention times and resolution of peaks in the polar region (I) more than in regions II and III. At the optimum ammonium acetate level (11%) peaks 1 and 2 were better resolved (I, Fig. 3.8b) with acceptable resolution obtained for peaks 3 and 4 (Fig. 3.8b).

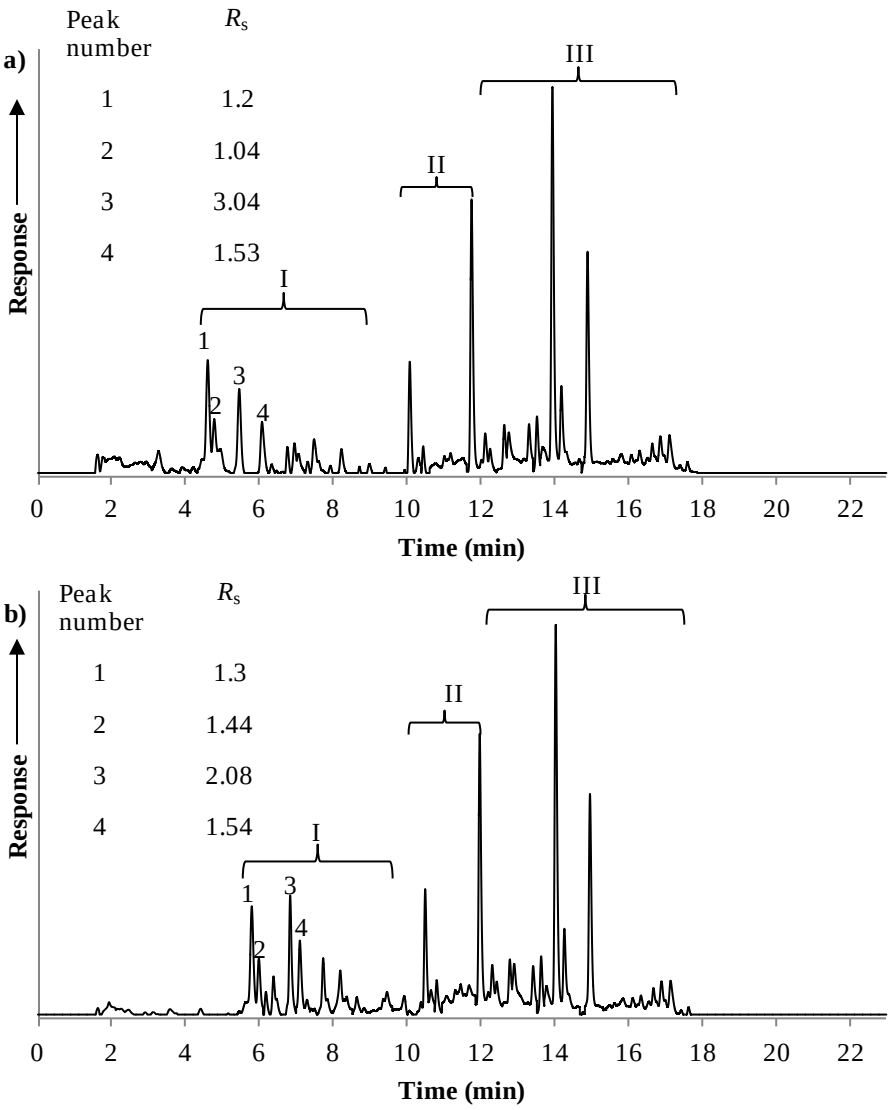

Figure. 3.8. UHPLC-PDA (300-800 nm) chromatogram of the sediment extract from Priest Pot performed on an Acquity UPLC BEH C_{18} 1.7 µm column (150 mm × 3 mm i.d.) analysed with (a) Method 6 (Table 3.4) and (b) Method 7B (Table 3.5).

Table 3.5. UHPLC gradients tested during evaluation of the Acquity UPLC BEH C_{18} 1.7 µm column (150 mm × 3 mm i.d.)

Method	Time (min)			Methanol (%)			Ethyl acetate (%)			Ammonium acetate (0.01 *M*) (%)			Acetonitrile (%)			Injection volume (µL)	Flow rate (mL min^{-1})
UHPLC Method 7	**A**	**B**	**C**	**A**	**B**	**C**	**A**	**B**	**C**	**A**	**B**	**C**	**A**	**B**	**C**		
	0	0	0	80	79	78	0	0	0	10	11	12	10	10	10	2	0.47
	1.2	1.2	1.2	80	79	78	0	0	0	10	11	12	10	10	10		0.47
	2.5	2.5	2.5	78.5	78.5	78.5	4.7	4.7	4.7	6.8	6.8	6.8	10	10	10		0.47
	16	16	16	37	37	37	53	53	53	0	0	0	10	10	10		0.47
	21	21	21	1	1	1	98	98	98	0	0	0	1	1	1		0.47
	22.5	22.5	22.5	1	1	1	98	98	98	0	0	0	1	1	1		0.47
	23	23	23	80	79	78	0	0	0	10	11	12	10	10	10		
UHPLC Method 8	**A**	**B**	**C**	**A**	**B**	**C**	**A**	**B**	**C**	**A**	**B**	**C**	**A**	**B**	**C**		
	0	0	0	79	79	79	0	0	0	11	11	11	10	10	10	2	0.6
	1	1	1	79	79	79	0	0	0	11	11	11	10	10	10		0.6
	2.5	2.5	2.5	78.5	78.5	78.5	4.7	4.7	4.7	6.8	6.8	6.8	10	10	10		0.6
	16	16	16	37	40	50	53	50	40	0	0	0	10	10	10		0.6
	21	21	21	2	2	2	97	97	97	0	0	0	1	1	1		0.6
	22.5	22.5	22.5	2	2	2	97	97	97	0	0	0	1	1	1		0.6
	23	23	23	79	79	79	0	0	0	11	11	11	10	10	10		0.6
UHPLC Method 9	**A**	**B**	**C**	**A**	**B**	**C**	**A**	**B**	**C**	**A**	**B**	**C**	**A**	**B**	**C**		
	0	0	0	79	79	80	0	0	0	11	11	10	10	10	10	2	0.6
	0.5	0.5	0.5	79	79	80	0	0	0	11	11	10	10	10	10		0.6
	5.0	7	7	70.8	64.7	64.7	13.6	20.8	20.8	5.6	4.6	4.6	10	10	10		0.6
	16	16	16	50	50	50	40	40	40	0	0	0	10	10	10		0.6
	21	21	21	2	2	2	97	97	97	0	0	0	1	1	1		0.6
	22.5	22.5	22.5	2	2	2	97	97	97	0	0	0	1	1	1		0.6
	23	23	23	79	79	79	0	0	0	11	11	10	10	10	10		0.6

Column temperature of all methods was maintained at 45°C

An increase in the flow rate to 0.6 mL min^{-1} coupled with a decrease in the duration of the initial isocratic period from 1.2 to 1 min (Method 8A, Table 3.5) caused earlier elution of all components, with reduced separation of peaks in the apolar region (Fig. 3.9a). Reduction in the slope of the methanol to ethyl acetate gradient over the interval 2.5 and 16 min improved separation of the components in the apolar region (Fig. 3.9b), the resolution of phaeophytin *a* (**11**, peak no. 18) and its epimer (peak no. 19) increasing from 1.97 to 2.14 (Fig. 3.9b). Under these conditions peak no. 7^{*} (6.5 min, Fig. 3.9b) showed evidence of co-elution.

Reducing the initial isocratic time from 1 min to 0.5 min (Method 9A, Table 3.5) and inserting an extra line into the gradient programme at 7 min (Method 9B, Table 3.5) to create a more gradual ethyl acetate gradient than that of Method 9A (Table 3.5) led to a slight decrease in the total analysis time and resolution of peaks 7 and 7′ (Fig. 3.9c; Method 9B).

Decreasing the ammonium acetate to 10% (Method 9C; Table 3.5) gave faster elution and greater resolution of compounds in the polar region. For example, resolution of the unidentified carotenoid (peak no.3) and phaeophorbide *a* (**20**, peak no.4) was increased from 1.27 (Method 9B, Fig. 3.9c) to 1.65 (Method 9C, Fig.10a). The UV/vis spectrum of pyrophaeophytin *b* (**19**, peak no. 18′) showed its co-elution with an unidentified compound exhibiting a λ_{max} at 414 nm. The final and optimal method for the Acquity column (Method 10, Table 3.6) was achieved by adjusting the mobile phase solvent at 7 min to an integer value. Inserting an additional line into the gradient at 18 min to mimic the gradient between 16 and 19 min for Method 9C (Table 3.5), shortening the column wash at the end of the program to 1 min and reducing ethyl acetate to 80% (balanced by increases in methanol led to compounds in the polar region eluting around 0.01 min faster (Fig. 3.10b) and those in the apolar region eluting around 0.1 to 0.3 min slower. Notably, this mobile phase composition is the same as the final mobile phase composition of Airs Method C (Airs et al., 2001a). The analysis time is below 18 min, though it did not prove possible to resolve the component coleuting with pyrophaeophytin *b* (**19**, peak no. 18′) (Fig. 3.10b). Although the small modification to the gradient did not affect the $W_{50\%}$, peak height or improve resolution, the separation more closely matches that of Airs et al.,

(2001a) and so can be expected to provide a similar level of efficiency for the analysis of complex pigment extracts. As a result, Method 10 (Table 3.6) was selected as the optimal method for the Acquity column.

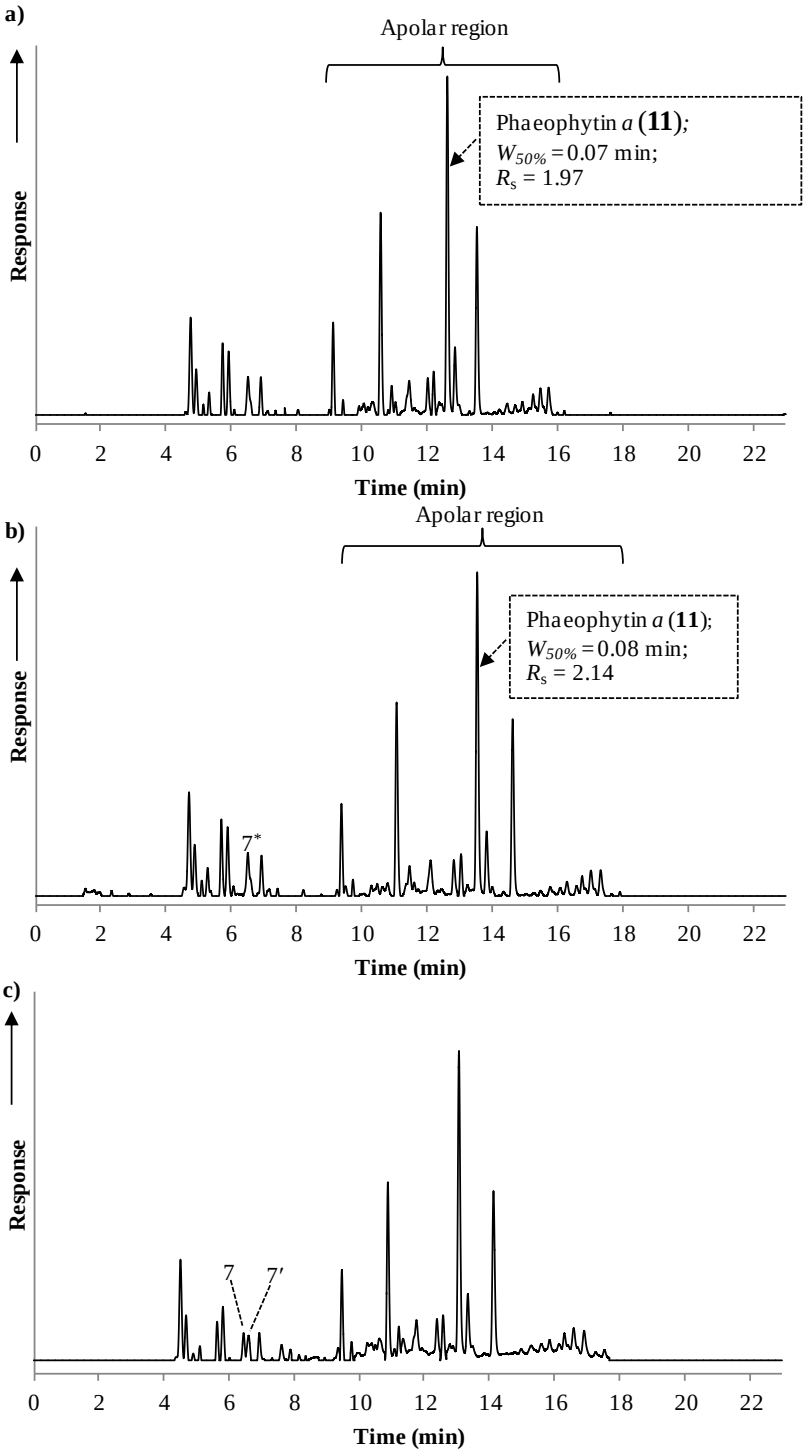

Figure 3.9. UHPLC-PDA (300-800 nm) chromatogram of the sediment extract from Priest Pot obtained using (a) Method 8A (Table 3.5), (b) Method 8C (Table 3.5) and (c) Method 9B (Table 3.5).

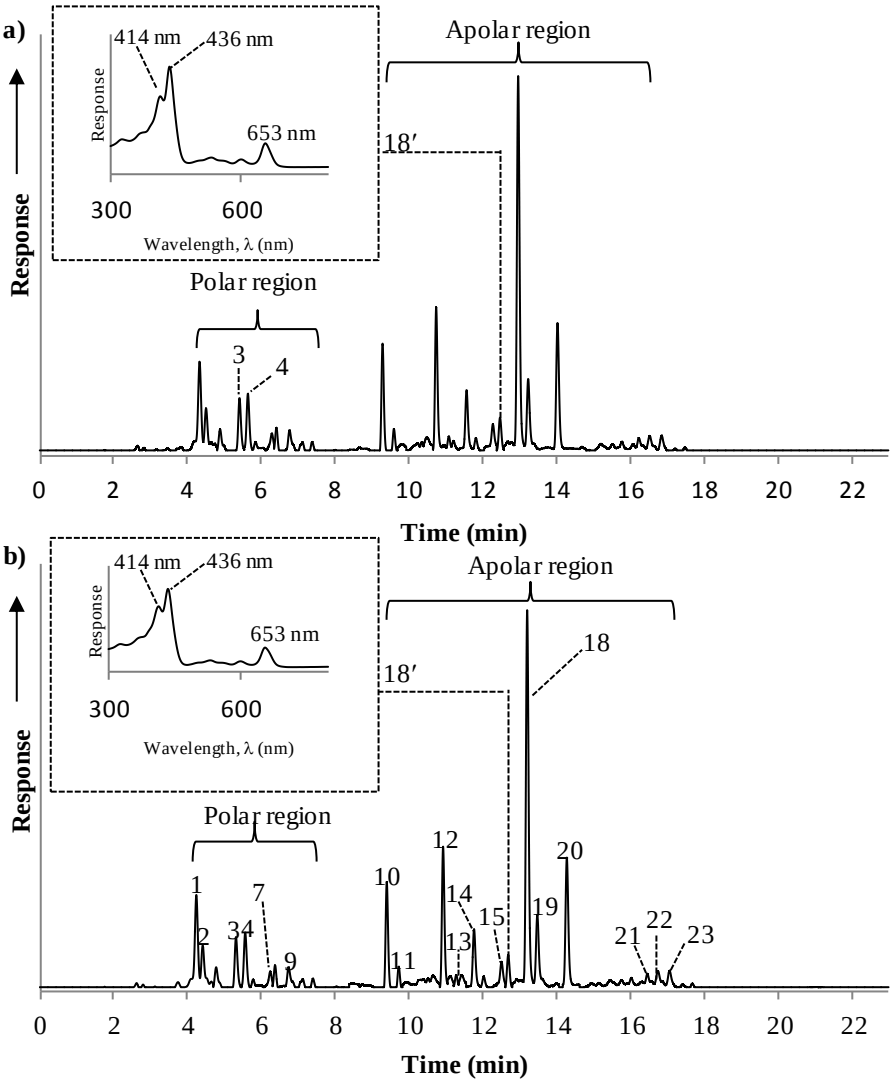

Figure 3.10. UHPLC-PDA (300-800 nm) chromatogram of the sediment extract from Priest Pot obtained using (a) Method 9C (Table 3.5) and (b) Method 10 (Table 3.6, major chlorins identification shown in Table 3.7).

Table 3.6. Optimal UHPLC method for the Acquity UPLC BEH C_{18} 1.7 µm column (150 mm × 3 mm i.d.).

Method	**Time (min)**	**Methanol (%)**	**Ethyl acetate (%)**	**Ammonium acetate (0.01 *M*) (%)**	**Acetonitrile (%)**	**Flow rate (mL min^{-1})**
Method 10	0	80	0	10	10	0.60
	0.5	80	0	10	10	0.60
	7	64	21	5	10	0.60
	16	50	40	0	10	0.60
	18	31	63	0	6	0.60
	18.5	19	80	0	1	0.60
	19.5	19	80	0	1	0.60
	20	80	0	10	10	0.60

Injection volume was 2 µL and the column was maintained at 45°C.

Table 3.7. Peaks assignments for chlorophylls and their derivatives in a sediment extract from Priest Pot analysed by the UHPLC Method 6 (Fig. 3.7c) and Method 10 (Fig. 3.10b).

Peak number [a]	Assignment [b]	t_R (min)		Main UV/vis absorption bands (nm)		$[M+H]^{+}$ [b]	Diagnostic fragment ions [b]		Esterifying alcohol [b]
		UHPLC Method 6	UHPLC Method 10	UHPLC Method 6	UHPLC Method 10		UHPLC Method 6	UHPLC Method 10	
1	Chlorophyllone (**24**)	4.7	4.2	407, 664	407, 664	533	515	515	-
2	Chlorophyllone (**25**)	4.9	4.4	406, 669	406, 669	533	515	515	-
3	Unidentified carotenoid	6.3	5.3	443, 470	443, 470	551	533	533	-
4	Phaeophorbide *a* methyl ester (**20**)	6.4	5.6	406, 664	405, 664	607	547, 461	547, 461	methanol
6	Unidentified carotenoid	7.0	-	444, 473	-				
7	Unidentified chlorin [c]	7.4	6.3	386, 520, 674	386, 514, 674	563	-	-	-
7′	Unidentified carotenoid	-	6.4	-	415, 475, 412	-	-	-	-
8	Unidentified chlorin [c]	7.5	-	407, 540, 670	-	579	-	-	-
9	Pyrophaeophorbide *a* methyl ester (**22**)	7.9	6.7	408, 665	408, 665	549	-	-	methanol
10	Chlorophyll *b* (**5**)	10.5	9.4	463, 648	463, 648	907	-	-	phytol
11	Chlorophyll *b* epimer (**37**)	10.9	9.7	463, 648	463, 648	907	-	-	phytol
12	Chlorophyll *a* (**4**)	12.1	10.9	430, 663	430, 663	893	615, 555	-	phytol
13	Chlorophyll *a* epimer (**38**)	12.5	11.3	430, 663	430, 663	893	-	-	phytol
14	Phaeophytin *b* (**17**)	13.3	11.8	434, 658	434, 658	885	607	607	phytol
15	Hydroxyphaeophytin *a* (**34**)	13.8	12.5	406, 665	406, 665	887	-	-	phytol
16	Hydroxyphaeophytin *a* epimer (**35**)	14.0	-	405, 666	-	887	-		phytol
18′	Pyrophaeophytin *b* (**19**)	14.3	12.7	436, 653	414, 436, 650	827	549, 521	-	phytol
18	Phaeophytin *a* (**11**)	14.5	13.2	407, 665	407, 665	871	593, 533	593, 533	phytol
19	Phaeophytin *a* epimer (**32**)	14.8	13.5	407, 665	407, 665	871	593, 533	593, 533	phytol
20	Pyrophaeophytin *a* (**18**)	15.6	14.3	408, 665	408, 665	813	535	535	phytol
21	Pyrophaeophorbide *a* steryl ester (**26**)	17.6	16.5	407, 666	408, 666	903	-	-	C_{27} sterol [c]
22	Pyrophaeophorbide *a* steryl ester (**27**)	17.7	16.6	409, 666	408, 666	929	-	-	C_{29} sterol [c]
23	Pyrophaeophorbide *a* steryl ester (**28**)	18.0	16.8	408, 666	408, 666	931	-	-	C_{29} sterol [c]

[a] Peak number refers to the peak labels in Fig. 3.7c and 3.10b. [b] Identification has been reported in previous study (Airs, 2001b). [c] Tentative assignment.

3.2.6 Comparison of the UHPLC methods 6 and 10 with Airs Method A (Airs et al., 2001a)

Sediment from Priest Pot (Cumbria, UK) was collected by Professor Brendan Keely, University of York, in 1996. The frozen sediment was freeze-dried and homogenised by griding and sieving. Sediment was extracted with acetone using ASE at 70°C as described in Chapter 2. The pigment extract was analysed by Airs Method A (Airs et al., 2001a) and the two UHPLC Methods 6 (Table 3.4) and 10 (Table 3.6) coupled with online UV/Vis and multistage tandem mass spectrometric (up to MS^3) detection. Comparison of the LC chromatogram of the Priest Pot extract obtained by those three methods reveals them to exhibit broadly similar pigment compositions (Fig. 3.11, retention times and peaks assignments are reported in Table 3.8). The sequence of major chlorins eluted by UHPLC methods 6 and 10 was similar to that obtained from Airs Method A (Airs, et al., 2001a) with the exception of pyrophaeophytin *b* (**19**, peak no. 16 shown in Fig. 3.11) which eluted before phaeophytin *a* (**11**, peak no. 15 shown in Fig. 3.11). Comparison between UHPLC Method 6 (Fig. 3.11b) and Method 10 (Fig. 3.11c) found that the resolution in the polar region (Fig. 3.11c) was slightly higher (e.g. R_s of peak no.3 shown in Fig. 3.11b and c) and retention times were shorter for Method 10 (Fig. 3.11c), though a coelution is apparent in the apolar region. The absence of the hydroxyphaeophytin *a* (**34**) peak in the chromatogram from Method 10 (Table 3.7) indicates this to be the compound that coelutes with pyrophaeophytin *b* (**19**).

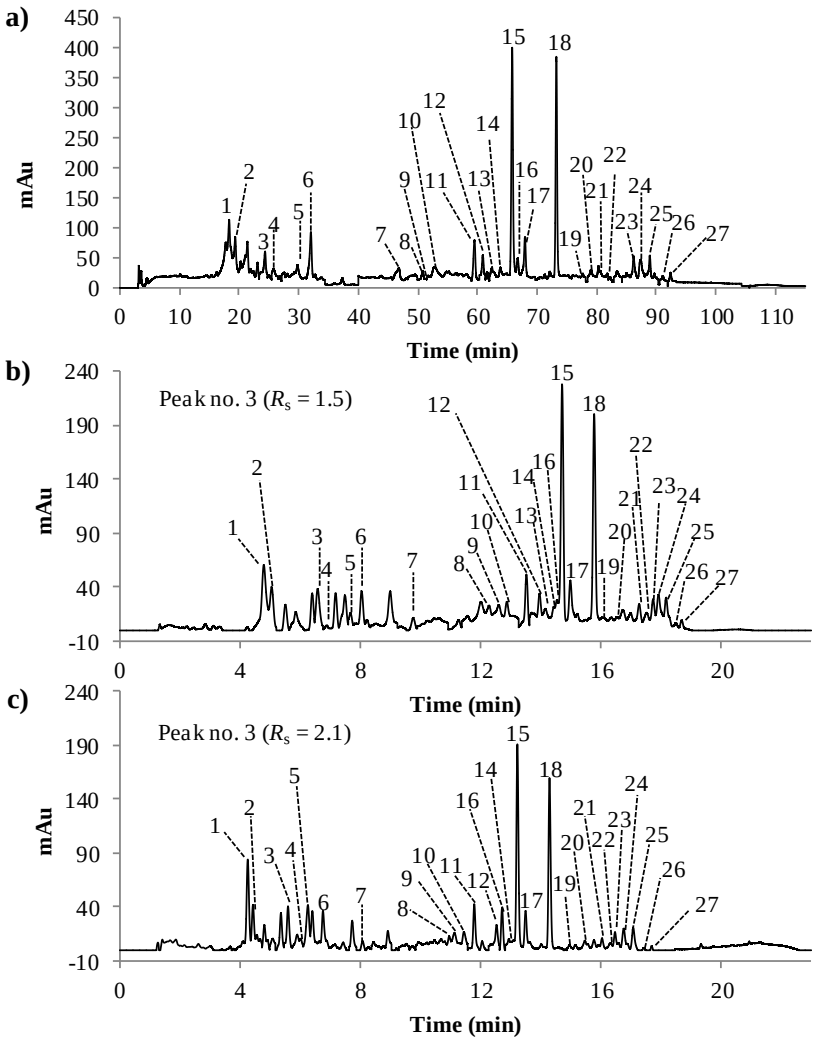

Figure 3.11. LC-PDA (300-800 nm) chromatogram of the sediment extract from Priest Pot obtained using (a) HPLC Airs Method A (Table 3.1), (b) the UHPLC Method 6 (Table 3.4) and (c) the UHPLC Method 10 (Table 3.6). For peak assignment, see Table 3.8.

Table 3.8. Peaks assignments for chlorophylls and their derivatives in a sediment extract from Priest Pot analysed by the Airs Method A (Airs et al., 2001a) (Fig. 3.11a), UHPLC Method 6 (Fig. 3.11b) and UHPLC Method 10 (Fig. 3.11c).

Peak number [a, b]	**Assignment** [b,c]	t_R **(min)**			**Main UV/vis absorption bands (nm)**			**[M+H]$^+$** [b] **(*m/z*)**	**Diagnostic fragment ions** [b]			**Esterifying alcohol** [b, d]
		Airs Method A [d]	UHPLC Method 6	UHPLC Method 10	Airs Method A [d]	UHPLC Method 6	UHPLC Method 10		Airs Method A [d]	UHPLC Method 6	UHPLC Method 10	
1	Chlorophyllone (**24**)	18.4	4.8	4.3	407, 665	407, 664	407, 664	533	515	515	515	-
2	Chlorophyllone (**25**)	19..4	5.1	4.4	407, 664	406, 669	406, 669	533	515	515	515	-
3	Phaeophorbide *a* methyl ester (**20**)	24.4	6.6	5.6	407, 664	406, 664	405, 664	607	547, 461	547, 461	547, 461	methanol
4	Phaeophorbide *a* methyl ester epimer	25.3	6.9	6.0	404, 669	404, 669	400, 664	607	547, 461	-	-	methanol
5	Unidentified chlorin	29.8	7.7	6.3	407, 670	407, 670	388, 672	-	-	-	-	-
6	Pyrophaeophorbide *a* methyl ester (**22**)	32.1	8.0	6.8	407, 670	408, 665	408, 665	549	521, 435	521, 435	-	methanol
7	Unidentified chlorin	46.8	9.8	8.1	431, 663	431, 663	431, 663	-	-	-	-	-
8	Chlorophyll *a* (**4**)	50.8	12.3	11.0	430, 663	430, 663	430, 663	-	-	-	-	phytol
9	Unidentified chlorin	51.7	12.6	11.1	408, 666	406, 665	407, 665	-	-	-	-	-
10	Unidentified chlorin	52.6	12.9	11.4	408, 661	408, 663	408, 663	-	-	-	-	-
11	Phaeophytin *b* (**17**)	59.5	13.5	11.8	434, 658	434, 658	434, 658	885	-	-	-	phytol
12	Hydroxyphaeophytin *a* (**34**)	60.9	14.0	12.5	406, 665	406, 665	406, 665	887	609	-	-	phytol
13	Hydroxyphaeophytin *a* epimer (**35**)	62.4	14.2	-	407, 666	405, 666	-	887	-	-	-	phytol
14	Unidentified chlorin	63.9	14.4	12.9	405, 674	400, 671	400, 674	-	-	-	-	-
15	Phaeophytin *a* (**11**)	65.8	14.7	13.2	406, 665	407, 665	407, 665	871	593, 533	593, 533	593, 533	phytol
16	Pyrophaeophytin *b* (**19**)	66.7	14.5	12.7	436, 653	436, 653	414, 436, 550	827	549, 521	-	-	phytol
17	Phaeophytin *a* epimer (**32**)	68.0	15.0	13.5	407, 665	407, 665	407, 665	871	-	-	-	phytol
18	Pyrophaeophytin *a* (**19**)	73.2	15.8	14.3	408, 665	408, 665	408, 665	813	535, 507	535, 507	535, 507	phytol
19	Unidentified chlorin	77.7	16.1	15.0	408, 665	402, 661	402, 664	-	-	-	-	-
20	Unidentified chlorin	79.0	16.5	15.5	408, 665	407, 664	409, 664	-	-	-	-	-
21	Unidentified chlorin	80.3	17.3	16.0	395, 496, 656	396, 500, 661	396, 496, 567	-	-	-	-	-
22	Unidentified chlorin	81.8	17.5	16.3	395, 494, 658	398, 502, 663	397, 500, 662	-	-	-	-	-
23	Pyrophaeophorbide *a* steryl ester (**26**)	86.2	17.7	16.5	408, 666	408, 666	408, 666	903	535, 507	-	-	C_{27} sterol [c]
24	Pyrophaeophorbide *a* steryl ester (**27**)	87.4	17.9	16.8	408, 666	408, 666	408, 666	929	535, 507	-	-	C_{29} sterol [c]
25	Pyrophaeophorbide *a* steryl ester (**28**)	88.9	18.2	17.1	408, 666	408, 666	408, 666	931	535, 507	-	-	C_{29} sterol [c]
26	Unidentified chlorin	91.8	18.5	17.4	408, 666	408, 666	408, 666	-	-	-	-	-
27	Pyrophaeophorbide *a* steryl ester	92.4	18.7	17.7	408, 666	408, 666	408, 666	948	535, 507	-	-	C_{30} sterol [c]

[a] Peak number refers to the peak labels in Fig. 3.11. [b] Identification has been reported in Ruth Airs' s thesis (Airs, 2001b). [c] Tentative assignment [d] Airs et al., 2001a.

Application to a distinctly different complex mixture of pigments was evaluated by analysis of an extract from Little Long Lake (North-America Great Lakes Area, Wisconsin, sediment provided by Carles Borrego, University of Girona and extracted by Ruth Airs (Airs, 2001b)), which contains homologues of bacteriophaeophytins *d* and *c* and was analysed previously to demonstrate the separations capabilities of Airs Method A (Airs et al., 2001b). The chromatogram (Fig. 3.12a) reveals a broadly similar profile of bacteriophaeophytins *d* and *c* to that presented by Airs (Airs, 2001b) Peak identities were confirmed by the *m/z* values of the protonated molecules $[M+H]^+$ and MS^2 product ions (Table 3.9). The slightly shorter retention times observed than in the previous study (Airs, 2001b) are due to the absence of a guard column (Experimental). In addition, the absorption maxima in the online UV-Vis spectra were a few nanometres lower (Table 3.9) than in the previous study (Airs, 2001b) due to a different photodiode array detector being used.

Comparison of the HPLC chromatograms obtained by Airs Method A (Airs et al., 2001a) and the two UHPLC methods 6 (Fig. 3.12b) and 10 (Fig. 3.12c) reveals that, at more than four times the total analysis time of the UHPLC methods, Airs Method A (Airs et al., 2001a) gives more efficient separation. For example, peaks 10 and 11 (Fig. 3.12a, Table 3.9) were separated whereas they co-eluted using UHPLC Methods 6 and 10 (Fig. 3.12b and 3.12c, respectively). Furthermore, owing to the greater peak width, Airs Method A (Airs et al., 2001a) enabled MS^2 to be observed for all peaks (Table 3.8), while only product ions from the first two components (peak no. 1 and 2; Table 3.9) were obtained by Method 6 and four components (peak no. 1, 2, 3 and 16; Table 3.9) obtained by Method 10 during mass-dependent MS/MS. On the other hand, the two optimal UHPLC methods both allowed elution of all components in under 20 min, representing a 5-5.8 fold reduction in total run time. The combination of the online UV-Vis absorption and mass spectra (Table 3.9) enabled the identification of the components in the chromatograms in Fig. 3.12b and c. Notably, the chromatogram obtained by Method 6 (Fig. 3.12b) reveals higher resolution of components in the more apolar regions (peaks 10-16, Fig. 3.12b and Table 3.9) than Method 10 (Fig. 3.12c). Also, slight separation could be observed for peaks 12, 13 and 14. This can be rationalised by the less polar solvent composition in this region effecting greater separation of the components. In the

more polar regions, the UHPLC-chromatogram obtained by Method 10 shows better resolution of peaks 1 and 2, as well as peaks 6 and 7 (Fig. 3.12c, Table 3.9), attributable to the greater initial polarity of the mobile phase (10% ammonium acetate) which has allowed greater retention and resolution of polar components.

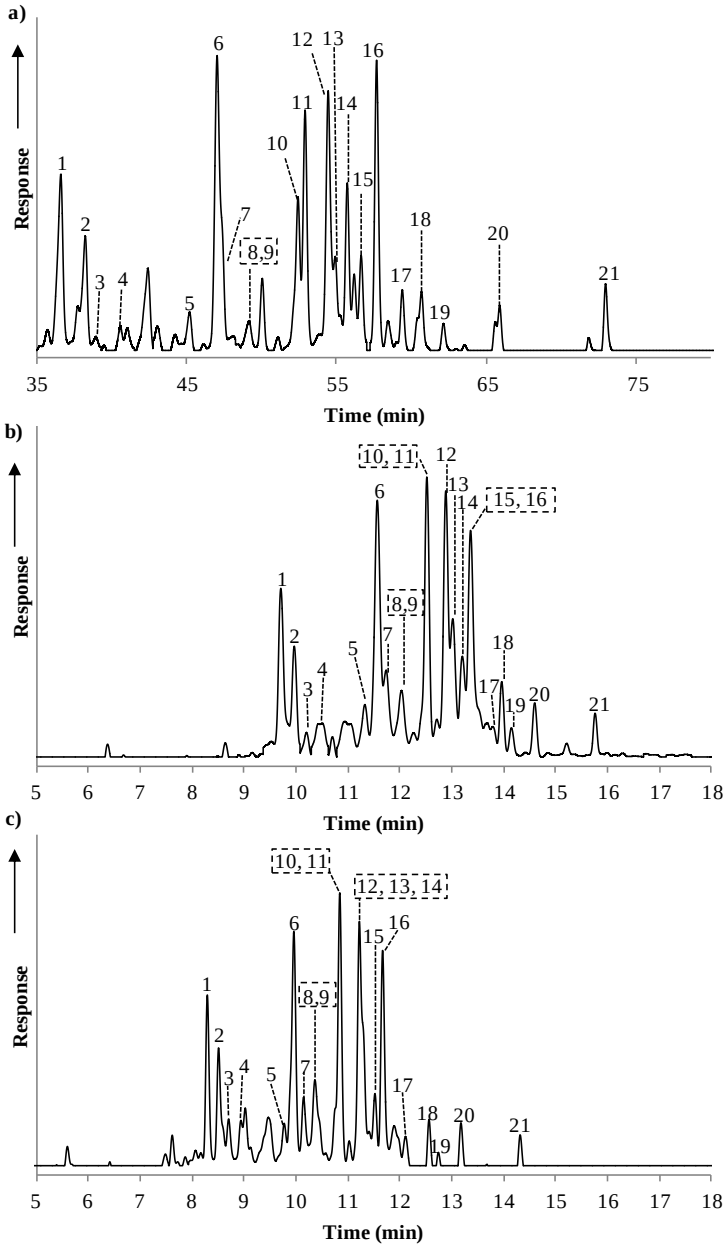

Figure 3.12. Expansion section of LC-PDA (300-800 nm) chromatogram of the sediment extract from Little Long Lake obtained using (a) HPLC Airs Method A (Table 3.1), (b) the UHPLC Method 6 (Table 3.4) and (c) the UHPLC Method 10 (Table 3.6). For peak assignment, see in Table 3.9.

Table 3.9. Peak assignments for bacteriophaeophytin *c* and *d* homologues in a pigment extract from Little Long Lake water particulates obtained by HPLC Airs Method A (Airs et al., 2001) and UHPLC Method 6 and Method 10. (continued over)

Peak number [a, b]	**t_R (min)**			**Main UV/vis absorption bands (nm)**			**Assignment** [b,c]	**$[M+H]^+$** [b] **(*m/z*)**	**Diagnostic fragment ions** [b]			**Esterifying alcohol** [b, d]	**[C-8, C-12] Substituents** [b]
	Airs Method A [d]	UHPLC Method 6	UHPLC Method 10	Airs Method A [d]	UHPLC Method 6	UHPLC Method 10			Airs Method A [d]	UHPLC Method 6	UHPLC Method 10		
1	36.6	9.7	8.3	404, 657	404, 657	404, 657	Bphe *d* (**40**)	771	567	567	567	Farnesol	[Et, Et] / [*n*-Pr, Me]
2	38.3	10.0	8.5	410, 667	409, 667	409, 668	Bphe *c* (**39**)	785	581	581	581	Farnesol	[Et, Et] / [*n*-Pr, Me]
3	38.97	10.2	8.7	404, 654	404, 654	404, 654	Bphe *d* (**40**)	785	581	-	785	Farnesol	[*n*-Pr, Et] / [*i*-Bu, Me]
4	40.7	10.5	8.9	410, 667	409, 667	410, 667	Bphe *c* (**39**)	799	595	-	-	Farnesol	[*n*-Pr, Et] / [*i*-Bu, Me]
5	45.3	11.3	9.8	404, 657	404, 657	404, 657	Bphe *d* (**40**)	839	567	-	-	Geranylgeraniol	[Et, Et] / [*n*-Pr, Me]
6	47.0	11.6	10.0	404, 657	405, 657	405, 658	Bphe *d* (**40**)	789	567	-	-	Hexadecenol	[Et, Et] / [*n*-Pr, Me]
7	47.0	11.8	10.1	404, 657	405, 677	405, 658	Bphe *d* (**40**)	853	581	-	-	Geranylgeraniol	[*n*-Pr, Et] / [*i*-Bu, Me]
8	49.2	12.1	10.4	404, 657	405, 657	405, 657	Bphe *c* (**39**)	803	581	-	-	Hexadecenol	[Et, Et] / [*n*-Pr, Me]
9	49.2	12.1	10.4	404, 657	405, 657	405, 657	Bphe *d* (**40**)	867	595	-	-	Geranylgeraniol	[*i*-Bu, Et] /[*n*-Pent, Me]
10	52.5	12.5	10.9	404, 657	405, 657	404, 657	Bphe *d* (**40**)	817	567	-	-	Octadecenol	[Et, Et] / [*n*-Pr, Me]

Peak number [a, b]	t_R (min)			Main UV/vis absorption bands (nm)			Assignment [b,c]	$[M+H]^+$ [b] (*m/z*)	Diagnostic fragment ions [b]			Esterifying alcohol [b, d]	[C-8, C-12] Substituents [b]
	Airs Method A [d]	UHPLC Method 6	UHPLC Method 10	Ai_{rs} Method A [d]	UHPLC Method 6	UHPLC Method 10			Airs Method A [d]	UHPLC Method 6	UHPLC Method 10		
11	52.9	12.5	10.9	404, 657	405, 657	404, 657	Bphe *d* (**40**)	791	567	-	-	Hexadecenol	[Et, Et] / [*n*-Pr, Me]
12	54.5	12.9	11.2	405, 657	405, 657	405, 657	Bphe *d* (**40**))	831	581	-	-	Octadecenol	[*n*-Pr, Me] / [*i*-Bu, Me]
13	55.0	13.0	11.2	405, 657	405, 657	405, 657	Bphe *d* (**40**)	805	581	-	-	Hexadecanol	[*n*-Pr, Et] / [*i*-Bu, Me]
14	55.7	13.2	11.2	404, 657	405, 657	405, 657	Bphe *d* (**40**)	805	567	-	-	Heptadecanol	[Et, Et] / [*n*-Pr, Me]
15	56.7	13.4	11.5	404, 657	404, 657	405, 657	Bphe *d* (**40**)	819	581	-	-	Heptadecanol	[*n*-Pr, Et] / [*i*-Bu, Me]
16	57.7	13.4	11.7	405, 657	404, 657	405, 657	Bphe *d* (**40**)	819	581	-	581	Heptadecanol	[*n*-Pr, Et] / [*i*-Bu, Me]
17	59.4	13.8	12.1	405, 656	405, 657	404, 657	Bphe *d* (**40**)	833	595	-	-	Heptadecanol	[*i*-Bu, Et] / [*n*-Pent, Me]
18	60.7	14.0	12.7	406, 665	406, 666	405, 666	OH-Phe *a* (**34**)	887	609, 591	-	-	Phytol	[Et, Me]
19	62.2	14.1	12.8	407, 664	406, 667	408, 666	OH-Phe *a*' (**35**)	887	609, 591	-	-	Phytol	[Et, Me]
20	65.8	14.6	13.2	399, 665	399, 665	399, 665	Phe *a* (**11**)	871	593, 533	-	-	Phytol	[Et, Me]
21	72.9	15.8	14.3	408, 665	408, 665	408, 665	Pphe *a* (**18**)	813	535, 507	-	-	Phytol	[Et, Me]

[a] Peak number refers to the peak labels in Fig. 3.12.

[b] Identification has been reported in Ruth Airs' s thesis (Airs, 2001b).

[c] Bphe = bacteriophaeophytin; OH-Phe = hydroxyphaeophytin; Phe = phaeophytin; Pphe = pyrophaeophytin.

[d] Airs et al., 2001a.

3.3 Conclusions

UHPLC methods have been developed and optimised for two different types of C_{18} stationary phase. Method 6 was developed on two Acclaim 120 C_{18} columns (100 mm × 2.1 mm i.d.) with 2.2 µm particle size. Method 10 was developed on an Acquity UPLC BEH C_{18} (1.7 µm, 150 mm x 3 mm i.d.) column. Both methods have been demonstrated to be capable of separating the complex distributions of chlorophylls present in the extracts from Priest Pot and bacteriochlorophyll homologues in Little Long Lake. Although separation efficiency was not as good with Method 6 (23 min) and Method 10 (20 min) as with Method A (115 min), the majority of the components of the extracts could be identified from their online UV-Vis absorption and mass spectra. Notably, some isobaric pigments require MS^2 data to be distinguished. The two UHPLC Methods 6 and 10 lead to significant reductions in solvent consumption (≥ 85 %), sample injected (90%), and analysis time (≥ 80 %). Thus, these methods will enable the high throughput screening of extremely complex pigment distributions in sediment extracts where the greater analysis times of the Airs Method prove prohibitive.

Chapter 4

Application of ASE and UHPLC to high resolution studies of pigments in sediment cores

4.1. Introduction

Photosynthetic pigments preserved in aquatic sediment have been used successfully in palaeoenvironmental reconstruction (e.g. Squier et al., 2002; Squier et al., 2005; Tani et al., 2009). At one level, variations in chlorin pigment concentrations have been used to estimate the intensity of primary production in the past (Harris et al., 1996). At a more detailed level of investigation, many previous studies have used variations within pigment distributions to reveal past changes in environmental conditions. For example, interpretation of the algal and bacterial pigment signatures from Kirisjes Pond, a low altitude lake in Antartica, indicated changes in relative sea level (Squier et al., 2002). Similarly, variations in the composition of the photosynthetic community in a meromictic lake indicated changes in water column stratification that relate to climatic changes (Romero-Viana et al., 2010) and in periods of ice cover for Progress Lake, another Antarctic lake (Squier et al., 2005). The transformation products of photosynthetic pigments can also be used as environmental indicators; for example, sedimentary steryl chlorin esters (SCEs), which form in the gut of zooplankton, can indicate the grazing of phytoplankton (King and Repeta, 1991; Soma et al., 2001; Soma et al., 2007; Talbot et al., 1999a; Talbot et al., 1999b) and purpurins, formed by the oxidative scission of ring E, can indicate oxidising conditions in the water column (Naylor and Keely, 1998).

Owing to the value of photosynthetic pigments as indicators in palaeoenvironmental interpretation, high resolution studies of sediment sequences have the potential to be of great value for obtaining more detailed reconstruction of palaeoenvironments. Palaeoenvironmental reconstructions typically involve the profiling of biomarkers in sediment cores. This is done by sampling horizons of the core, extracting the organic components using solvent, analysing the extract and interpreting the distributions of biomarkers as a function of depth (and therefore time) (Castaneda and Schouten, 2011; Squier et al., 2002; Squier et al., 2004; Tani et al., 2009; Watanabe et al., 2012). As the vertical span of each horizon represents a period of time, determined by the accumulation rate of the sediment, the extract from each represents an average for that period. Thus, variations occurring on a shorter timescale will not be visible and will impact the accuracy of the palaeoenvironmental reconstruction. The accuracy of the reconstruction can be improved by increasing the sampling

resolution, sampling narrower horizons at higher frequency to observe changes occurring on smaller timescales. The limits to high resolution studies are a) the limit of detection and b) the speed of analysis. Sampling narrower horizons naturally results in less material to be analysed, requiring an analytical technique with good limits of detection. The resulting increase in the number of samples with increased stratigraphic resolution increases the time needed to process the samples, requiring high throughput methods for extraction and analysis.

High resolution studies have been developed based on spectroscopic methods. For example, chlorophyll *a* concentrations have been analysed by spectrofluorometry (Pirtle-Levy et al., 2009; Sane et al., 2011). Notably, however, the pigment analysed by this method and attributed to chlorophyll *a* was in fact a mixture of chlorophylls (Sane et al., 2011). More detailed analysis of photosynthetic pigments for palaeoenvironmental reconstruction is based on the use of chromatographic techniques (Romero-Viana et al., 2010; Squier et al., 2002; Squier et al., 2004; Tani et al., 2009; Watanabe et al., 2012). Although such methods can generate the stratigraphic profiles of each individual pigment, they are more time consuming. As a result, the methods developed for the rapid extraction and analysis of sedimentary pigments (Chapters 2 and 3) are evaluated in this chapter. The high-throughput methods developed are applied to the study of sediment cores from three Antarctic lakes, Lake Heidi, Lake Nella and Lake 14 from Larsemann Hills, to provide greater detail than was possible with previous methods. The evaluation of the methods developed is focused on the analytical performance and potential for use in high-throughput analysis rather than on detailed palaeoenvironmental interpretation.

4.2. Results and Discussion

4.2.1. Sample set

Three sediment cores collected from Lake Heidi (latitude 76°06′, longitude 69°24′), Lake Nella (latitude 76°22′, longitude 69°24′) and Lake LH14 (latitude 76°07′, longitude 69°24′), Larsemann Hills, East Antarctica (Hodgson et al., 2001). The locations of these Lakes are shown in Fig. 4.1. The cores were sectioned in the field at 1 cm resolution with depth by the British Antarctic Survey team and the sections were stored below -20°C. Results from radiocarbon dating reveals their similar modern age at the core tops, while the age of the bases of the cores varied (1380 ± 40, 1570 ± 50 and 1650 ± 50; yr BP ± 1σ (Hodgson et al., 2001) for Lake Heidi, Lake Nella and Lake 14; respectively). In total there were 91 sectioned sediment samples from Lake Heidi (46 samples; depth 1-45 and 47-48 cm), Lake Nella (23 samples; depth 3-25 cm) and Lake LH14 (22 samples; depth 1-22 cm) which were analysed in this study. The analytical methods for use in high resolution stratigraphic profiling of sedimentary pigments, sampling and analysis were applied to the entire sample set, representing all of the individual horizons from each core, as if they represented a single batch. This was done in order to test the suitability of the methods for application in intensive studies of sediment cores.

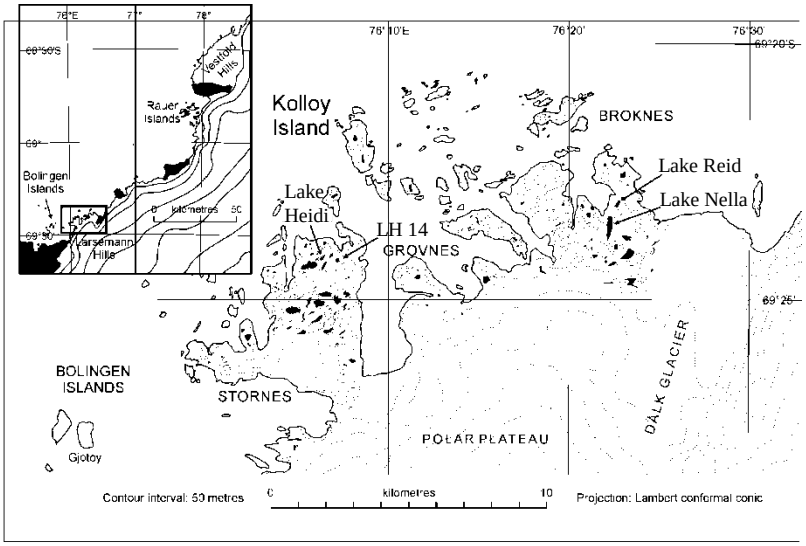

Figure 4.1. Locations of Lake Heidi, Lake Nella and Lake LH14 in Larsemann Hills, Antarctica.

4.2.2. Analytical workflow

The high-throughput methods developed in Chapters 2 and 3 were used for sediment preparation, pigment extraction and analysis. A flow diagram outlining the different stages and timeframes associated with the analysis of the 91 sediment samples by the conventional and newly developed analytical procedures (Fig. 4.2) allows comparison of the timescales involved for the two methods. The scheme shows that the extraction and analysis by the conventional method would take 30 days based on operations being performed in a linear fashion. By contrast, ASE extraction and UHPLC analysis reduces the time taken for these operations by about 4 times for the sample set (7 days, Fig. 4.2). When the additional preparation steps of freeze drying, grinding and sieving are considered, the analysis time is still 2.7 times shorter (12 days, Fig. 4.2) than for the conventional method in which the samples were processed wet and with mixing to homogenise them (total time 32 days, Fig. 4.2). The preparation steps are necessary to obtain homogenised samples and generate more accurate data (Chapter 2), hence they are equally applicable to studies using conventional extraction and analysis methods. Thus, a more appropriate comparison, incorporating the sample preparation steps in the conventional method, would give a total of 35 days for the analysis of the complete sample set. The efficiency of ASE extraction reported is based on a rate of 16 samples/day, the limitation being the number of extraction cells in the laboratory. This extraction step could be increased to 24 samples/day if more extraction cells were available (reducing the processing time by 1.5 days). Moreover, the duration for the high-throughput method could be reduced further, to less than 12 days for the whole process, by processing multiple batches in parallel (e.g. freeze drying one batch while another is subjected to automated ASE extraction). By contrast to the high-throughput approach, the lack of automation in the conventional method means that processing parallel batches of samples is not possible. Clearly, therefore, the high throughput method offers a significant advantage in sample throughput.

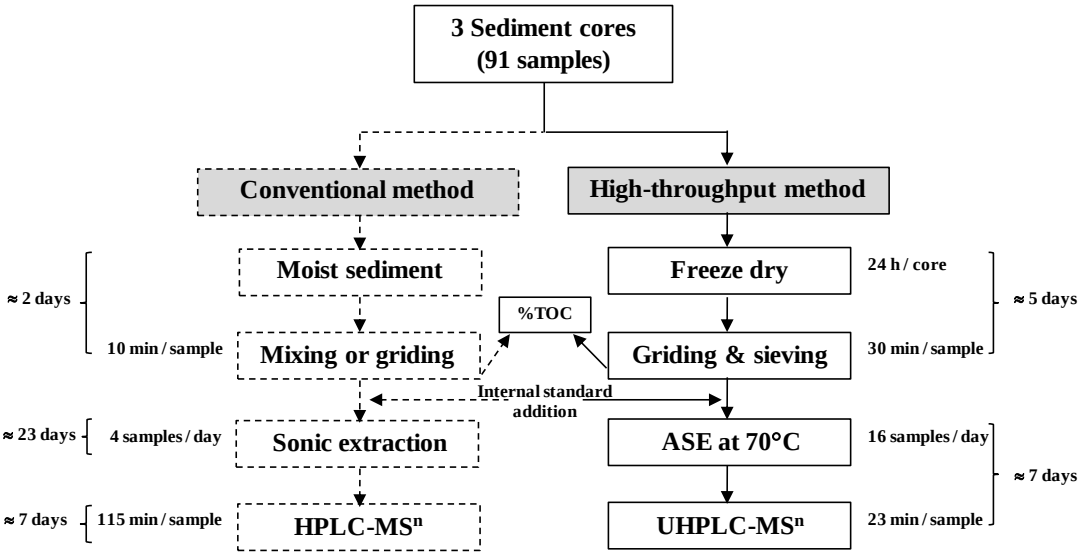

Figure 4.2. Procedure for the processing of 91 sediment samples. The solid line illustrates the time taken to process 91 samples by the high-throughput method while the dashed line refers to the estimated time to process the 91 samples using the conventional method for pigment extraction.

In terms of solvent consumption, the high-throughput method using the ASE at 70°C (Chapter 2) and the UHPLC method (Chapter 3) requires 5 and 5.8 times less solvent than for sonic extraction and HPLC analysis using Airs Method A (115 min), respectively. Similarly, the sample requirement was reduced to around 50-80 mg of dried sediment for Lake Heidi and Lake 14 (see Table 6.2, Chapter 6) while that required for Lake Nella varied from 12.4 - 286 mg (see Table 6.2, Chapter 6) dependent on the amount of sample available from the British Antarctic Survey. This represents a dramatic reduction in sample requirement compared with that conventionally used (3-5 g; (Airs, 2001b).

An internal standard was added to the sediment before ASE. This technique delivers high precision for quantitative chromatography (Skoog et al., 1998), reduces uncertainties introduced by sample injection on chromatography (Skoog et al., 1998) and can correct for errors/losses arising during the extraction process. A synthetic pyrophaeophorbide *a* stearyl (C_{18}) ester (**41**) was selected as the standard because it was not naturally present in the pigment extract and eluted in the chromatographic region between pyrophaeophytin *a* and pyrophaeophorbide *a* steryl ester, where other

pigments do not elute. Thus, the synthetic pigment standard did not interfere with other analytes in the pigment extract. The pyrophaeophorbide *a* steryl C_{18} ester (**41**) (3.03 nmol, $[M+H]^+$ *m/z* 787, Table 4.1) was spiked into each sediment sample in the ASE extraction cell prior to extraction. Each pigment in the extract was calculated based on this internal standard concentration, corrected where necessary by the molar extinction coefficient for each particular pigment. The formula for calculation and molar extinction coefficients are given in the Experimental (Section 6.6.2 and Table 6.5, Chapter 6).

4.2.3 Lake Heidi

4.2.3.1 Pigment distribution

The sediment extracts from Lake Heidi were analysed by UHPLC with online UV/vis and MS^n detection. Notably, analysis of the first 15 samples from depths 1-2 to 15-16 cm was performed on the UHPLC system before replacement of the pump piston seals was carried out. Thus, the chromatographic retention times of the pigments obtained from these runs were slightly later than for chromatograms obtained after replacement of the seals; this did not affect peak assignments, however, as these were based on their UV/vis and MS^n spectra (Table 4.1). Comparison of all of the chromatograms for the core analysis reveals four distinct distribution patterns of chlorin pigments. The first pigment distribution pattern was found in sediment extracted from the depth 1-2 cm (Fig. 4.3a). Besides phaeophytin *a* (**11**, peak 20 Fig. 4.3a), which was a dominant peak in the chromatogram, the extract contained chlorophyll *a* (**4**) (peak no. 11, Fig. 4.3a), its oxidative transformation product hydroxychlorophyll *a* (**42**) (peak no. 7, Fig. 4.3a) and chlorin e_6 dimethyl phytyl ester (**16**) (peak no.15, Fig. 4.3a). The relative abundance of phaeophytin *a* (**11**) was greater in the second distribution pattern obtained from depths 2-3 (Fig. 4.3b) through to 5-16 cm. Below this horizon the extracts exhibited a steadily decreasing relative abundance of phaeophytin *a* (**11**) and increasing relative abundance of pyrophaeophytin *a* (**18**) until the relative abundance of the both peaks were similar (third pattern, depth 23-24 cm, Fig. 4.3c). The fourth and final pattern (Fig. 4.3d) was obtained from sediment extracted from 24-25 cm depth. In this pattern, pyrophaeophytin *a* (**18**) is the dominant peak. Even without

quantification of pigments, the high-throughput method can be used as a screening method to generate a rough pigment distribution profile that enables samples of similar distributions to be grouped and a representative selection chosen for further analysis as necessary. For example, if more data is required, extracts can be analysed again using HPLC-MS^n with Airs Method A (Airs et al., 2001a).

Notably, the sample sizes of Lake Heidi sediment used for the high-throughput methods were below 50-80 mg (see Table 6.2, Chapter 6) and gave good signals on the UHPLC chromatograms. For example, Lake Heidi sediment around 73, 76 and 78 mg obtained from depths 2-3, 23-24 and 24-25 cm; respectively, show good quality UHPLC chromatograms (Fig. 4.3).

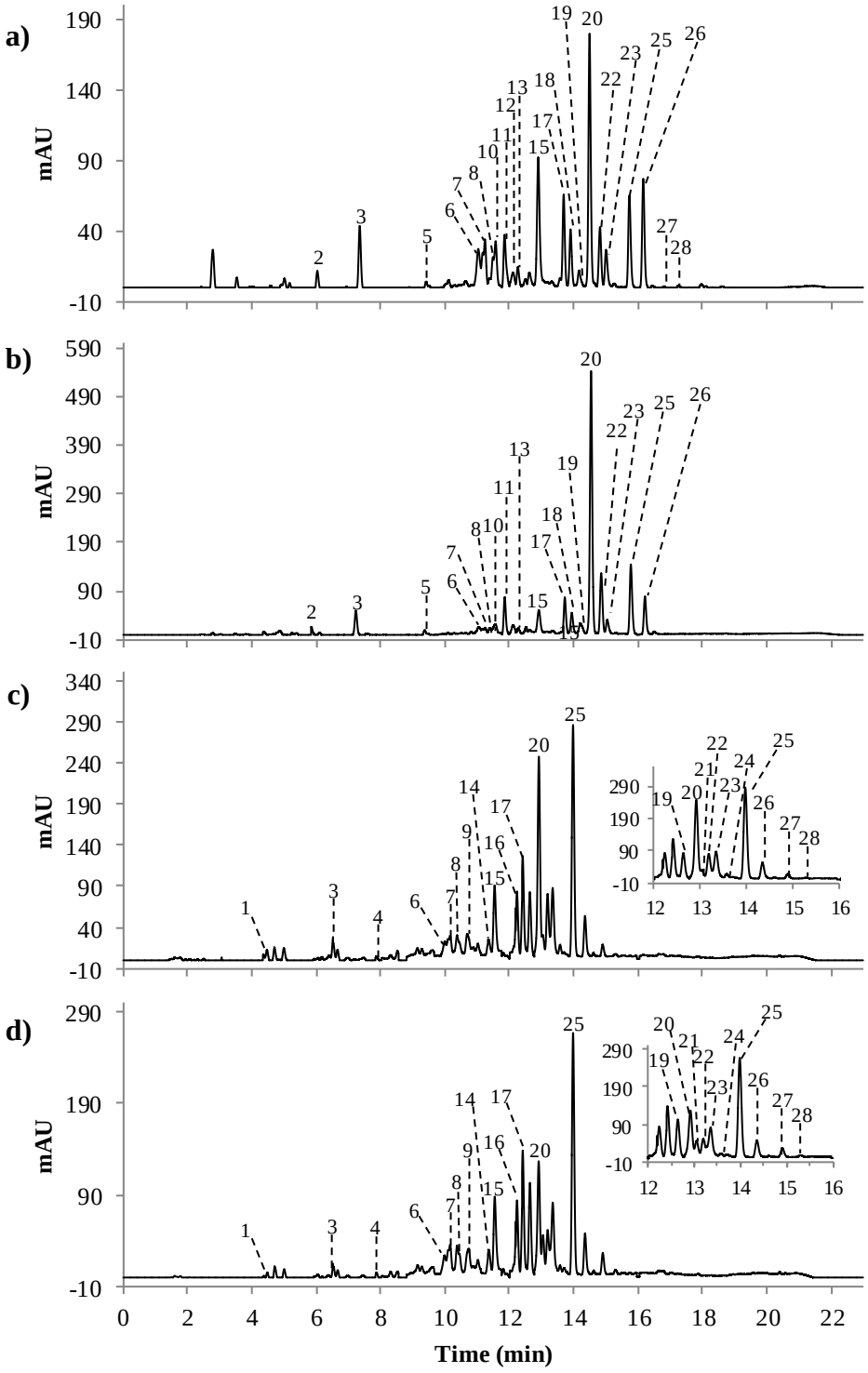

Figure 4.3. UHPLC-PDA (300-800 nm) chromatogram of sediment extracts from Lake Heidi (a) depth 1-2 cm, (b) depth 2-3 cm, (c) depth 23-24 cm and (d) depth 24-25 cm obtained using UHPLC method 10 (Table 3.6 in Chapter 3). Insert shows an expansion of the chromatographic region at 12-16 min. For peak assignment, see Table 4.1.

Table 4.1. Peak identification of pigments extracted from Lake Heidi sediment core.

Peak	t_R (min)	UV/vis absorption (nm)	$[M+H]^+$ (*m/z*)[b]	Fragment ion MS^n (*m/z*)	Assignment
1	4.6	403, 664	533	-	Chlorophyllone (**24**)
2	6.0[a]	406, 664	607	547, 461	Phaeophorbide *a* (**20**)
3	6.5	409, 665	549	521, 435	Pyrophaeophorbide *a* (**22**)
4	7.9	400, 422, 651	610	582, 496	Unidentified metal chlorin
5	9.2[a]	404, 658	-	-	Unidentified chlorin
6	10.0	417, 653	587	-	Unidentified chlorin
7	10.1	428, 663	887	631, 558	Hydroxychlorophyll *a* (**42**)
8	10.4	418, 665	-	-	Unidentified chlorin
9	10.7	413, 655	-	-	Unidentified chlorin
10	11.6[a]	417, 654	-	-	Unidentified metal chlorin
11	11.9[a]	429, 663	871	593, 533	Chlorophyll *a* (**4**)
12	12.1[a]	407, 664	-	-	Unidentified chlorin
13	12.3[a]	420, 663	871	593, 533	Chlorophyll *a* epimer (**38**)
14	11.4	417, 656	-	-	Unidentified chlorin
15	11.5	399, 667	903	-	Chlorin e_6 dimethyl phytyl ester (**16**)
16	12.2	407, 665	590	-	Unidentified chlorin
17	12.4	408, 665	887	-	Hydroxyphaeophytin *a* (**34**)
18	13.9[a]	408, 665	887	609, 591	Hydroxyphaeophytin *a* epimer (**35**)
19	12.6	400, 669	917	-	Purpurin-7 phytyl ester (**14**)
20	12.9	406, 666	871	593, 533	Phaeophytin *a* (**11**)
21	12.9	399, 420, 651	-	-	Unidentified metal chlorin
22	13.2	406, 666	871	593, 533	Phaeophytin *a* epimer (**32**)
23	13.4	359, 406, 543, 696	843	565, 503	Purpurin-18-phytyl ester (**15**)
24	13.6	399, 421, 651	-	-	Unidentified metal chlorin
25	14.0	408, 665	813	535, 507	Pyrophaeophytin *a* (**18**)
26	14.3	321, 408, 665	787	759, 507	Pyrophaeophorbide *a* C_{18} ester (**41**)
27	14.9	400, 422, 651	874[c]	-	Copper pyrophaeophytin *a* (**43**)
28	15.3	401, 422, 650	848[c]	820[c], 496	Copper pyrophaeophorbide *a* C_{18} ester (**44**)

[a] Retention time obtained from analysis before replacing the rear seal on the instrument. [b] All metallated pigments appear in MS as their demetallated counterparts due to post column demetallation prior to MS (Airs and Keely, 2000). [c] Copper complex which cannot be demetallated by post column formic acid.

In addition to advantages in terms of saving time (4 and 5 times for extraction and UHPLC analysis, respectively, Fig. 4.2), the lower solvent consumption and lower sample size requirement, the high throughput methods generate high quality data sets. This was illustrated by applying error bars representing the relative errors measured during development of the ASE method (Chapter 2) to the sediment from Lake Heidi. The Estanya sediment (in Chapter 2) was prepared in a similar way to that of Lake Heidi (freeze dried, ground and sieved, extracted by ASE at 70°C with

acetone) and gave approximate errors of 20% and 10% (± 1 standard deviation) for pigments yields of less than 0.02 and greater than 0.02 (μmol), respectively (values represent average percentage errors calculated from those of ASE at 70°C in Table 2.10, Chapter 2). By contrast, the conventional sonic extraction method from moist Priest Pot sediment of gave approximately 25% and 20% error (± 1 standard deviation) for pigment yields for less than 0.02 and greater than 0.02 (μmol), respectively (values represent average percentage errors calculated from those of sonic extraction in Table 2.1, Chapter 2). The errors estimated for sonic extraction (Table 2.1, Chapter 2) are a combination of both the errors associated with extraction method and those associated with the extraction of moist rather than freeze dried sediment. Comparison of the pigment profiles throughout the Lake Heidi core with each of the two sets of error bars (from ASE at 70°C and sonic extraction) applied is illustrated in Figs. 4.4a and b, respectively. It is clear that there is a significant degree of uncertainty associated with profiles generated from sonic extraction of moist sediment (Fig. 4.4b) with the potential for variations in sedimentary components to be both moderated and exaggerated within the boundaries indicated by the error bars. By contrast, there is a greater confidence in the profiles generated from freeze dried sediment that has been ASE extracted (Fig. 4.4a). For example, purpurin-7 phytyl ester, pyrophaeophytin *a* and phaeophytin *a* yields in the regions numbered 1 to 6 (Fig. 4.4a) show significant changes, but these are not significantly different when the error bars from the conventional sonic extraction method are applied (Fig. 4.4b). Clearly, using the high throughput methods together with the sample preparation methods developed in this work can improve the quality of data, providing greater confidence that the observed profiles accurately reflect the genuine variations in sedimentary pigment yields and, hence, enabling more reliable interpretation of the significance of the distributions. Accordingly, all pigment yields are represented in this chapter with ± 1 s.d. (n = 3) to reflect errors appropriate to ASE at 70°C followed by chromatographic analysis.

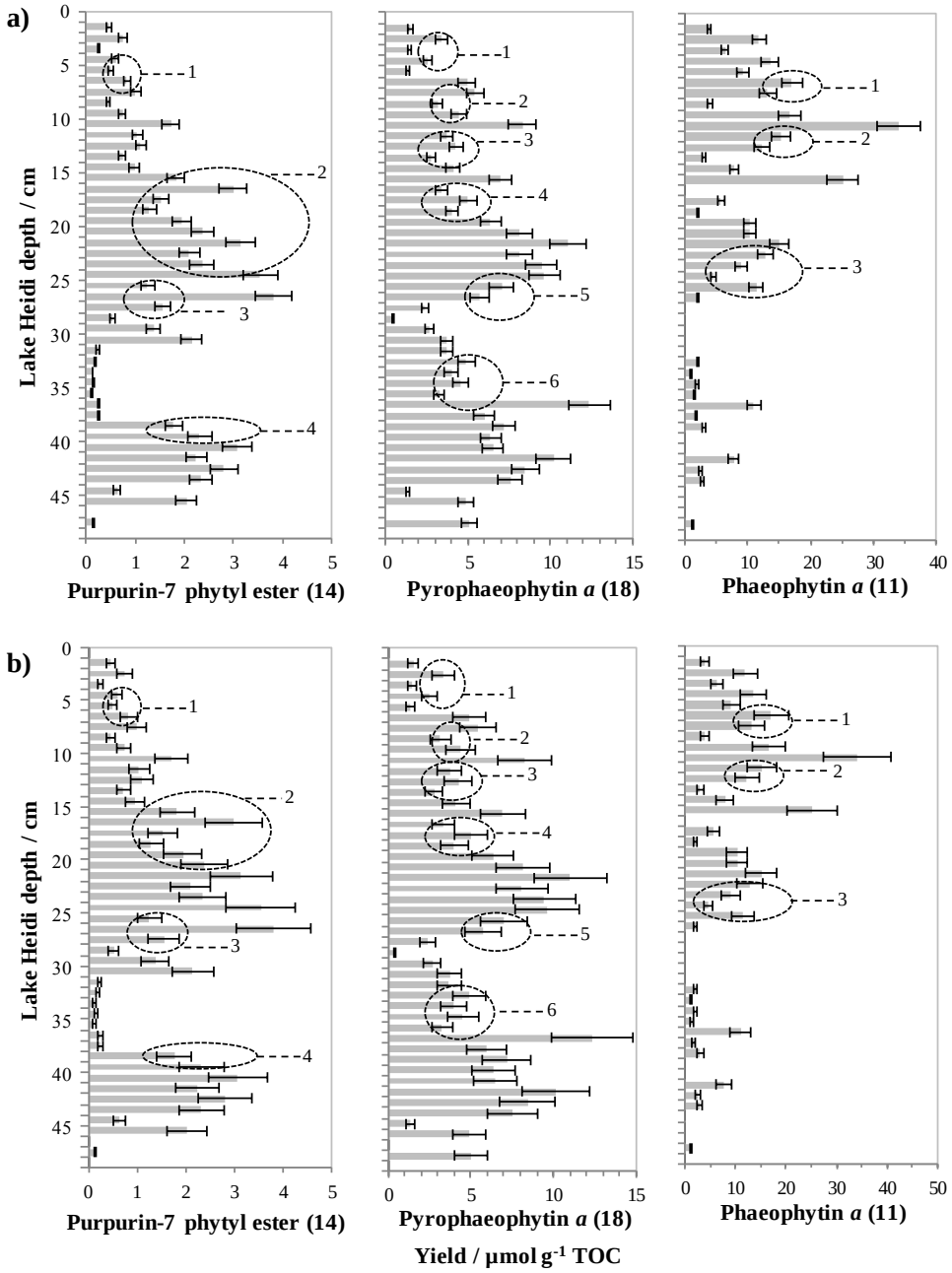

Figure 4.4. Purpurin-7 phytyl ester (**14**), pyrophaeophytin *a* (**18**) and phaeophytin *a* (**11**) yields in sediment extracts from Lake Heidi. (a) With 10% and 20% error estimate applied when the pigment yield is less than 0.02 and greater than 0.02, respectively (error bars obtained from average error of Estanya sediment extraction using ASE at 70°C, Chapter 2). (b) With 20% and 25% error estimate applied when the pigment yield is less than 0.02 and greater than 0.02, respectively (error bars obtained from the results of sonic extraction of moist Priest Pot sediment, Chapter 2).

4.2.3.2 Pigment yields stratigraphic profile

The pigment yields profile of Lake Heidi sediment core extracted and analysed by the high-throughput method indicates both regular transformation products of chlorophyll; such as, pyrophaeophorbide *a* (**22**), phaeophytin *a* (**11**) and pyrophaeophytin *a* (**18**) (Fig. 4.5a) and oxidised transformation products; such as hydroxychlorophyll *a* (**42**), hydroxyphaeophytin *a* (**34**), chlorin e_6 dimethyl phytyl ester (**16**), purpurin-7 phytyl ester (**14**) and purpurin-18 phytyl ester (**15**) (Fig. 4.5b) are presented. These profiles provide information on the environmental conditions at the time of deposition. Total pigment yields reflect chlorin accumulation and have been used to estimate the intensity of palaeo-productivity (Harris et al., 1996). Total pigment yields from Lake Heidi generally fluctuate around 10-30 μmol g^{-1} TOC with a maximum at 10-11 cm depth (~70 μmol g^{-1} TOC). This suggests that the sediment at depth 10-11 cm reflects deposition during a period when primary productivity was high. In addition, the presence of chlorophyll *a*, which still has its complexed magnesium, found from the depth 1-16 cm indicates good preservation. After 16-17 cm depth, chlorophyll *a* (**4**) is largely absent, total pigment yields compared to depth 15-16 cm are generally lower and the abundance of oxidised transformation products increase. For example, the abundance of purpurin-18 phytyl ester (**15**) increases dramatically below the upper 15 cm and remains high to the bottom of the core. The lower yields of total pigment and abundance of oxidised pigments products indicates that the lower portion of the Lake Heidi core was deposited under a more oxidising water column (1380 ± 40 yr. BP, Hodgson et. al, 2001). The systematic changes in the profiles of non-oxidised versus oxidised pigments with depth, but with subtle differences in the profiles of individual compounds within each class, add further confidence that the trends in the data accurately reflect changes in environmental conditions at the time of sediment deposition.

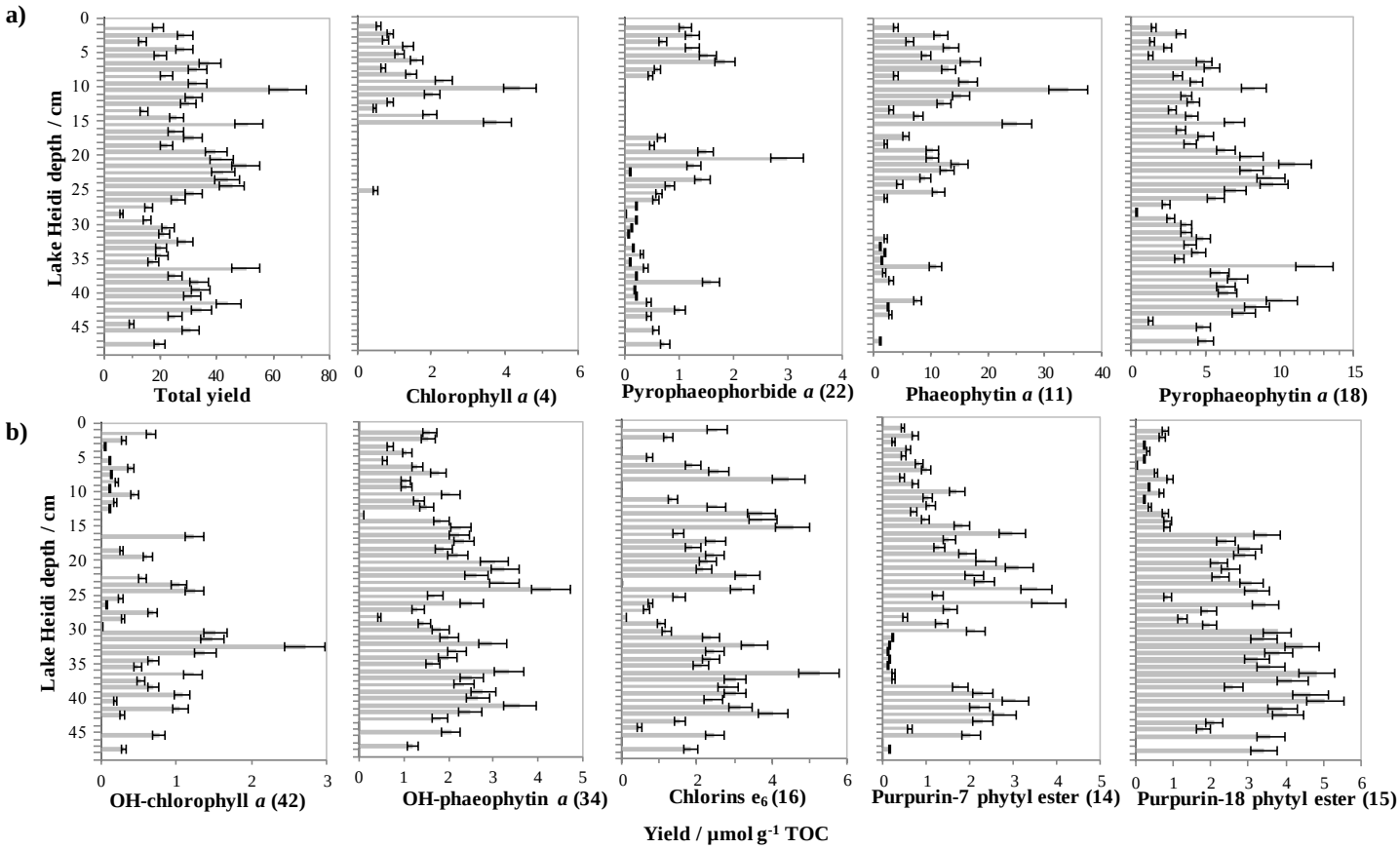

Figure 4.5. Yields of (a) total pigments and regular transformation (of pigment) products and (b) oxidative pigment transformation products obtained from Lake Heidi sediment. Error bars represent ± 1 standard deviation (n = 3) estimated from study of the Estanya sediment extraction using ASE 70°C (in Chapter 2).

4.2.4 Lake Nella (LH72)

4.2.4.1 Pigment distribution

Unlike the Lake Heidi sediment core, the UHPLC chromatograms obtained from Lake Nella pigment extract revealed a similar pigment distribution from 3-4 cm depth at the core top to 23-24 cm depth. In general, the component with the highest relative abundance in the chromatograms was the copper complex of the internal standard (peak no. 17, Table 4.2 and Fig. 4.6a). Only chromatograms obtained from the extracts from depths 24-25 and 25-26 cm (Fig. 4.6b and c; respectively, Table 4.2) show relative abundances of the natural chlorophyll derivatives above those of the copper pyrophaeophorbide *a* C_{18} ester (**44**) ($[M+H]^+$ *m/z* 848 and fragment ions at *m/z* 820 and 496, Table 4.2).

Table 4.2. Peak identification of pigments extracted from Lake Nella sediment core.

Peak	t_R (min)	UV/vis absorption (nm)	$[M+H]^+$ [a] (*m/z*)	Fragment ion MS^n (*m/z*)	Assignment
1	6.5	409, 665	549	521, 435	Pyrophaeophorbide *a* (**22**)
2	7.9	400, 422, 651	610	-	Unidentified metal chlorin
3	11.9	434, 650	885	-	Phaeophytin *b* (**17**)
4	12.1	329, 427, 657	849	-	Unidentified metal chlorin
5	12.2	407, 665	590	531, 485	Unidentified chlorin
6	12.4	408, 665	887	609, 591	Hydroxyphaeophytin *a* (**34**)
7	12.6	400, 669	917	-	Purpurin-7 phytyl ester (**14**)
8	12.9	406, 666	871	593, 533	Phaeophytin *a* (**11**)
9	12.9	399, 420, 651	-	-	Unidentified metal chlorin
10	13.1	395, 409, 648	-	-	Unidentified metal chlorin
11	13.2	406, 666	871	593, 533	Phaeophytin *a* epimer (**32**)
12	13.3	387, 439, 678	-	-	Unidentified metal chlorin
13	13.4	359, 406, 543, 696	843	565, 503	Purpurin-18-phytyl ester (**15**)
14	14.0	408, 665	813	535, 507	Pyrophaeophytin *a* (**18**)
15	14.3	321, 408, 665	787	759, 507	Pyrophaeophorbide a C_{18} ester (**41**)
16	14.9	400, 422, 651	874[b]	-	Copper pyrophaeophytin *a* (**43**)
17	15.3	401, 422, 650	848[b]	820[b], 496	Copper pyrophaeophorbide *a* C_{18} ester (**44**)

[a] All metallated pigments appear in MS as their demetallated counterparts due to post column demetallation prior to MS (Airs and Keely, 2000). [b] Copper complex which cannot be demetallated by post column formic acid.

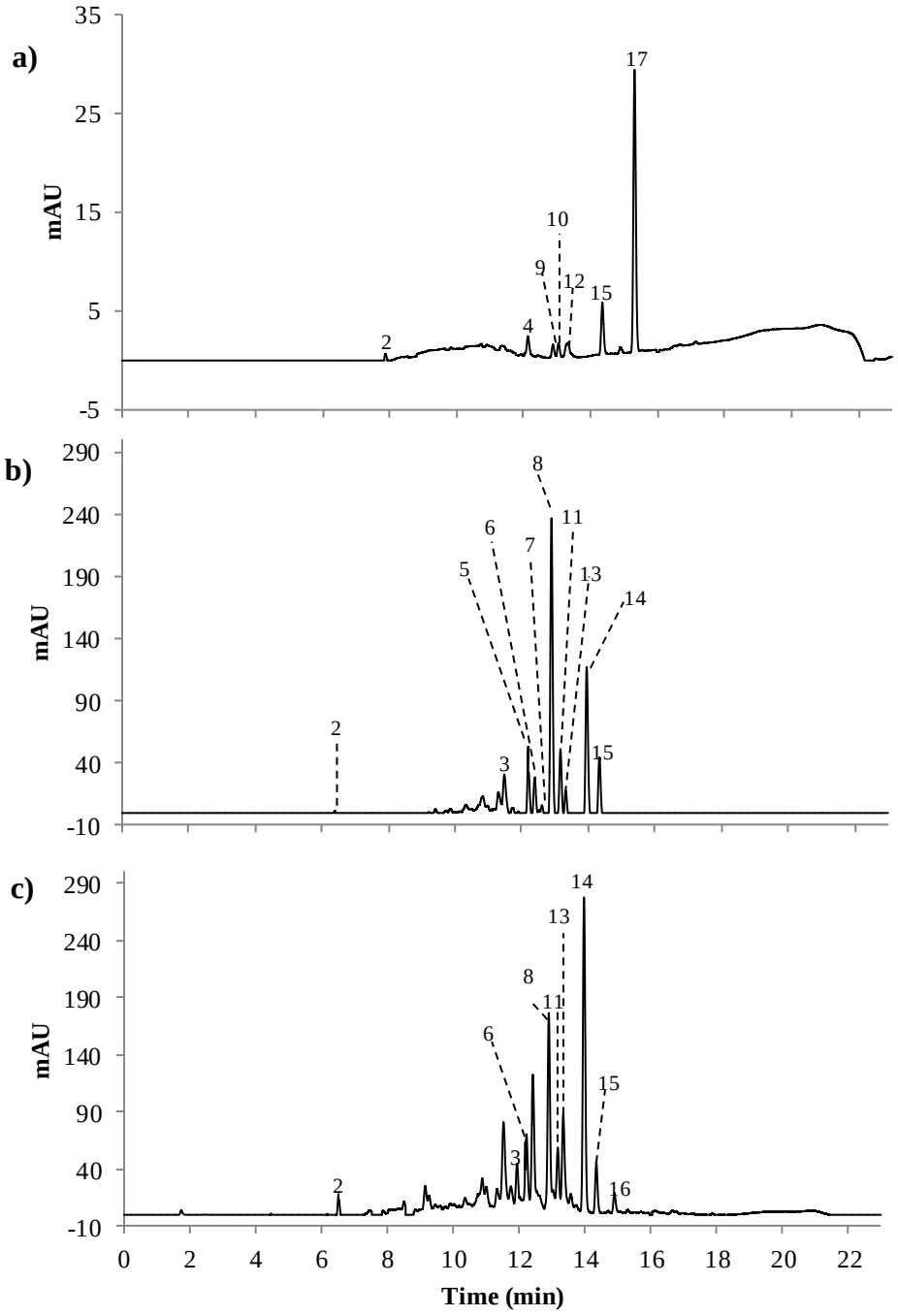

Figure 4.6. UHPLC-PDA (300-800 nm) chromatogram of the sediment extract from Lake Nella (a) depth 23-24 cm, (b) depth 24-25 cm and (c) depth 26-27 cm obtained using UHPLC method 10 (Chapter 3). For peak assignment, see Table 4.2.

The ready formation and greater stability of copper complexes of chlorophylls compared to magnesium complexes has been reported in previous work (Bobbio and Guedes, 1990; Humphrey, 1980). Thus, if the analytical process was contaminated with copper, copper chlorophylls should be detected. It appears that the abundance of copper metallated products, which occur throughout the analysis of the Lake Nella sediment core, is inversely proportional to sediment sample size (Fig. 4.7a). Notably, however, the sample at 24-25 cm depth from Lake Heidi, for which 78.1 mg dried sediment was examined, gave 9.9% copper metallation of the pigment standard (Fig. 4.7b) while the sample at 23-24 depth for Lake Nella (251.2 mg) gave 88% copper metallation (Fig. 4.7a). Thus, sample size is not the main factor controlling the extent copper metallation. Comparison between the total organic carbon (TOC) contents obtained from Lake Heidi 24-25 cm depth and Lake Nella 23-24 cm depth reveals higher TOC of Lake Heidi (25.4%) than Lake Nella (2.2%). Thus, it is possible that one of major factors governing the extent of metallation is the concentration of pigment in the sediment.

4.2.4.2 Source of copper contamination

In order to determine the source of copper contamination, three possible metal sources involved in sediment preparation, sieving, ASE extraction and UHPLC analysis were assessed. The sieving may be a source of copper contamination due to the small amount of dry sediment used. A 200 mg sample of Priest Pot sediment, which had been analysed in the studies reported in Chapters 2 and 3, was freeze dried and sieved. A 50 mg sample of the freeze dried Priest Pot sediment was extracted by ASE at 70°C and analysed by UHPLC method 10. The UHPLC chromatogram and online UV/vis spectra of the extract do not show any copper chlorophyll complexes in the extract. To test whether the copper contamination arises from the UHPLC analysis step, pyrophaeophorbide *a* C_{18} ester (**41**), at the same concentration as that used when spiking the sediment extracts, was injected and analysed. Like the sieving test, the copper complex of pyrophaeophorbide *a* C_{18} ester (**44**) was not present in the UHPLC chromatogram. From these two tests, it is clear that the sieving and UHPLC analysis steps were not the source of the copper contamination. The final test was performed on the ASE extraction process. ASE extraction at 70°C of empty stainless steel cells (5 mL, Dionex) spiked with pyrophaeophorbide *a* C_{18} ester (**41**) led to the

formation of the copper complex (Fig. 4.8a). The UHPLC chromatogram of the extract when the experiment was repeated using a zirconium extraction cell (66 mL, Dionex) only showed a small amount of the copper complex (Fig. 4.8b).

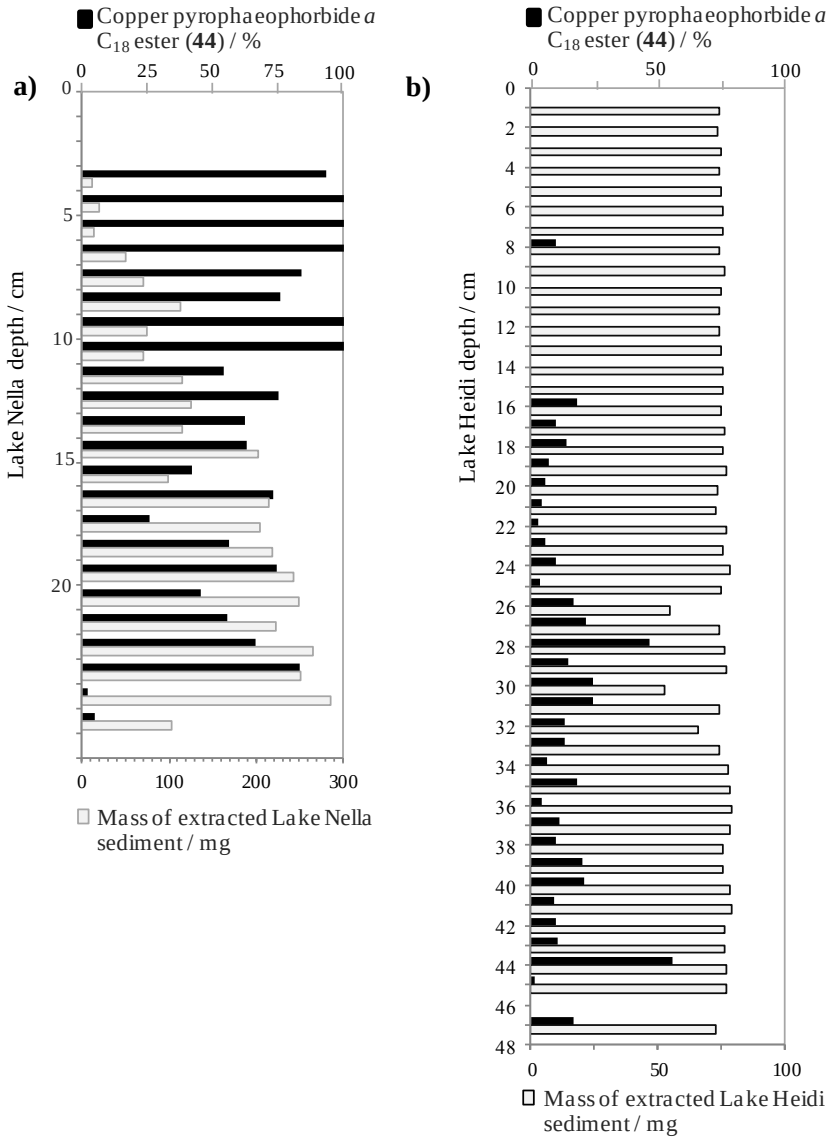

Figure 4.7. (a) Comparison between mass of Lake Nella sediment extracted and % copper pyrophaeophorbide *a* C_{18} ester (**44**) observed when those sample sizes were extracted by ASE at 70°C. (b) Comparison between mass of Lake Heidi sediment extracted and % copper pyrophaeophorbide *a* C_{18} ester (**44**) observed when those sample sizes were extracted by ASE at 70°C.

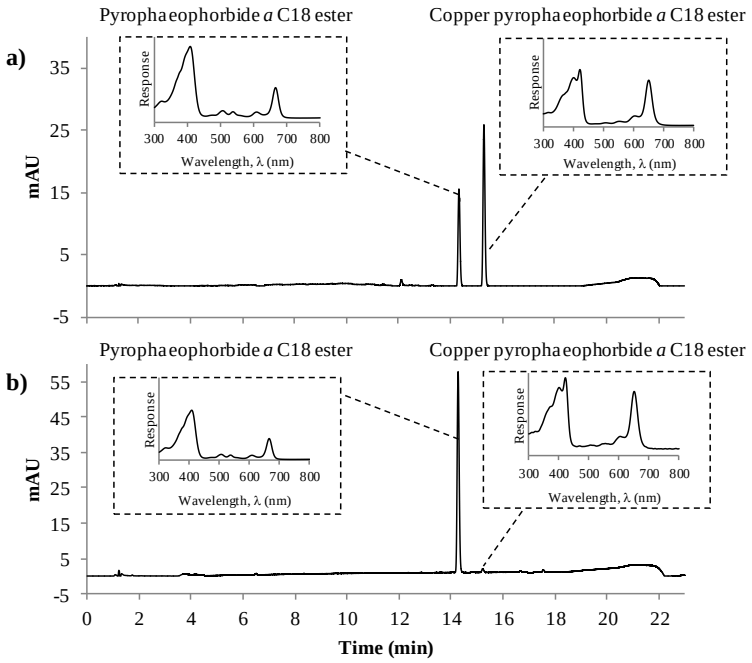

Figure 4.8. UHPLC-PDA (300-800 nm) chromatogram of pyrophaeophorbide *a* C_{18} ester (**41**) extracted by ASE 70°C using (a) stainless steel (5 mL, Dionex) and (b) Zirconium cell (66 mL, Dionex). The inserts show the UV/vis absorption spectra of the standard and its copper metallated product.

Clearly, the stainless steel extraction cells employed in the ASE extraction are the major source of copper contamination. Owing to the limited number of zirconium cells available and their large cell volume all further extractions were performed using the stainless steel extraction cell. Thus, pigment quantification was calculated as before, relative to the free base internal standard, with its concentration modified to account for any of the copper complex formed during the extraction (see Section 6.6.2, Chapter 6).

4.2.4.3 Pigment stratigraphic profiles

Pigment profiles for Lake Nella (Fig. 4.9a) were generated for the regular chlorophyll transformation products, oxidative transformation products and all metallated pigment products. Notably, the total yield from the 3-6 cm depth (Fig. 4.9a) was high even though the mass of sediment sample extracted was less than 20 mg (Fig. 4.7a). The total pigment yields obtained from 12 -24 cm depth, for which the sediment sample size extracted ranged from 100-250 mg (Fig. 4.7a), were close to zero. Thus, the lack of chlorins pigments over this range most likely indicates low intensity primary productivity at the time of deposition or a significantly higher sedimentation rate. The intensity of primary production appears to have been greater during the period when the sediments at 24-25 and 25-26 cm depth were deposited, as indicated by relatively high total pigment yields. In addition, oxidative transformation product including hydroxyphaeophytin *a* (**34**) and purpurin-7 phytyl ester (**14**) were found at these depths, especially at 25-26 cm depth. Their occurrence indicates the presence of an oxidising water column at the time of sediment deposition. Interestingly, even though the pigment yields in the Lake Nella were low, they show significant variations, reflecting palaeoenvironmental change.

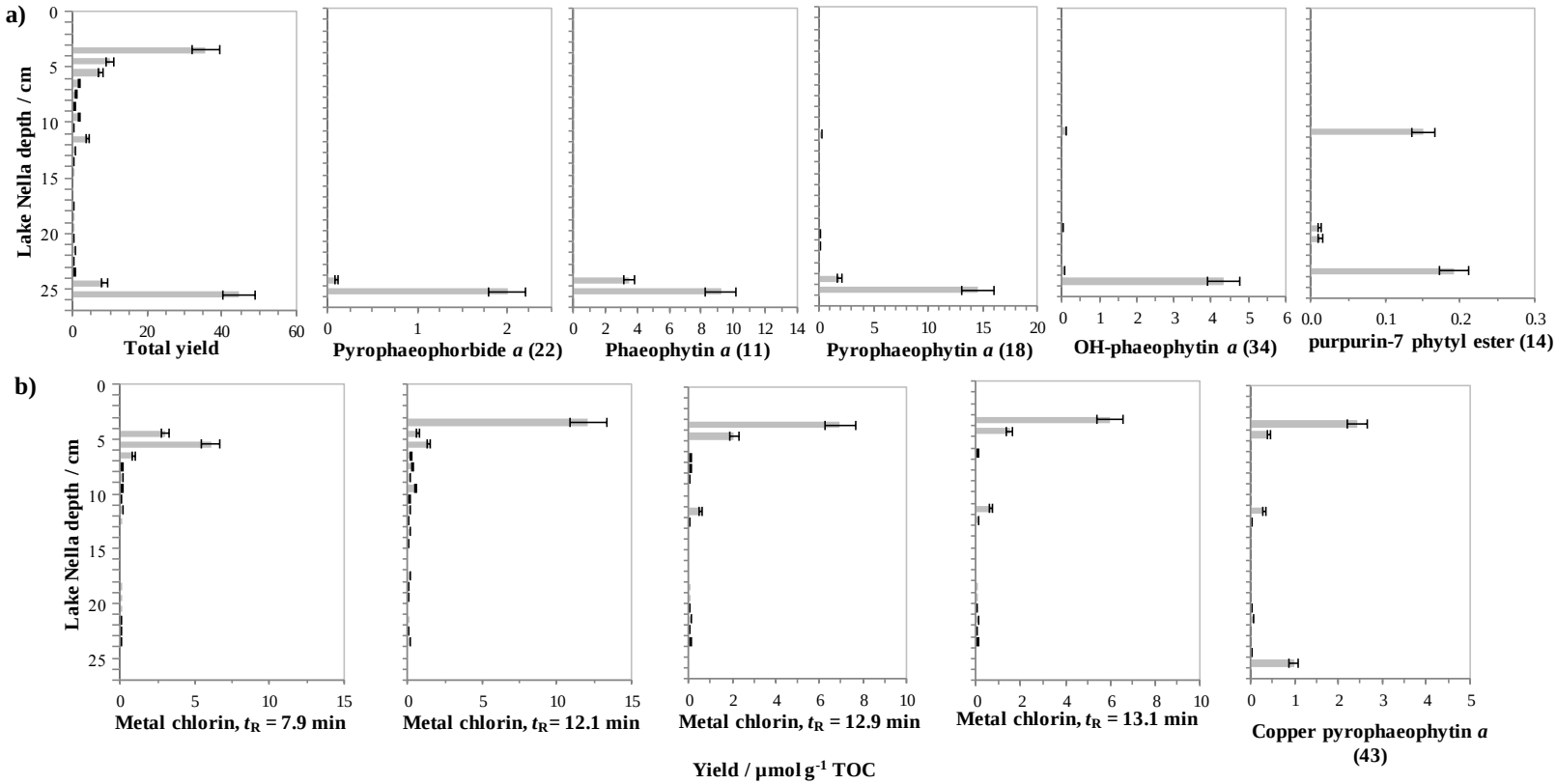

Figure 4.9. Pigment yield profiles from a Lake Nella sediment core between 3-4 and 25-26 cm depth. (a) Total yield and free base pigment yields. (b) Yields of metallated pigments involving unidentified metal chlorins at t_R = 7.9, 12.1, 12.9, and 13.1 and copper pyrophaeophorbide *a* C_{18} ester (**44**). Error bars represent ± 1 standard deviation *(n* = 3) estimated from study of the Estanya sediment extraction using ASE 70°C (Chapter 2).

4.2.5 Larsemann Hills (LH14)

4.2.5.1 Pigment distribution

The third sediment core analysed during the evaluation of the high-throughput methods was Lake 14 in the Larsemann Hills region, Antarctica. The UHPLC chromatograms show three distinct distribution patterns throughout the core (Fig. 4.10). Peak no. 15 (Fig. 4.10a), phaeophytin *a* (**11**) (Table 4.3), was the dominant peak at 1-2 cm depth but was less prominent at 2-3 cm depth (Fig. 4.10b). At the latter depth, two coeluting peaks, an unidentified chlorin (peak no. 4, Table 4.3) and hydroxychlorophyll *a* (**42**) (peak no.5, Table 4.3), were found in high abundance. The UHPLC chromatograms of the extracts obtained from 3 to 15 cm depth (1 cm intervals) were broadly similar to that for 2-3 cm depth (Fig. 4.10b). Between 16 – 23 cm depth similar distributions occur, represented by that at 16-17 cm depth in Fig. 4.10c. In this distribution type, phaeophytin *a* (**11**) (peak no. 15, Fig. 4.10c, Table 4.3) and pyrophaeophytin *a* (**18**) (peak no. 20, Fig. 4.10c, Table 4.3) dominate.

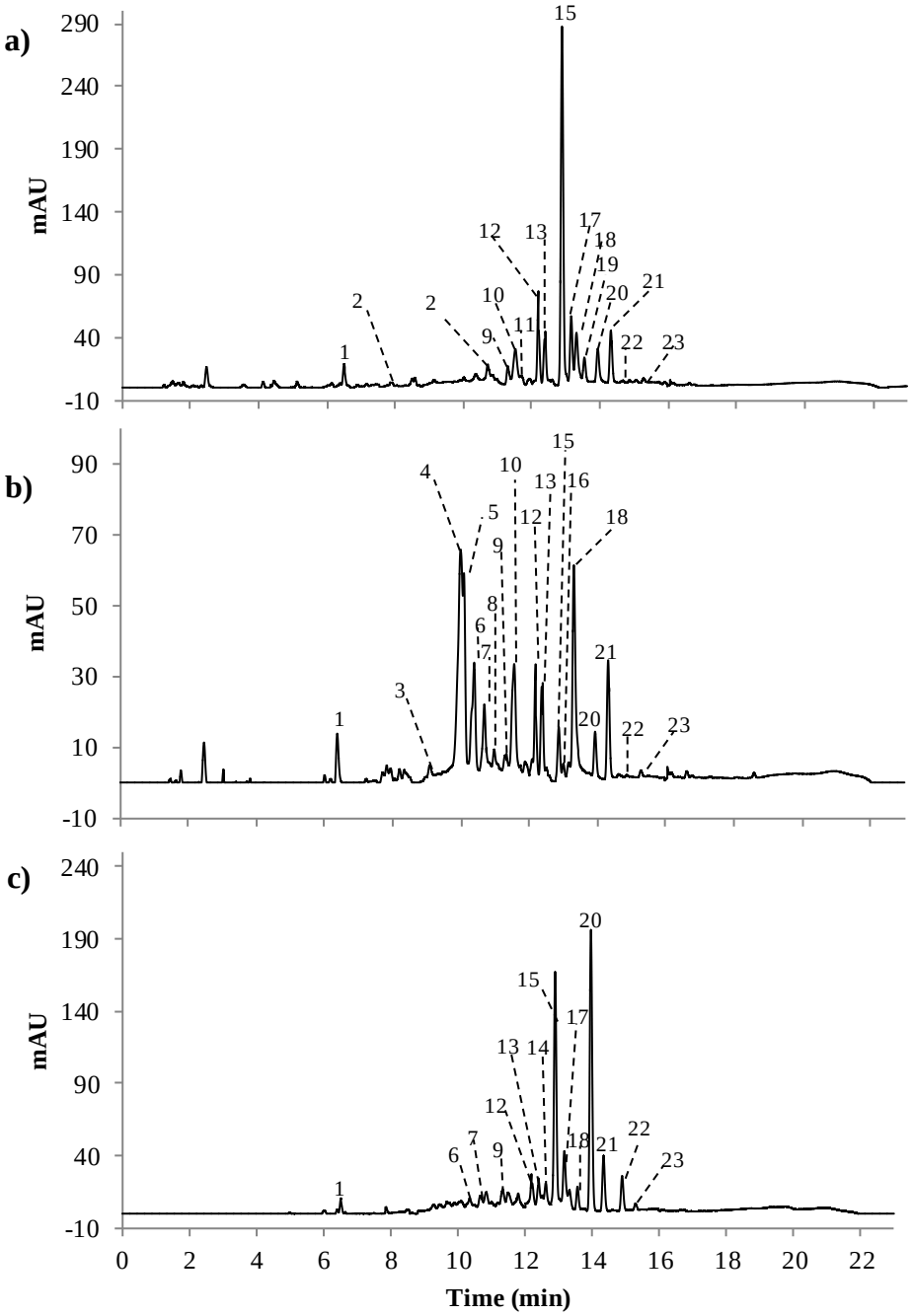

Figure 4.10. UHPLC-PDA (300-800 nm) chromatogram of the sediment extract from Larsemann Hills Lake 14 (a) depth 1-2 cm, (b) depth 2-3 cm and (c) depth 16-17 cm obtained using UHPLC method 10 (Chapter 3). For peak assignment, see Table 4.3.

Table 4.3. Peak identification of pigments extracted from Larsemann Hills Lake 14 sediment core.

Peak	t_R (min)	UV/vis absorption (nm)	$[M+H]^+$ (*m/z*)[a]	Fragment ion MS^n (*m/z*)	Assignment
1	6.5	409, 665	549	521, 435	Pyrophaeophorbide *a* (**22**)
2	7.9	400, 422, 651	610	-	Unidentified metal chlorin
3	9.1	420, 666	-	-	Unidentified chlorin
4	10.0	417, 653	587	-	Unidentified chlorin
5	10.1	428, 663	887	631, 558	Hydroxychlorophyll *a* (**42**)
6	10.4	418, 665	-	-	Unidentified chlorin
7	10.7	415, 654	-	-	Unidentified chlorin
8	11.0	423, 660	-	-	Unidentified metal chlorin
9	11.3	417, 656	-	-	Unidentified chlorin
10	11.5	399, 667	903		Chlorin e_6 dimethyl phytyl ester (**16**)
11	11.7	434, 650	885	-	Phaeophytin *b* (**17**)
12	12.2	407, 665	590	531, 485	Unidentified chlorin
13	12.4	408, 665	887	609, 591	Hydroxyphaeophytin *a* (**34**)
14	12.6	400, 669	917	-	Purpurin-7 phytyl ester (**14**)
15	12.9	406, 666	871	593, 533	Phaeophytin *a* (**11**)
16	12.9	399, 420, 651	-	-	Unidentified metal chlorin
17	13.2	406, 666	871	593, 533	Phaeophytin *a* epimer (**32**)
18	13.4	359, 406, 543, 696	843	565, 503	Purpurin-18-phytyl ester (**15**)
19	13.6	399, 421, 651	-	-	Unidentified metal chlorin
20	14.0	408, 665	813	535, 507	Pyrophaeophytin *a* (**18**)
21	14.3	321, 408, 665	787	749, 507	Pyrophaeophorbide a C_{18} ester (**41**)
22	14.9	400, 422, 651	874[b]	-	Copper pyrophaeophytin *a* (**43**)
23	15.3	401, 422, 650	848[b]	820[b], 496	Copper pyrophaeophorbide *a* C_{18} ester (**44**)

[a] All metallated pigments appear in MS as their demetallated counterparts due to post column demetallation prior to MS (Airs and Keely, 2000). [b] Copper complex which cannot be demetallated by post column formic acid.

4.2.5.2 Pigment yields stratigraphic profile

Unlike Lake Nella, chlorin pigments were observed throughout the sediment core from Larsemann Hills Lake 14 (Fig. 4.11a). The highest total yield was found at 5-6 cm depth and the lowest was found at 17-18 cm depth. The total pigment yields most likely reflect the intensity of primary production, being greatest during deposition of the horizon at 5-6 cm depth and lowest during deposition of the horizon at 17-18 cm. Regular transformation products of chlorophyll *a* (**4**), such as pyrophaeophorbide *a* (**22**), phaeophytin *a* (**11**) and pyrophaeophytin *a* (**18**), were represented throughout the core and might indicate grazing activity. Notably, the profile of purpurin-7 phytyl ester (**14**) (Fig. 4.11b) was different to those of the oxidation products chlorin e_6 dimethyl phytyl ester (**16**) and purpurin-18 phytyl ester (**15**). The profile of purpurin-7 phytyl ester (**14**) was high when chlorin e_6 dimethyl phytyl ester (**16**) and purpurin-18 phytyl ester (**15**) were not detected. It is likely that the purpurin-7 phytyl ester (**14**) is formed by a different transformation mechanism to the other two oxidation products. Further consideration of the reasons for the differences, for example in the oxidative transformation mechanism, are beyond the scope of this study.

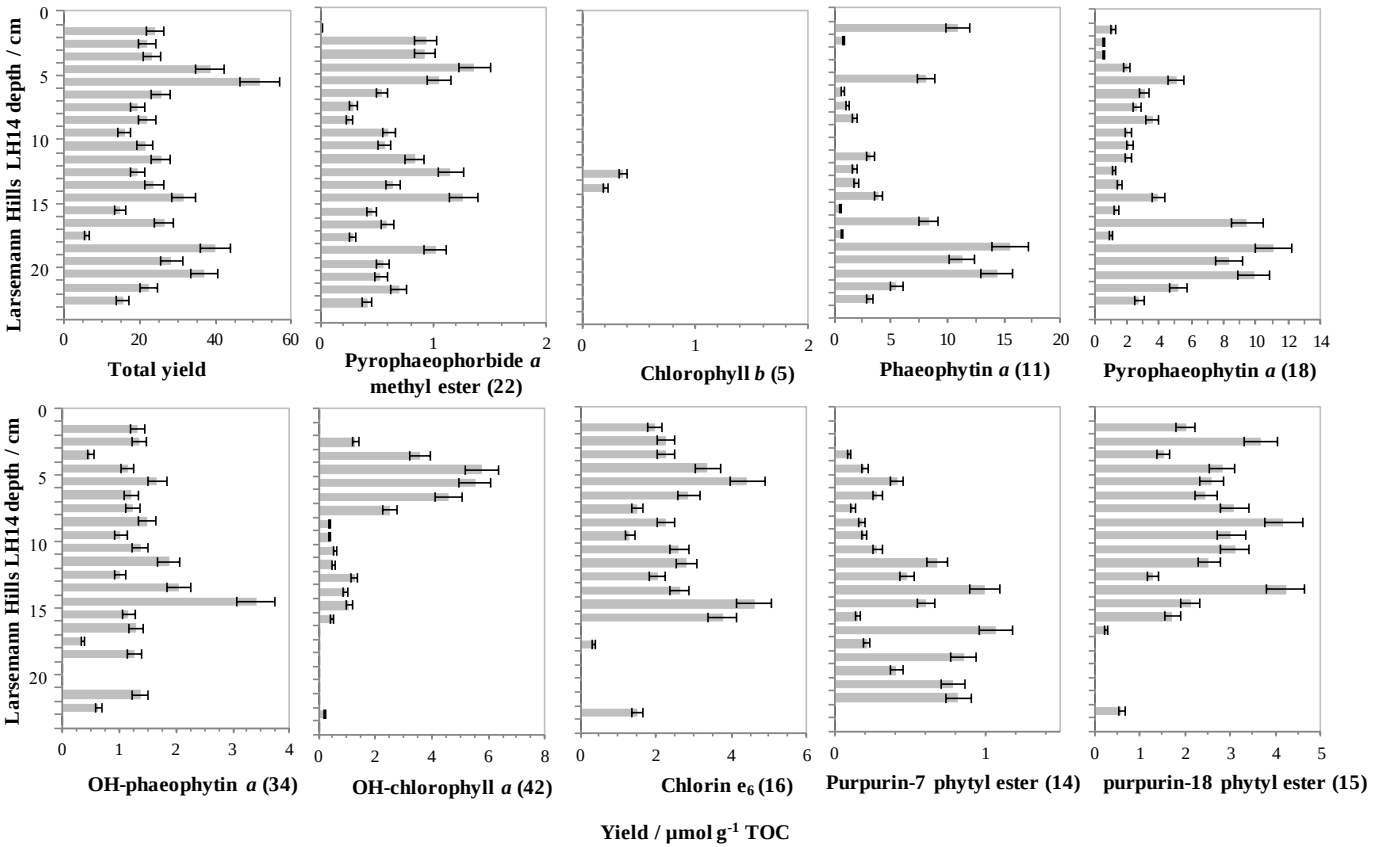

Figure 4.11. Histogram plots showing pigments extracted from a sediment core from the Larsemann Hills Lake 14 between 1-2 and 23-24 cm depth. (a) Total yield and regular transformation products and (b) yields of oxidative transformation products. Error bars represent ± 1 standard deviation (n = 3) estimated from study of the Estanya sediment extraction using ASE 70°C (Chapter 2).

4.3 Conclusions

The high-throughput methods developed in Chapters 2 and 3 were applied to the analysis of three lake sediment cores from the Larsemann Hills region of Antarctica. Sediment cores were sectioned at reasonably high resolution (1 cm scale) to generate a total of 91 sample horizons for study. The high-throughput method enabled all samples to be processed at least 2.5 times faster than the estimated analysis time for the conventional method with greater control on sample preparation being subsumed within the reduced total analysis time. The automation of the extraction and analysis steps allowed several batches of samples to be processed in parallel. Solvent consumption was reduced by approximately 5 and 5.8 times for extraction and UHPLC analysis, respectively, compared with conventional methods. Sediment sample sizes were reduced from 3-5 g (typically extracted) to below 50-80 mg for Lake Heidi and Lake 14 (TOC contents 13- 37%) while for Lake Nella the smallest sample size was 12.4 mg of sediment (depth 3-4 cm, %TOC = 15.46).

As a consequence of working at such low samples sizes, copper metallation products were observed and the source of copper contamination was investigated. The sieving and UHPLC analysis were ruled out as sources of the copper contamination. The source of the copper contamination was found to be the stainless steel extraction cells used in ASE extraction. Performing the ASE extraction in zirconium cells immediately reduced the formation of copper pigment complexes. The lack of availability of sufficient numbers of zirconium cells and large volume of those available prevented the use of the zirconium cells in validating the high-throughput methods discussed in this chapter. As a result, the stainless steel cells were employed for the ASE extraction process and the amount of internal standard metallated by copper was deducted from the original amount of internal standard before quantifying pigment yields.

In terms of the quality of the data produced, the high throughput extraction and chromatographic methods have been used to establish pigment distribution profiles and yield profiles for the three sediment cores. In addition, by applying the percentage errors from ASE method development (Chapter 2) it has been shown that the new methods generate pigment profiles with a greater degree of confidence (Fig.

4.4). Thus, they more accurately reflect the genuine sedimentary distributions and provide a more reliable estimate of the environmental conditions in times past. For example, high total pigment yields can reveal to intense primary production in Lake Heidi and Lake 14 whereas it was low in Lake Nella over the similar time period. Chlorophyll *a* was present in the top 15 samples (from the depth 1-16 cm shown in Fig. 4.5a) of the core from Lake Heidi, indicating environmental conditions suited to preservation of this highly reactive biomarker at the time of deposition. The decreased chlorophyll *a* yield and increasing levels of oxidative transformation products in the deeper sections of the core indicate more oxidising conditions within the depositional environment during the earlier period of the lake's history. In addition, the different profiles of purpurin-7 phytyl ester (**14**) and other oxidative transformation products obtained from analysis of Lake 14 probably reflect different mechanisms of oxidation involved with their formation.

In conclusion, the results obtained during the study clearly demonstrate the applicability of the high-throughput methods to the analysis of large numbers of small sediments from sediment cores. The methods offer significant savings in time, solvent and sample consumption and generate more reliable data.

Chapter 5

Conclusions and future work

5.1 Overall summary and conclusions

The overall aim of the work described in this thesis was to develop high-throughput methods for the extraction and analysis of sedimentary pigments. The approach involved both the evaluation of accelerated solvent extraction (ASE) for the extraction of pigments from sediments (described in Chapter 2) and development of a rapid UHPLC method for pigment analysis (Chapter 3). Both of the methods developed in the study were applied to the analysis of the pigments in three sediment cores to demonstrate the quality of the pigment profiles, the improvements in the speed of analysis and the applicability of the methods to the analysis of environmental samples (Chapter 4).

The use of ASE for the extraction of sedimentary pigments was evaluated by comparison of the yields and distributions of extracted pigments, obtained over a range of extraction temperatures, to the conventional method of sonic extraction for sediment samples from Lake Reid, Priest Pot, Loch Ness, Chiprana and Estanya Lake and bacterial cell material. These samples were chosen because they contain a range of sensitive pigments representative of both oxygenic primary producers (chlorophylls and their derivatives) and anoxygenic primary producers (bacteriochlorophyll *a* and its derivatives). The optimal ASE conditions were found to be 3 × 5 min extraction cycles with acetone at 70°C. Pigment yields and repeatability were found to suffer for extractions performed at temperatures below 60°C, whereas, temperatures of 75°C and above caused degradation of some of the more sensitive pigment structures. The result is a rapid, high-throughput alternative to sonication for the extraction of chlorophyll pigments from sediments.

During the development of the ASE extraction variations in yield of repeat extractions were noted and inconsistencies arising from working with moist sediments were highlighted. The study confirms the importance of freeze-drying for the preparation of sediment samples for the extraction of pigments (*cf.* McClymont et al., 2007) and illustrates the importance of homogenisation (by grinding and sieving) for achieving high repeatability in yields. The improvements arising from freeze drying and sieving are apparent in the much narrower error bars for individual pigments for replicate measurements. Spiking the sediment with target analytes, an

approach that is used to test extraction efficacy in a wide range of applications, including many outside geochemistry, gave poor repeatability for chlorophyll *a* (**4**) and chlorophyll *b* (**5**) as a result of their alteration via demetallation. The alteration of the spiked components under conditions in which their sedimentary counterparts are stable indicates that caution should be exercised when assuming identical behaviour for components that are integrated with a matrix and those that are introduced during laboratory manipulation. This observation has wider implications, beyond geochemistry, for studies where the integrity and extraction efficiency of spiked samples are considered.

In Chapter 3, the HPLC Method A of Airs, et. al. (2001a), capable of separating complex mixtures of sedimentary pigments, was transferred to UHPLC. Variables including injection volume, mobile phase composition, gradient, flow rate, column length, and column temperature were optimised for two different UHPLC column phases to generate two rapid and sensitive methods for pigment analysis (Methods 6 and 10). Method 6 (23 min) was developed using two 2.2 µm Acclaim 120 C_{18} columns (100 mm × 2.1 mm i.d.) coupled in series. Method 10 (20 min) was developed on an Acquity UPLC BEH C_{18} (1.7 µm, 150 mm x 3 mm i.d) column. Both methods are capable of separating the complex distributions of chlorophyll derivatives present in the extracts from Priest Pot, and bacteriochlorophyll homologues in Little Long Lake. Although the efficiency of separation was not as good with Methods 6 (23 min) and 10 (20 min) as that with Method A (115 min, Airs et al., 2001a), the majority of the components of the extracts could be identified from their elution order, online UV-Vis absorption and mass spectra and all of the main components were confirmed from their spectral characteristics. Notably, MS^2 spectra could not be obtained for analysis of the complex mixture from Little Long Lake extract using both UHPLC methods 6 and 10. The inability to acquire MS^2 spectra was due to the scan speed of ion trap mass analyser not being fast enough to allow a sufficient number of scans over the narrow chromatographic peaks obtained by these methods. This shortcoming might be overcome by utilising a mass spectrometer with a faster scan speed, as described in Section 5.2. The two UHPLC methods 6 and 10 lead to significant reductions in solvent consumption (≥ 85 %), sample injected (90%), and analysis time (≥ 80 %). Thus, these methods will enable the high throughput screening of extremely complex pigment distributions in

sediment extracts where the greater analysis times of the Airs Method prove prohibitive.

The ASE and UHPLC methods developed in Chapters 2 and 3 were applied to the analysis of the pigment profiles in three lake sediment cores from the Larsemann Hills region of Antarctica (Chapter 4). Sediment cores were sectioned at reasonably high resolution (1 cm scale) generating a total of 91 sample horizons for study.

The high-throughput extraction and analysis methods enabled all samples to be processed at least 2.5 times faster than the estimated analysis time for the conventional method and solvent consumption was reduced by approximately 5 and 5.8 times for extraction and UHPLC analysis, respectively. Hence, the entire set of 91 samples was processed from the frozen samples through freeze drying, sieving, extraction and UHPLC analysis in a total of 12 days. In addition, the greater detection limits of the methods enabled a significant reduction in sediment sample sizes from 3-5 g (typically extracted) to below 50-80 mg for Lake Heidi and Lake 14 (TOC contents 13- 37%) while for Lake Nella the smallest sample size was 12.4 mg of sediment (depth 3-4 cm, %TOC = 15.46). This reduction in sample sizes did not compromise the data obtained or the quality of the chromatograms generated. Furthermore, the improvement in repeatability arising from sample preparation (freeze drying and homogenisation) and ASE results in an increased confidence in the data produced. Thus, the pigment profiles generated using these methods more accurately reflect the genuine sedimentary distributions and provide more reliable assessments of the environmental conditions in times past. The dramatic reduction in the sample size required for the analysis meets one of the main requirements for high resolution profiling of sediment cores, where sample sizes are often limited by the demands of the various complementary analyses planned for their examination. Furthermore, the lower sample requirements will enable sectioning of sediment cores at considerably higher stratigraphic resolution, thereby enabling the recovery of profiles that reflect much higher temporal resolution in the signatures of environmental change.

Notably, when working with small sample sizes copper metallated artefacts dervied from the chlorins were observed, which were not detected during ASE and UHPLC

method development. The source of copper contamination was investigated at all stages of the sample processing, extraction and analysis. The sieving and UHPLC stages were ruled out as sources of the copper contamination. The absence of copper pigment complexes formed when the ASE extraction was performed using zirconium cells indicated that the stainless steel extraction cells used in ASE were the source of the copper contamination. Thus, in future studies ASE extraction of pigments from very small sediment samples should be performed using zirconium extraction cells.

In conclusion, the work in this thesis clearly demonstrates the applicability of the high-throughput ASE and UHPLC methods developed to the analysis of complex distributions of sedimentary pigments. The methods offer significant savings in time, solvent and sample consumption and generate more reliable data. Furthermore, the ability to process small sample sizes with short analysis times enables the profiling of sediment cores at high sampling resolutions within reasonable timescales.

5.2 Future work

The ASE and UHPLC methods presented in this thesis could be applied to the high-throughput, high resolution analysis of samples from other sediment cores. The improved sensitivity of the methods, requiring smaller sample sizes, mean that sediment cores could realistically be profiled at resolutions as high as 1 mm intervals. This would allow variations in pigment distributions to be observed at a greater temporal resolution, enabling a much more detailed reconstruction of the changes in palaeoenvironmental conditions.

Although Methods 6 and 10 provided acceptable chromatographic separation for the highly complex mixture of bacteriophaeophytin *c* and *d* homologues, coeluting peaks are evident in the chromatograms (Fig. 3.10, Chapter 3). Accordingly, a specific UHPLC method for bacteriophaeophytin *c* and *d* homologues should be developed to increase the separation efficiency. In terms of pigment identification by UHPLC combined with ion trap mass spectrometry, the reduced peak widths observed in UHPLC coupled with the slow scan speed of the mass spectrometer meant that MS^2 spectra were not always observed (cf. $>MS^6$ attainable with HPLC Method A (Airs et

al., 2001a)). This could be solved by coupling the UHPLC separation to a faster mass spectrometer such as a time-of-flight instrument. Furthermore, coupling the UHPLC separation to a time-of-flight/time-of-flight mass spectrometer (TOF/TOF MS) could enable MS^2 spectra to be acquired. Thus, future work should be aimed at validating the use of the UHPLC methods with TOF/TOF MS detection.

A significant effort in future work should be directed towards the application of the high-throughput methods in the examination of sediment cores as part of multi-proxy studies targeted at monitoring environmental change. By analysing photosynthetic pigments at very high stratigraphic resolution, further understanding of the fate and significance of these crucial biomarkers of the primary producer community will be possible. Notably, these studies should be complemented by radiocarbon dating of individual pigment components from selected horizons, using methods developed recently by Ballantyne (2012) in order to provide a rigorous age model for the interpretation of changes in the pigment distributions.

Chapter 6

Experimental and analytical procedures

6.1 General procedures

6.1.1 Solvents and reagents

All solvents used in sample preparation of pigment analysis were analytical grade or HPLC grade purity (Fisher, Loughborough, UK) unless specified otherwise. For HPLC analysis, solvents were used as purchased, while for UHPLC analysis, all solvents were filtered through a 0.2 µm nylon membrane (Waters Corporation, US) before use.

6.1.2 Glassware

All glassware was cleaned thoroughly prior to using to avoid contamination. The cleaning procedure involved rinsing with acetone (laboratory grade) and deionised water before soaking in a 1% solution of Decon-90 (Decon, Hove, UK) for 24 hr and washing with tap water, deionised water and finally acetone (laboratory grade).

6.1.3 Storage and handling of sediment and pigment

Sediment samples were stored in the dark at -20°C before extraction. Pigment extracts and standards were stored dry in the dark at +4°C. Extraction and manipulation of pigments was carried out in a low light environment to avoid pigment photodegradation.

6.1.4 Accelerated solvent extraction cell

All extraction cells used in ASE were rinsed with deionised water and sonicated with acetone (laboratory grade) for 30 min. The cells were re-rinsed with acetone (analytical grade) and allowed to dry before use.

6.2 Reagent and standard preparation

6.2.1 Diazomethane

Fresh diazomethane was prepared from the reaction between diazald, *N*-methy-*N*-nitroso-*p*-toluenesulfonamide (0.3 g) in ethanol:diethyl ether (1:1, v/v, 2 mL), and aqueous potassium hydroxide (6.6 M, 1.5 mL). The reaction was performed in special apparatus and the distillated diazomethane trapped in cold diethyl ether (2 mL). Excess diazomethane was destroyed immediately using dilute HCl (0.1 M) to reduce hazards associated with its storage (Pickering, 2009).

6.2.2 Standard pigments

A mixture of chlorophyll *a* (**4**), phaeophorbide *a* (**20**) and phaeophytin *a* (**11**) standards (prepared by Matt Pickering) was used for generating the calibration curve in Chapter 2.

6.2.2.1 Standard mixture of chlorophylls *a* (4) and *b* (5)

Chlorophylls *a* and *b* were isolated from spinach leaves as described previously (Iriyama et al., 1974; Walker, 2004a) but without purification by sugar column chromatography. The chlorophyll extract was analysed by reversed phase high performance liquid chromatography (RP-HPLC) using Method B of (Airs et al., 2001a). The chlorophyll *a* and *b* extract was dissolved in acetone, pipetted into vials (2 mL) and the solvent was removed using a vacuum concentrator (1310 rpm for 15 min, CHRIST, RVC 2-25) prior to storage in a freezer. Each vial contained a mixture of chlorophyll *a* (32.7 µg) and chlorophyll *b* (12.9 µg).

6.2.2.2 Preparation of internal standard pyrophaeophorbide *a* C_{18} ester (**41**)

Pyrophaeophorbide *a* C_{18} ester (**41)** (606.412 nmol; 99% purity, $[M+H]^+$ *m/z* 787, prepared by Chris Knappy) was dissolved with acetone (AR grade) in a volumetric flask (20 mL). 2 ml aliquots of the solution were pipetted into 9 separate vials. Acetone was removed by a rotary vacuum concentrator (Christ, 2-25 RVC, 1310 rpm for 15 min) and stored at 4°C in the dark. The standard pigment in each vial was re-dissolved in acetone (2 mL) and a portion (100 µL; 3.03 nmol) pipetted onto the sediment sample in the extraction cell.

6.3 Sediment and culture samples

6.3.1 Samples in Chapter 2

The origin and preparation of all of the samples studied in Chapter 2 is described below. These samples were extracted by both sonic and ASE extraction (masses given in Table 6.1). The extraction procedure is described in Section 6.4. Three replicates were performed for each extraction temperature, except in the case of the sediment from Lake Reid which was extracted once for each temperature.

6.3.1.1 Lake Reid sediment

Sediment from Lake Reid (Larsemann Hills, Antarctica), collected and frozen by the British Antarctic Survey (BAS) in 1997, was thawed and excess water removed by pipette. Coarse grains of sediment (diameter > 0.3 mm) were removed and the resulting matrix, comprising sandy silt, was homogenised by griding using a pestle and mortar. The homogenised sediment was kept in a freezer until use and was thawed before extraction.

6.3.1.2 Priest Pot sediment

Priest Pot sediment was collected by Brendan J. Keely in 1985 from Cumbria, UK. Frozen sediment was defrosted, thawed and excess water removed by pipette. The fine black moist sediment was homogenized by grinding using a pestle and mortar. The homogenized sediment was kept in a freezer until use and was thawed before extraction. Moist Priest Pot sediment (1 g) was spiked with chlorophylls *a* (**4**) and *b* (**5**) in acetone (250 µL), 32.7 and 12.9 µg, respectively and the acetone was removed under a stream of N_2 before extraction.

6.3.1.3 Loch Ness sediment

The sediment from Loch Ness, Scotland, collected from 150 m water depth in the southern basin of the Loch by Bracewell (1993) using a modified Kullenburg corer, was stored at room temperature and extruded and sectioned within 7 days (Bracewell, 1993; Naylor and Keely, 1998). A section from 67-74 cm depth in the core was freeze dried overnight (HETO PowerDry PL3000; Thermo Scientific) and subsequently homogenized by grinding using a pestle and mortar. Dried sediment was kept in a freezer until use and was thawed before extraction.

6.3.1.4 Chiprana sediment

Sediment was collected from La Salada de Chiprana, Spain, by Brendan J. Keely in 1996, using a box core. A 2.5 cm long vertical section from the Chiprana box core was freeze dried overnight (HETO PowerDry PL3000; Thermo Scientific) and subsequently homogenized by grinding using a pestle and mortar. Dried sediment was kept in a freezer until use and was thawed before extraction.

6.3.1.5 Estanya sediment

Sediment from Lake Estanya, Spain was collected by Brendan J. Keely in 1996, using a gravity corer. A vertical quarter section from the frozen Estanya sediment was freeze dried overnight (HETO PowerDry PL3000; Thermo Scientific) and subsequently homogenized by grinding using a pestle and mortar. The dried

sediment was sieved (BS410-1, 400 µm) after homogenization, stored in a freezer until use and was thawed before extraction.

6.3.1.6 *Allochromatium vinosum* cell paste

Frozen cell paste of the bacterium *Allochromatium vinosum* (supplied by Sigma Aldrich in 1984, strain not declared) was thawed and homogenized by grinding using a pestle and mortar. The homogenized cell paste was divided into Whirl-Pak® bags (2 g bag^{-1}, Nasco, USA). Homogenized cell paste was stored in a freezer and thawed immediately before extraction.

Table 6.1. Extraction conditions and extract volumes for the ASE extraction of sediments and cell paste (Chapter 2).

Sample	Mass (g)	ASE extraction temperatures (°C)	Acetone (µL[a])
Lake Reid sediment	4	20, 50, 75, 100, 125, 150 and 175	1000
Priest Pot sediment[b]	1	50, 70, 75, 80, 85 100, 125, 150 and 175	500
Loch Ness sediment	1.5	50, 60, 65, 70, 75 and 80	80
Chiprana sediment	1	50, 60, 65, 70, 75, 80, 85 and 90	1000
Estanya sediment	1	50, 60, 65, 70, 75, 80, 85 and 90	400
Allochromatium vinosum	1	50, 65, 70, 75 and 80	-[c]

[a] Volume of acetone added to extracts for RP-HPLC and LC-MS^n analysis.

[b] The sediment was spiked with known concentrations of chlorophylls *a* (**4**) and *b* (**5**) in acetone and solvent was removed under a gentle stream of N_2 gas for 30 min.

[c] Stock solution of extract was prepared by adding acetone (3 mL) and diluting 200 µL of solution with acetone (200-1000 µL)

6.3.2 Samples in Chapter 3

6.3.2.1 Priest Pot extract spiked with chlorophylls *a* and *b*

Priest Pot sediment described above (Section 6.3.1.2) 3 g was spiked with chlorophylls *a* (**4**) (98.1 µg) and *b* (**5**) (38.7 µg) prepared as described in section 6.2.2.1 and subjected to sonic extraction (Section 6.4.1).

6.3.2.2 Estanya extract

Dried sediment from Lake Estanya (1 g; prepared as described in Section 6.3.1.5) was extracted by ASE at 75°C (Section 6.4.2). The extract was spiked with bacteriochlorophyll *a* (**6**) (19.3 µg) in acetone (2 mL). Aliquots of the spiked Estanya extract, (50 µL) were pipetted into 35 vials (2 mL), dried by vacuum concentrator (1310 rpm for 15 min) and stored in the dark at 4°C. Aliquots of spiked Estanya extract were dissolved in acetone (50 µL) prior to LC analysis.

6.3.2.3 Priest Pot extract for comparison of Airs Method A (Airs et al., 2001a) and UHPLC methods 6 and 10

Priest Pot sediment was collected by Brendan J. Keely in 1985 from Cumbria, UK. Frozen sediment was freeze-dried (HETO PowerDry PL3000; Thermo Scientific) overnight, subsequently homogenized by grinding using a pestle and mortar and sieved (BS410-1, 400 µm). Sediment (1 g) was extracted in acetone using the ASE at 70°C method as described in Section 6.4.2. The pigment extract was dissolved in acetone (500 µL), pipetted (60 µL) into 6 vials (200 µL), dried by vacuum concentrator (1310 rpm for 15 min) and stored in the dark at 4°C. Aliquots of Priest Pot extract were dissolved in acetone (60 µL) prior to LC analysis using Airs Method A (Airs et. al., 2001a), UHPLC Method 6 and UHPLC Method 10.

6.3.2.4 Little Long Lake extract

A water column sample from Little Long Lake, located in the North American Great Lake Area (Wisconsin), was taken at 3.2 m and filtered through 0.45 µm pore diameter membrane filters by Carles Borrego, University of Girona (Airs, 2001b). The photosynthetic pigments from the water-column filtrand were extracted with acetone by Ruth Airs (Airs, 2001b) and the extract stored in a freezer (-20°C) since 2001. The frozen extract was left at room temperature to thaw for 1 h before adding acetone (500 µL). Aliquots (60 µL) of this stock solution were pipetted into 6 vials (containing 200 µL glass inserts), dried using a vacuum concentrator (1310 rpm for 15 min) and stored in the dark at 4°C. The aliquots of Little Long Lake extract were redissolved in acetone (60 µL) prior to LC analysis using the Airs Method A (Airs et. al., 2001a), UHPLC Method 6 and UHPLC Method 10.

6.3.3 Samples in Chapter 4

The location and sample collection of Lake Heidi, Lake Nella, and Lake 14 sediment cores is described in Chapter 4. The sectioned sediment was freeze dried overnight (HETO PowerDry PL3000; Thermo Scientific) and sieved (BS410-1, 400 µm) before analysis. Dried and homogenised sediment (sample size see in Table 6.2) was loaded into a stainless steel extraction cell (size 5 mL) and the internal standard pyrophaeophorbide *a* C_{18} ester **(41)** (3.03 nmol) was added. The extraction was performed by ASE at 70°C (Dionex ASE 350) with acetone (AR grade; Fisher, Loughborough, UK) (extraction conditions listed in Table 6.3). Pigment extracts were dried, filtered and treated with a solution of diazomethane in ether according to Section 6.4.2. before drying under a stream of nitrogen. Samples were dissolved in acetone (50 µL) for UHPLC analysis (method 10, Table 6.4). For more detail of UHPLC-MS^n see Section 6.5.

Table 6.2. Sediment sample size of sectioned sediment cores of Lake Heidi, Lake Nella and Lake 14 (LH14) from Larsemann Hills extracted by ASE at 70°C and percentage total organic carbon (TOC) measurements.

No	Depth (cm)	Lake Heidi		Lake 14 (LH14)		Lake Nella	
		Extracted sample size (mg)	%TOC[a]	Extracted sample size (mg)	%TOC[a]	Extracted sample size (mg)	%TOC[a]
1	1-2	74.08	30.30	70.73	32.63	-	-
2	2-3	73.34	29.20	71.52	33.44	-	-
3	3-4	74.81	32.73	70.76	35.40	12.41	15.46
4	4-5	74.58	36.63	54.91	30.83	20.65	18.39
5	5-6	74.67	27.08	71.46	30.82	14.53	22.15
6	6-7	75.4	27.62	74.89	31.65	49.98	15.22
7	7-8	75.56	17.50	72.75	33.91	70.22	12.26
8	8-9	74.34	12.53	73.94	33.37	112.75	9.76
9	9-10	76.28	18.24	70.46	29.56	74.63	11.00
10	10-11	74.68	22.32	71.32	29.66	70.26	24.68
11	11-12	74.44	29.48	71.52	25.58	114.5	9.51
12	12-13	74.13	27.62	73.68	28.54	124.51	14.50
13	13-14	75.11	27.28	74.21	29.98	115.37	8.97
14	14-15	75.94	25.60	74.91	25.89	202.35	9.47
15	15-16	75.33	28.16	73.68	25.33	98.56	7.99
16	16-17	74.97	27.04	72.41	26.85	214.28	5.85
17	17-18	76.13	19.18	73.70	22.93	204.68	5.41
18	18-19	75.88	14.67	71.25	28.38	217.91	14.27
19	19-20	76.8	23.12	74.79	20.37	243.35	11.05
20	20-21	73.8	26.61	76.16	21.70	248.58	9.64
21	21-22	73.05	26.93	71.15	21.94	221.93	10.91
22	22-23	76.89	25.80	70.85	27.44	265.45	2.86
23	23-24	75.8	28.00	-	-	251.16	2.17
24	24-25	78.12	25.42	-	-	286.02	4.57
25	25-26	75.1	27.08	-	-	102.84	11.10
26	26-27	55.03	26.97	-	-	-	-
27	27-28	74.55	18.61	-	-	-	-
28	28-29	76.63	27.45	-	-	-	-
29	29-30	77.29	28.72	-	-	-	-
30	30-31	52.82	26.63	-	-	-	-
31	31-32	74.06	27.01	-	-	-	-
32	32-33	65.8	27.78	-	-	-	-
33	33-34	74.3	28.91	-	-	-	-
34	34-35	77.88	29.80	-	-	-	-
35	35-36	78.16	31.02	-	-	-	-
36	36-37	79.03	27.85	-	-	-	-
37	37-38	78.21	29.99	-	-	-	-
38	38-39	75.68	28.69	-	-	-	-
39	39-40	75.76	25.81	-	-	-	-
40	40-41	78.73	26.26	-	-	-	-
41	41-42	78.89	27.72	-	-	-	-
42	42-43	76.36	24.12	-	-	-	-
43	43-44	76.64	30.39	-	-	-	-
44	44-45	76.84	24.91	-	-	-	-
45	45-46	76.85	23.10	-	-	-	-
46	47-48	73.16	30.93	-	-	-	-

[a] Analysis of total organic carbon (TOC) is described in Section 6.5.5.

6.4 Pigment extraction

6.4.1 General procedure for sonic extraction

Sediment was sonicated for 10 min (Decon FS100b, Hove, UK) in acetone (10 mL; AR grade; Fisher, Loughborough, UK) followed by centrifugation for 5 min at 2000 *g* (Denley BR401). The supernatant was filtered through a plug of defatted cotton-wool in a Pasteur pipette. The procedure was repeated until the supernatant was colourless (up to 10 times) and the combined extracts were reduced to dryness by rotary evaporation. Free acids in the extracts were methylated using freshly prepared diazomethane in diethyl ether and the extracts were stored dry, in the dark, at 4°C (Airs et al., 2001a).

6.4.2 General procedure for accelerated solvent extraction (ASE)

Sediment was extracted using an accelerated solvent extraction apparatus (Dionex ASE 350). Sediment was placed in stainless steel cells (5 mL) between cellulose filters. Extractions were performed with acetone (AR grade; Fisher, Loughborough, UK) at 1500 psi at each of a series of temperatures for the work in Chapter 2 (see Table 6.1) or at the optimised temperature for the work in Chapter 4 (see Table 6.3). The static time was set to 5 min. The heat up time was 5 min for temperatures below 100°C and ranged between 6-8 min for temperatures above 100°C. Three extraction cycles were performed followed by a rinse with acetone (50% cell volume); extraction used a total of 15-20 mL solvent. The solvent was purged from the sample cell using N_2 (60s at 1500-1600 psi) and the extracts were dried using a vacuum concentrator (1310 rpm for 2 h, CHRIST, RVC 2-25). Extracts were dissolved in acetone (10 mL; AR grade; Fisher, Loughborough, UK), filtered through a defatted cotton-wool plug in a Pasteur pipette and dried using the vacuum concentrator. Free acids in the extracts were methylated using freshly prepared diazomethane in diethyl ether and the extracts were stored dry, in the dark, at 4°C (Airs et al., 2001a).

Table 6.3. Optimal ASE conditions for high-throughput method evaluation (Chapter 4)

ASE at 70°C	
Temperature	70°C
Heat up time	5 min
Static time	5 min
Cycles	3
Rinse volume	50%
Purge	60s

6.5 Pigment analysis

6.5.1 RP-HPLC analysis (Chapter 2)

Reversed-phase high-performance liquid chromatography (RP-HPLC) was carried out using a Waters (Milford, MA USA) system comprising a 717 autosampler, 600MS system controller and 996 photodiode array (PDA) detector recording between 350 and 800 nm. Reversed-phase separation of total pigment extracts was performed using two Waters Spherisorb 3µ particle size ODS2 columns (4.6 × 150 mm) with gradient elution by Method A described in a previous study (Airs et al., 2001a) for sediment extracts and with Method B (Airs et al., 2001a) for the extracts from *Allochromatium vinosum* Samples were dissolved in acetone (Table 6.1; AR grade; Fisher, Loughborough, UK) and 10 µL was injected.

6.5.2 RP-HPLC and UHPLC analysis (Chapter 3)

Both RP-HPLC and RP-UHPLC were carried out using an Ultimate 3000 RSLC system (Dionex, USA). The RSLC system comprised a pump, auto-sampler, column compartment and diode array detector. Three types of C_{18} column were selected for this study: two Waters Spherisorb 3µ ODS2 columns (4.6 × 150 mm) used for the gradient elution Method A described in a previous study (Airs et al., 2001a); one, two or three Acclaim® RSLC 120 C_{18} 2.2 µm columns (100 mm × 2.1 mm i.d.) (Dionex, USA) coupled in series; and an Acquity UPLC® BEH C_{18} 1.7 µm column (150 mm × 3 mm i.d.) combined with a VanGuard™ column (2.1 mm × 5 mm i.d.)

(Waters, Ireland) of the same stationary phase. The gradient systems employed for both UHPLC column types are discussed in the Chapter 3. All HPLC and UHPLC chromatograms were generated at the maximum UV/Vis absorption spectrum of each of the compounds. Resolution values are quoted according to the expression;

$$R_s = 1.18 \times \frac{t_R B - t_R A}{W_{50\%}\, A + W_{50\%} B}$$

6.5.3 UHPLC analysis (Chapter 4)

Pigment extracts were dissolved in acetone (50 µL) for analysis by UHPLC (method 10, Table 6.4) carried out by an Ultimate 3000 RSLC system (Dionex, USA) and an Acquity UPLC® BEH C_{18} 1.7 µm column (150 mm × 3 mm i.d.) combined with an VanGuard™ column (2.1 mm × 5 mm i.d.) of the same stationary phase. For more detail of the UHPLC-MS^n see Section 6.5.4.

Table 6.4. UHPLC method 10 for sediment sample analysis

UHPLC	Time (min)	Methanol (%)	Ethyl acetate (%)	Ammonium acetate (0.01 *M*) (%)	Acetonitrile (%)	Flow rate (mL min^{-1})
Method 10	0	80	0	10	10	0.60
	0.5	80	0	10	10	0.60
	7	64	21	5	10	0.60
	16	50	40	0	10	0.60
	18	31	63	0	6	0.60
	18.5	19	80	0	1	0.60
	19.5	19	80	0	1	0.60
	20	80	0	10	10	0.60
	23	80	0	10	10	0.60

Injection volume was 2 µL and the column was maintained at 45°C.

6.5.4 LC-MS^n analysis

For the Lake Reid extracts, liquid chromatography-multistage mass spectrometry (LC-MS^n) was carried out using a Finnigan MAT LCQ ion trap (San Jose, CA, USA) equipped with an APCI source operated in positive ion mode. MS parameters were as follows: capillary temperature 150°C; APCI Vapouriser temperature 450°C; discharge current 5 µA; sheath gas flow 60 (arbitrary units); auxiliary gas flow 10 (arbitrary units); default isolation width 2; collision energy 38% (Airs et al., 2001a). The HPLC conditions were as described above.

For all other sedimentary pigment extracts, liquid chromatography-multistage mass spectrometry (LC-MS^n) was performed using an HCTultra ETD-II (Bruker, Germany) ion trap instrument coupled to an Ultimate 3000 RSLC system (Dionex, USA) as detailed in Section 6.5.2. The HCTultra ETD-II was equipped with an APCI source operated in positive ion mode. MS parameters were follows: vaporizer temperature 450°C; nebulizer 40 psi, drying gas 8.5 L min^{-1} ; mass scan range 400-1000 *m/z***.**

6.5.5 Total organic carbon (TOC) analysis (adapted from Columbo and Baccanti, 1990)

Total organic carbon (TOC) elemental analysis was performed using a Thermo Flash 2000 Elemental Analyser fitted with MAS200R autosampler, chromatographic column and thermal conductivity detector. Helium was used as a carrier gas at a flow rate of 140 ml min^{-1}. Soil samples (10-15 mg) were weighed using a XS3DU microbalance (Mettler Toledo) into silver foil capsules for TOC analysis. Dried sediment samples for TOC analysis were treated with 2 drops of hydrochloric acid (6 M) to destroy carbonates and then heated to 80°C for 6 min to drive of excess acid solution. Foil capsules were folded to exclude air. Samples were combusted in a quartz reactor tube, packed with copper oxide granules and electrolytic copper wires, held at 900°C. Sample introduction coincided with a pulse of oxygen (250 ml min^{-1}, 5 s).

6.6 Calculation

6.6.1 Quantification of pigments (Chapter 2)

Yields of chlorophyll *a* (**4,** Scheme 2.1 Chapter 2), phaeophytin *a* (**11**) and phaeophorbide *a* (**20**) were calculated from calibration curves for the pure standards. The yields of phaeophytin *a* epimer (**31**), pyrophaeophytin *a* (**18**), hydroxyphaeophytin *a* (**34**) and its 13^2 diastereomer (**35**) were calculated *via* the molar response from the calibration curve for phaeophytin *a* (**11**). Pyrophaeophorbide *a* (**23**), and the diastereomeric chlorophyllones (**24** and **25**) were estimated *via* the molar response from the calibration curve for phaeophorbide *a* (**20**). The yields of chlorophyll *b* (**5**) and bacteriochlorophyll *a* (**6**) were calculated by correcting the standard chlorophyll *a* (**4**) calibration curve using published absorption coefficients for the red absorption bands of chlorophyll *b* (**5**) ($\varepsilon = 47.6 \times 10^3$ L mol^{-1} cm^{-1}) (Watanabe et al., 1984), bacteriochlorophyll *a* (**6**) ($\varepsilon = 69.3 \times 10^3$ L mol^{-1} cm^{-1}) (Permentier et al., 2000) and chlorophyll *a* (**4**) ($\varepsilon = 81.3 \times 10^3$ L mol^{-1} cm^{-1}) (Watanabe et al., 1984) to compute correction factors for the Soret band absorption coefficients. Phaeophytin *b* (**17, 33**), pyrophaeophytin *b* (**19**), bacteriophaeophytin *a* (**29, 30**) and pyrobacteriophaeophytin *a* (**31**) were similarly quantified by correcting the calibration curve for phaeophytin *a* (**11**) using the molar absorption coefficients phaeophytin *b* (**17** and **19**: $\varepsilon = 29.3 \times 10^3$ L mol^{-1} cm^{-1}) (Watanabe et al., 1984), bacteriophaeophytin *a* (**29**) ($\varepsilon = 47.5 \times 10^3$ L mol^{-1} cm^{-1}) (Straley et al., 1973) and phaeophytin *a* (**11**) ($\varepsilon = 46.0 \times 10^3$ L mol^{-1} cm^{-1}) (Watanabe et al., 1984).

6.6.2 Statistical methods (adapted from Field, 2013) to test for significance differences in the data in Chapter 2

Normality of data was tested by the Shapiro-Wilk test and homogeneity of variance was tested by a Levene test before performing a significant difference test at 95% confidence. To determine if the total pigment yields from sonic extraction and ASE over the range of temperature tested exhibit statistically significant differences, one-way analysis of variance (ANOVA) and a multiple comparison method (least significance difference; LSD) were applied to the data for spiked Priest Pot, Loch Ness and Estanya sediments.

In cases where data were not normally distributed or did not show homogeneity of variance the data were tested by the Kruskal-Wallis test. For data showing significant difference, the Mann-Whitney *U* test was applied. All statistical data analysis in Chapter 2 was performed using IBM SPSS software version 21.

6.6.3 Quantification of pigments (Chapter 4)

Quantification of pigments extracted by the high-throughput method for sediment core analysis was performed using Equations 6.1, 6.2 and 6.3, when both internal standard pyrophaeophobide *a* C_{18} and its copper metallation product were detected, and was based on equations 6.2 and 6.4 when the internal standard was metallated completely by copper.

$$Corrected\ STD\ conc\ (nmol)\ = spiked\ conc.STD - \left[\frac{\frac{A_2}{\varepsilon_2}}{\left(\frac{A_2}{\varepsilon_2}\right)+\left(\frac{A_1}{\varepsilon_1}\right)} \times\ conc.\ STD\right] \quad (6.1)$$

$$Pigment\ yield\ (nmol) = A_{pigment} \times \frac{\varepsilon_1}{\varepsilon_{\text{pigment}}} \times \frac{Corrected\ STD\ conc.}{A_1} \quad (6.2)$$

$$Pigment\ yield\ (\mu mol\ g^{-1} of\ TOC) = \frac{Pigment\ yield\ (nmol)}{Mass\ of\ dry\ sediment\ (g) \times \left(\frac{\%TOC}{100}\right)} \times 0.001 \quad (6.3)$$

$$Pigment\ yield\ (nmol) = A_{pigment} \times \frac{\varepsilon_2}{\varepsilon_{\text{pigment}}} \times \frac{3.03}{A_2} \quad (6.4)$$

Where; A_1 = Peak area of standard pphorb *a* C_{18} ester (**41**) (mAU min)

ε_1 = Molar extinction coefficient of phorb *a* (**20**) (43.98 mM^{-1}cm^{-1}, Lorenzen & Jeffrey, 1980)

A_2 = Peak area of copper pphorb *a* C_{18} ester (**41**) (mAU min)

ε_2 = Molar extinction coefficient of copper pphorb *a* (47.1 mM^{-1}cm^{-1}, Inoue et al., 1994)

$A_{pigment}$= Peak area of quantified pigment (mAU min)

$\varepsilon_{pigment}$ = Molar extinction coefficient of quantified pigment refer to Table 6.5

%TOC = Total organic carbon in dry sediment sample (%) Table 6.2

conc.STD = concentration of internal standard (pphorb *a* C_{18} ester, **41**) = 3.03 nmol

Table 6.5. Molar extinction coefficients used for quantification of pigments in Chapter 4

Pigment	**Molar extinction coefficient in acetone ($\varepsilon_{pigment}$) ($mM^{-1}cm^{-1}$)**	**Pigments using this the same ε in quantification**
Phaeophorbide *a*	43.98 (Lorenzen and Jeffrey, 1980)	Chlorophyllone (**24**, **25**)
		Pyrophaeophorbide *a* methyl ester (**22**)
		Pyrophaeophorbide *a* C_{18} ester (**41)**
		All unidentified chlorins
Chlorophyll *a* (**4)**	81.3 (Watanabe et al., 1984)	Chlorophyll *a* epimer
		Hydroxychlorophyll *a* (**13**)
Chlorophyll *b* (**5)**	47.6 (Watanabe et al., 1984)	Chlorophyllide *b*
Phaeophytin *b* (**17)**	29.3 (Watanabe et al., 1984)	-
Phaeophytin *a* (**11)**	46.0 (Watanabe et al., 1984)	Phaeophytin *a* epimer (**31**)
		Pyrophaeophytin *a* (**18**)
		Chlorin e_6 dimethyl phytyl ester (**16**)
		Hydroxyphaeophytin *a* (**33**)
		Purpurin-7 phytyl ester (**14**)
		Purpurin-18-phytyl ester (**15**)
Copper phaeophorbide *a*	46.0 (Inoue et al., 1994)	Copper pyrophaeophorbide *a* C_{18} ester (**44)**
		All unidentified metal chlorins

Appendix of structures

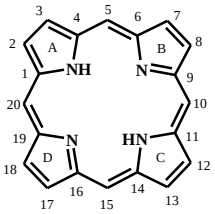

Porphyrin
(**1**)

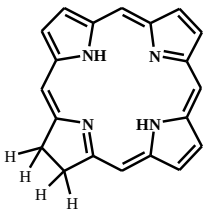

Chlorin
(**2**)

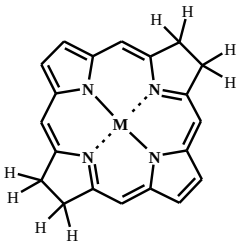

Bacteriochlorin
(**3**)

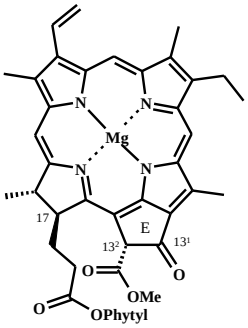

Chlorophyll *a*
(**4**)

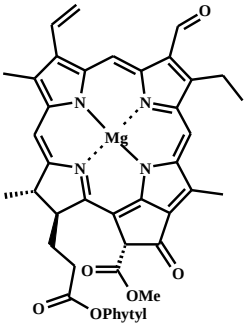

Chlorophyll *b*
(**5**)

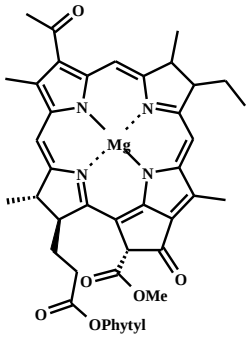

Bacteriochlorophyll *a*
(**6**)

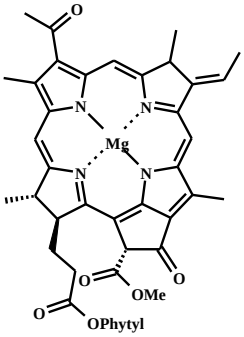

Bacteriochlorophyll *b*
(**7**)

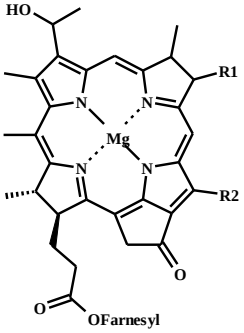

R1 = Et, *n*-Pr, or *i*-Bu
R2 = Et, or Me

Bacteriochlorophyll *c*
(**8**)

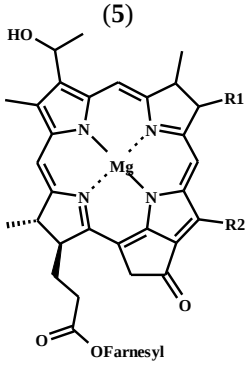

R1 = Et, *n*-Pr, *i*-Bu, *neo*-pent
R2 = Et, Me

Bacteriochlorophyll *d*
(**9**)

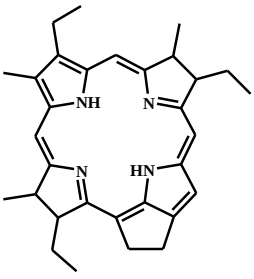

DPEP
(**10**)

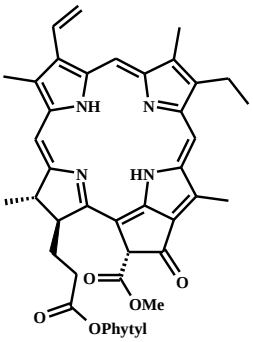

Phaeophytin *a*
(**11**)

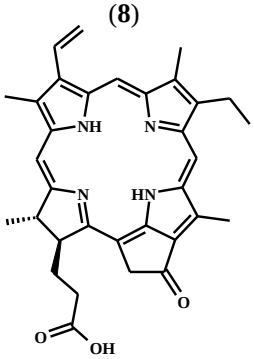

Pyrophaeophorbide *a*
(**12**)

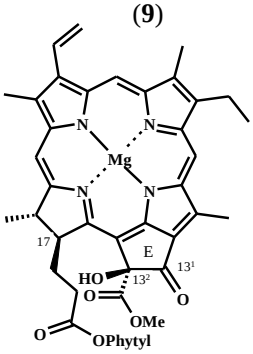

Hydroxychlorophyll *a*
(**13**)

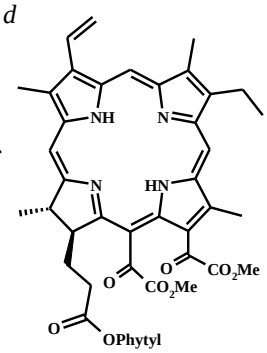

Purpurin-7 dimethyl phytyl ester
(**14**)

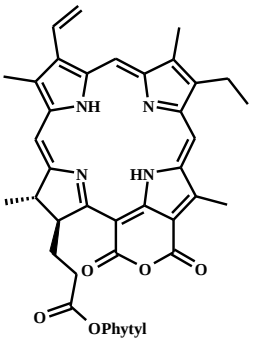

Purpurin-18 phytyl ester
(**15**)

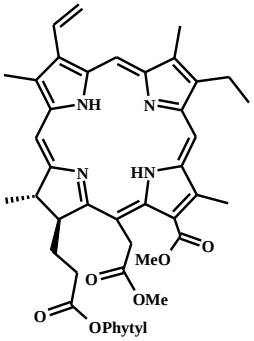

Chlorin e_6 dimethyl phytyl ester
(**16**)

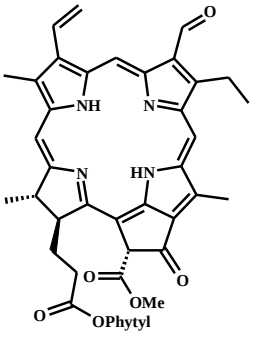

Phaeophytin *b*
(**17**)

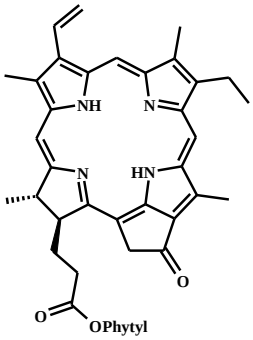

Pyrophaeophytin *a*
(**18**)

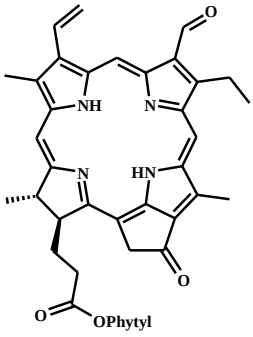

Pyrophaeophytin *b*
(**19**)

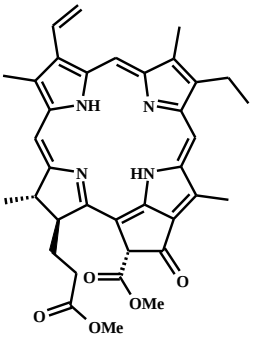

Phaeophorbide *a*
methyl ester (**20**)

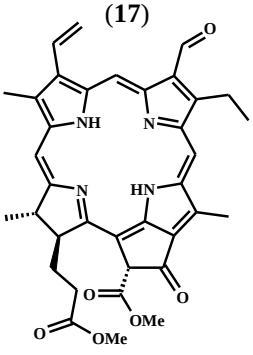

Phaeophorbide *b*
methyl ester (**21**)

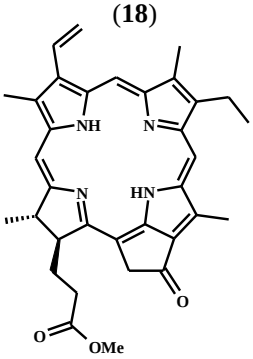

Pyrophaeophorbide *a*
methyl ester (**22**)

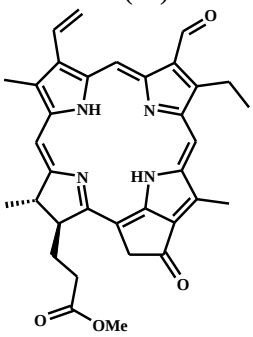

Pyrophaeophorbide *b*
methyl ester (**23**)

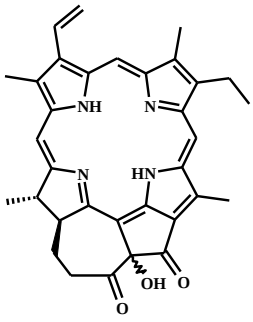

Chlorophyllone
diastereomers
(**24**) (**25**)

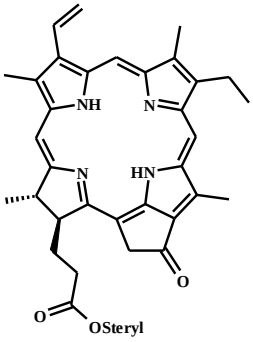

Pyrophaeophorbide *a*
steryl ester
Steryl = C_{27} sterol (**26**)
= C_{29} sterol (**27**) (**28**)

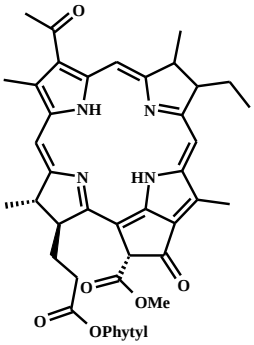

Bacteriophaeophytin *a*
(**29**)

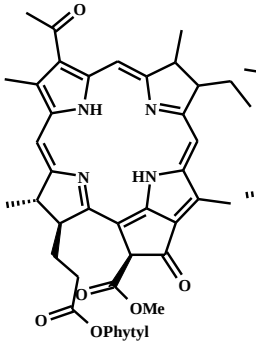

Bacteriophaeophytin *a*
epimer (**30**)

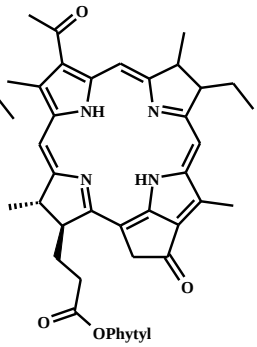

Pyrobacteriophaeophytin *a*
(**31**)

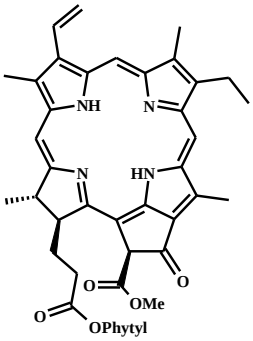

Phaeophytin *a* epimer
(**32**)

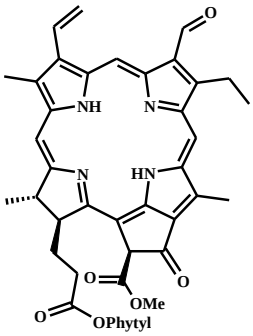

Phaeophytin *b* epimer
(**33**)

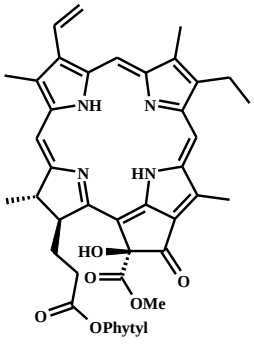

Hydroxyphaeophytin *a*
(**34**)

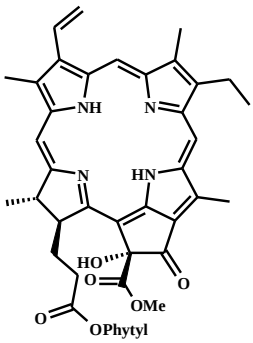

Hydroxyphaeophytin *a*
epimer (**35**)

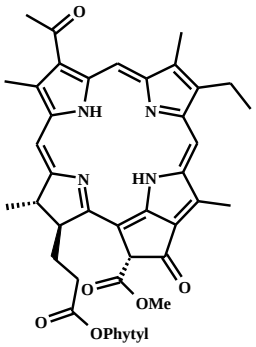

Bacterioviridin
(**36**)

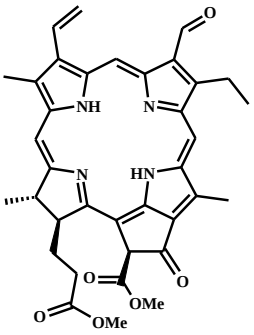

Chlorophyll *b* epimer
(**37**)

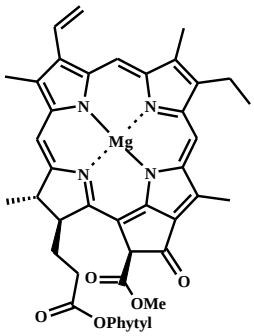

Chlorophyll *a* epimer
(**38**)

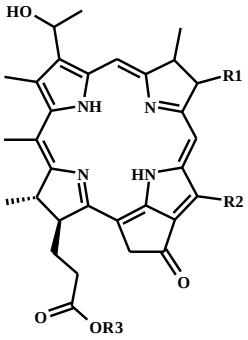

R1 = Et, *n*-Pr, *i*-Bu
R2 = Et, Me
R3 = Farnesyl, Hexadecenyl,

Bacteriophaeophytin *c*
(**39**)

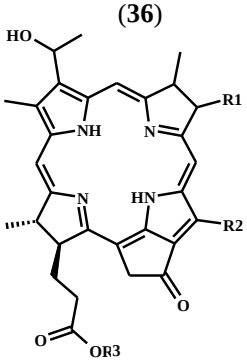

R1 = Et, *n*-Pr, *i*-Bu, *neo*-pent
R2 = Et, Me
R3 = Farnesyl, Geranylgeranyl, Hexadecenyl, Octadecenyl, Heptadecenyl

Bacteriophaeophytin *d*
(**40**)

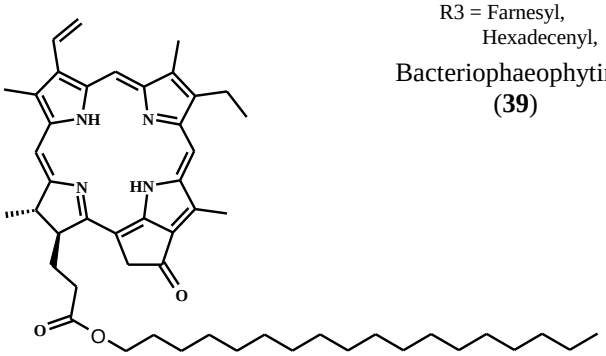

Pyrophaeophorbide *a* stearyl (C18) ester
(**41**)

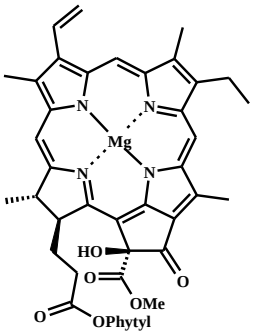

Hydroxychlorophyll *a*
(**42**)

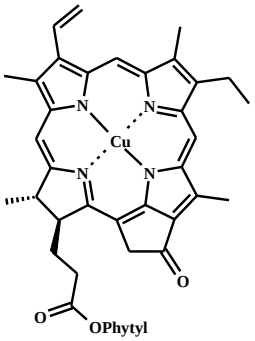

Copper pyrophaeophytin *a*
(**43**)

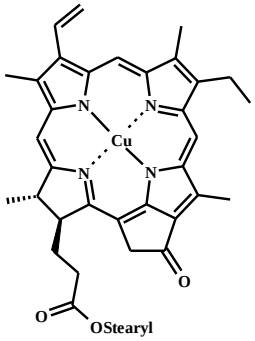

Copper pyrophaeophorbide *a* C18 ester
(**44**)

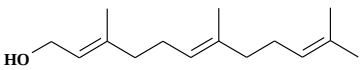

Farnesol
(**45**)

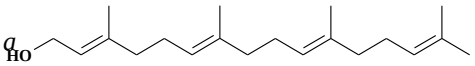

Geranyl geraniol
(**46**)

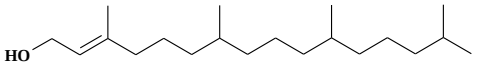

Phytol
(**47**)

List of definitions and abbreviations

°C	Degree of Celsius
λ_{max}	Wavelength of maximum absorbance
$[M+H]^+$	Protonated molecule
µL	Micro litre unit
µmol	Micro mole unit
ANOVA	One way analysis of variance for determining the degree of similarity or difference between two or more groups of data
ASE	Accelerated solvent extraction
B.F.	Boost factor used in the Method Speed-up Calculator from Dionex
bar	Unit of pressure
Bchl	Bacteriochlorophyll
Bphe	Bacteriophaeophytin
Chl	Chlorophyll
DPEP	Desoxophylloerythroetioporphyrin
F	*F*-ratio (test statistic used in ANOVA)
h	Hours
H	Kruskal-Wallis test statistic
i.d.	Internal diameter
L	Length of column
LC	Liquid chromatography
m/z	Mass-to-charge ratio
min	Minutes
MS	Mass spectrometry
MS/MS	Tandem mass spectrometry
nmol	Nano mole
OH-phe	Hydroxyphaeophytin
p	Significance of a statistic test
PAHs	Polycyclic aromatic hydrocarbons
Pbphe	Pyrobacteriophaeophytin
PCBs	Polychlorinated biphenyls
PDA	Photodiode array
Phe	Phaeophytin
Phorb	Phaeophorbide

Pphe	Pyrophaeophytin
Pphorb	Pyrophaeophorbide
RP-HPLC	Reversed phase-high performance liquid chromatography
R_s	Resolution of peak
s.d.	Standard deviation
TOC	Total organic carbon
t_R	Retention time
UHPLC	Ultra high performance liquid chromatography
UV/vis	Ultraviolet/visible
$W_{50\%}$	Peak width at half-height

References

Airs, R.L., Atkinson, J.E., Keely, B.J., 2001a. Development and application of a high resolution liquid chromatographic method for the analysis of complex pigment distributions. Journal of Chromatography A, 917, 167-177.

Airs, R.L., 2001b. Chlorophylls of phototrophic prokaryotes: Analytical developments and significance of natural distributions. Ph.D. Thesis. University of York.

Airs, R.L., Keely, B.J., 2000. A novel approach for sensitivity enhancement in atmospheric pressure chemical ionisation liquid chromatography/mass spectrometry of chlorophylls. Rapid Communications in Mass Spectrometry, 14, 125-128.

Airs, R.L., Keely, B.J., 2003. A high resolution study of the chlorophyll and bacteriochlorophyll pigment distributions in a calcite/gypsum microbial mat. Organic Geochemistry, 34, 539-551.

Ballantyne A.C., 2012. Photosynthetic pigments in sediments: development of applications in archaeology and compound-specific radiocarbon analysis. PhD Thesis, University of York, UK.

Bobbio, P.A., Guedes, M.C., 1990. Stability of copper and magnesium chlorophylls. Food Chemistry, 36, 165-168.

Bohoyo-Gil, D., Dominguez-Valhondo, D., García-Parra , J.J., González-Gómez, D., 2012. UHPLC as a suitable methodology for the analysis of carotenoids in food matrix. European Food Research and Technology, 235, 1055-1061.

Bracewell, C.E., 1993. A geochemical study of natureal and pollutant compounds in Loch Ness, Scotland., M.Sc. Thesis. University of Newcastle-upon-Tyne.

Brändli, R.C., Bucheli, T.D., Kupper, T., Stadelmann, F.X., Tarradellas, J., 2006. Optimised accelerated solvent extraction of PCBs and PAHs from compost. International Journal of Environmental Analytical Chemistry, 86, 505-525.

Braumann, T., Grimme, L.H., 1981. Reversed-phase high-performance liquid chromatography of chlorophylls and carotenoids. Biochimica et Biophysica Acta (BBA) – Bioenergetics, 637, 8-17.

Brockmann, H., 1968. The absolute configuration of chlorophyll. Angewandte Chemie International Edition in English, 7, 221-222.

Callot, H.J., Ocampo, R., Albrecht, P., 1990. Sedimentary porphyrins - correlations with biological precursors. Energy & Fuels, 4, 635-639.

Cartaxana, P., Jesus, B., Brotas, V., 2003. Pheophorbide and pheophytin *a* like pigments as useful markers for intertidal microphytobenthos grazing by *Hydrobia ulvae*. Estuarine Coastal and Shelf Science, 58, 293-297.

Castaneda, I.S., Schouten, S., 2011. A review of molecular organic proxies for examining modern and ancient lacustrine environments. Quaternary Science Reviews, 30, 2851-2891.

Chesnut, S.M., Salisbury, J.J., 2007. The role of UHPLC in pharmaceutical development. Journal of Separation Science, 30, 1183-1190.

Cho, S.K., Abd El-Aty, A.M., Choi, J.H., Kim, M.R., Shim, J.H., 2007. Optimized conditions for the extraction of secondary volatile metabolites in *Angelica* roots by accelerated solvent extraction. Journal of Pharmaceutical and Biomedical Analysis, 44, 1154-1158.

Columbo, B., Baccanti, M., 1990. Process and equipment for the determination of organic carbon content in complex matrixes, EP0401648. Erba, Strumentazione, Italy.

Currie, R.I., 1962. Pigments in zooplankton faeces. Nature, 193, 956-957.

Daemen, E., 1986. Comparison of methods for the determination of chlorophyll in estuarine sediments. Netherlands Journal of Sea Research, 20, 21-28.

Dionex, 2009. Easy method transfer from HPLC to RSLC with the Dionex Method Speed-up Calculator. Technical Note, 75, 1-10.

Downs, J.N., Lorenzen, C.J., 1985. Carbon - pheopigment ratios of zooplankton fecal pellets as an index of herbivorous feeding. Limnology and Oceanography, 30, 1024-1036.

Eglinton, G., Calvin, M., 1967. Chemical fossils. Scientific American, 216, 32.

Eskins, K., Scholfield, C.R., Dutton, H.J., 1977. High-performance liquid chromatography of plant pigments. Journal of Chromatography A, 135, 217-220.

Falkowski, P.G., Sucher, J., 1981. Rapid, quantitative separation of chlorophylls and their degradation products by high-performance liquid-chromatography. Journal of Chromatography, 213, 349-351.

Field, A., 2013. Discovering statistics using IBM SPSS statistics 4th edition. SAGE Publications Ltd., London.

Fleming, I.A.N., 1967. Absolute configuration and the structure of chlorophyll. Nature, 216, 151-152.

Fu, W., Magnúsdóttir, M., Brynjólfson, S., Palsson, B.Ø., Paglia, G., 2012. UPLC-UV-MSE analysis for quantification and identification of major carotenoid and chlorophyll species in algae. Analytical and Bioanalytical Chemistry, 404, 3145-3154.

Giergielewicz-Możajska, H., Dąbrowski, Ł., Namieśsnik, J., 2001. Accelerated solvent extraction (ASE) in the analysis of environmental solid samples-some aspects of theory and practice. Critical Reviews in Analytical Chemistry, 31, 149-165.

Gilpin, R.K., Zhou, W., 2008. Ultrahigh-pressure liquid chromatography: fundamental aspects of compression and decompression heating. Journal of Chromatographic Science, 46, 248-253.

Gruz, J., Novák, O., Strnad, M., 2008. Rapid analysis of phenolic acids in beverages by UPLC-MS/MS. Food Chemistry, 111, 789-794.

Guzzella, L., Pozzoni, F., 1999. Accelerated solvent extraction of herbicides in agricultural soil samples. International Journal of Environmental Analytical Chemistry, 74, 123-133.

Hall, D.O., Rao, K.K., 1999. Photosynthesis, 6th edition. Cambridge University Press, Cambridge.

Harradine, P.J., Harris, P.G., Head, R.N., Harris, R.P., Maxwell, J.R., 1996. Steryl chlorin esters are formed by zooplankton herbivory. Geochimica et Cosmochimica Acta, 60, 2265-2270.

Harris, P.G., Carter, J.F., Head, R.N., Harris, R.P., Eglinton, G., Maxwell, J.R., 1995. Identification of chlorophyll transformation products in zooplankton fecal pellets and marine sediment extracts by liquid-chromatography mass-spectrometry atmospheric-pressure chemical-ionization. Rapid Communications in Mass Spectrometry, 9, 1177-1183.

Harris, P.G., Zhao, M., Rosell-Melé, A., Tiedemann, R., Sarnthein, M., Maxwell, J.R., 1996. Chlorin accumulation rate as a proxy for Quaternary marine primary productivity. Nature, 383, 63-65.

Hayes, J.M., Takigiku, R., Ocampo, R., Callot, H.J., Albrecht, P., 1987. Isotopic compositions and probable origins of organic molecules in the Eocene Messel shale. Nature, 329, 48-51.

Hendry, G.A.F., Houghton, J.D., Brown, S.B., 1987. The degradation of chlorophyll *a* biological enigma. New Phytologist, 107, 255-302.

Hinrichs, K.U., Hayes, J.M., Sylva, S.P., Brewer, P.G., DeLong, E.F., 1999. Methane-consuming archaebacteria in marine sediments. Nature, 398, 802-805.

Hodgson, G.W., Hitchon, B., Elofson, R.M., Baker, B.L., Peake, E., 1960. Petroleum pigments from recent fresh-water sediments. Geochimica et Cosmochimica Acta, 19, 272-288.

Hodgson, D.A., Noon, P.E., Vyverman, W., Bryant, C.L., Gore, D.B., Appleby, P., Gilmour, M., Verleyen, E., Sabbe, K., Jones, V.J., Ellis-Evans, J.C., Wood, P.B., 2001. Were the Larsemann Hills ice-free through the last glacial maximum? Antarctic Science, 13, 440-454, doi:10.1017/S0954102001000608.

Hodgson, D.A., Wright, S.W., Tyler, P.A., Davies, N., 1998. Analysis of fossil pigments from algae and bacteria in meromictic Lake Fidler, Tasmania, and its application to lake management. Journal of Paleolimnology, 19, 1-22.

Huang, S.C., Hung, C.F., Wu, W.B., Chen, B.H., 2008. Determination of chlorophylls and their derivatives in Gynostemma pentaphyllum Makino by liquid chromatography-mass spectrometry. Journal of Pharmaceutical and Biomedical Analysis, 48, 105-112.

Humphrey, A.M., 1980. Chlorophyll. Food Chemistry, 5, 57-67.

Hurley, J.P., Armstrong, D.E., 1990. Fluxes and transformations of aquatic pigments in Lake Mendota, Wisconsin. Limnology and Oceanography, 35, 384-398.

Hynninen, P.H., 1973. Chlorophylls IV. Preparation and purification of some derivatives of chlorophyll *a* and *b*. Accta Chemica Scandinavica, 27, 1771-1780.

Hynninen, P.H., 1991. Chemistry of chlorophylls: Modifications. In: H.E. In: Sheer (Ed.), Chlorophylls. CRC Press, Boca Raton, Florida, 145-209.

Inoue, H., Yamashita, H., Furuya, K., Nonomura, Y., Yoshioka, N., Li, S., 1994.

Determination of copper (II) chlorophyllin by reversed-phase high-performance liquid-chromatography. Journal of Chromatography A, 679, 99-104.

Iriyama, K., Ogura, N., Takamiya, A., 1974. Simple method for extraction and partial-purification of chlorophyll from plant material, using dioxane. Journal of Biochemistry, 76, 901-904.

Jansen, B., Nierop, K.G.J., Kotte, M.C., de Voogt, P., Verstraten, J.M., 2006. The applicability of accelerated solvent extraction (ASE) to extract lipid biomarkers from soils. Applied Geochemistry 21, 1006-1015.

Jeffrey, S.W., Hallegraeff, G.M., 1987. Chlorophyllase distribution in 10 classes of phytoplankton - a problem for chlorophyll analysis. Marine Ecology-Progress Series, 35, 293-304.

Johnston, L.G., Watson, W.F., 1956. The allomerization of chlorophyll. Journal of the Chemical Society, 1203-1212.

Kao, T.H., Chen, C.J., Chen, B.H., 2011. An improved high performance liquid chromatography-photodiode array detection-atmospheric pressure chemical ionization-mass spectrometry method for determination of chlorophylls and their derivatives in freeze-dried and hot-air-dried Rhinacanthus nasutus (L.) Kurz. Talanta, 86, 349-355.

Kashiyama, Y., Yokoyama, A., Kinoshita, Y., Shoji, S., Miyashiya, H., Shiratori, T., Suga, H., Ishikawa, K., Ishikawa, A., Inouye, I., Ishida, K.-i., Fujinuma, D., Aoki, K., Kobayashi, M., Nomoto, S., Mizoguchi, T., Tamiaki, H., 2012. Ubiquity and quantitative significance of detoxification catabolism of chlorophyll associated with protistan herbivory 109, 17328-17335.

Keely, B.J., 2006. Geochemistry of chlorophylls. In: Grimm, B., Porra, R.J., Rüdiger, W., Scheer, H. (Eds.) Advances in Photosynthesis and Respiration, Volume 25. Chlorophylls and Bacteriochlorophylls: Biochemistry, Biophysics, Functions and Applications, Advances in Photosynthesis and Respiration. Springer, Dordrecht, The Netherlands. pp. 535-561.

Keely, B.J., Brereton, R.G., 1986. Early chlorin diagenesis in a recent aquatic sediment. Organic Geochemistry, 10, 975-980.

Keely, B.J., Maxwell, J.R., 1990. Fast-atom-bombardment mass-spectrometric and tandem mass-spectrometric studies of some functionalized tetrapyrroles derived from chlorophyll *a* and Chlorophyll *b*. Energy & Fuels, 4, 737-741.

Keely, B.J., Prowse, W.G., Maxwell, J.R., 1990. The Treibs hypothesis - an evaluation based on structural studies. Energy & Fuels, 4, 628-634.

Killops, S.D., Killops, V.J., 2004. An introduction to organic geochemistry 2nd edition. Blackwell, Oxford.

King, L.L., Repeta, D.J., 1991. Novel pyropheophorbide steryl esters in Black-Sea sediments. Geochimica et Cosmochimica Acta, 55, 2067-2074.

Kosiur, D.R., 1977. Porphyrin adsorption by clay-minerals. Clays and Clay Minerals, 25, 365-371.

Krstulović, A.M., Brown, P.R., 1982. Reversed-phse high performance liquid chromatography: Theory, practice, and biomedical applications. John Wiley & Sons, Inc., Canada.

Leandro, C.C., Hancock, P., Fussell, R.J., Keely, B.J., 2006. Comparison of ultra-performance liquid chromatography and high-performance liquid chromatography for the determination of priority pesticides in baby foods by tandem quadrupole mass spectrometry. Journal of Chromatography A, 1103, 94-101.

Lorenzen, C.J., Jeffrey, S.W., 1980. Determination of chlorophyll in seawater. UNESCO Technical Paper in Marine Science, 35, 1-20.

Louda, J.W., Loitz, J.W., Rudnick, D.T., Baker, E.W., 2000. Early diagenetic alteration of chlorophyll *a* and bacteriochlorophyll *a* in a contemporaneous marl ecosystem; Florida Bay. Organic Geochemistry, 31, 1561-1580.

Louda, J.W., Mongkhonsri, P., Baker, E.W., 2011. Chlorophyll degradation during senescence and death-III: 3-10 yr experiments, implications for ETIO series generation. Organic Geochemistry, 42, 688-699.

Mackinney, G., Joslyn, M.A., 1940. The conversion of chlorophyll to pheophytin. Journal of the American Chemical Society, 62, 231-232.

Mantoura, R.F.C., Llewellyn, C.A., 1983. The rapid determination of algal chlorophyll and carotenoid pigments and their breakdown products in natural waters by reverse-phase high-performance liquid chromatography. Analytica Chimica Acta, 151, 297-314.

McClymont, E.L., Martinez-Garcia, A., Rosell-Mele, A., 2007. Benefits of freeze-drying sediments for the analysis of total chlorins and alkenone concentrations in marine sediments. Organic Geochemistry, 38, 1002-1007.

Meyer, V.R., 1988. Practical high-performance liquid chromatography. John Wiley & Sons Ltd., Frankfurt.

Mühlecker, W., Kräutler, B., Ginsburg, S., Matile, P., 1993. Breakdown of chlorophyll: A tetrapyrrolic chlorophyll catabolite from senescent rape leaves. Preliminary communication. Helvetica Chimica Acta, 76, 2976-2980.

Naylor, C.C., Keely, B.J., 1998. Sedimentary purpurins: oxidative transformation products of chlorophylls. Organic Geochemistry, 28, 417-422.

Nguyen, D.T.T., Guillarme, D., Rudaz, S., Veuthey, J.L., 2006. Fast analysis in liquid chromatography using small particle size and high pressure. Journal of Separation Science, 29, 1836-1848.

Nováková, L., Matysová, L., Solich, P., 2006. Advantages of application of UPLC in pharmaceutical analysis. Talanta, 68, 908-918.

Ocampo, R., Callot, H.J., Albrecht, P., Popp, B.N., Horowitz, M.R., Hayes, J.M., 1989. Different isotope compositions of C32 DPEP and C32 etioporphyrin III in oil shale. Naturwissenschaften, 76, 419-421.

Owens, T.G., Falkowski, P.G., 1982. Enzymatic Degradation of Chlorophyll *a* by marine-phytoplankton *in vitro*. Phytochemistry, 21, 979-984.

Patterson, J., Parsons, T.R., 1963. Distribution of chlorophyll *a* and degradation products in various marine materials. Limnology and Oceanography, 8, 355-356.

Pawliszyn, J., 1993. Kinetic-model of supercritical fluid extraction. Journal of Chromatographic Science, 31, 31-37.

Pearce, G.E.S., Keely, B.J., Harradine, P.J., Eckardt, C.B., Maxwell, J.R., 1993. Characterization of naturally-occurring steryl esters derived from chlorophyll *a*. Tetrahedron Letters, 34, 2989-2992.

Permentier, H., Schmidt, K., Kobayashi, M., Akiyama, M., Hager-Braun, C., Neerken, S., Miller, M., Amesz, J., 2000. Composition and optical properties of reaction centre core complexes from the green sulfur bacteria Prosthecochloris aestuarii and Chlorobium tepidum. Photosynthesis Research, 64, 27-39.

Pickering, M.D., 2009. Low temperature sequestration of photosynthetic pigments: Model studies and natural aquatic environments. Ph.D. Thesis. University of York.

Pirtle-Levy, R., Grebmeier, J.M., Cooper, L.W., Larsen, I.L., 2009. Chlorophyll *a* in Arctic sediments implies long persistence of algal pigments. Deep-Sea Research Part II-Topical Studies in Oceanography, 56, 1326-1338.

Poole, C.F., Poole, S.K., 1991. Chapter 5: Instrumental aspects of high pressure liquid chromatography, Chromatography today. Elsevier Science, 545-599.

Purcaro, G., Moret, S., Bučar-Miklavčič, M., Conte, L.S., 2012. Ultra-high performance liquid chromatographic method for the determination of polycyclic aromatic hydrocarbons in a passive environmental sampler. Journal of Separation Science, 35, 922-928.

Renger, G., 2008. Chapter 1: Overview of primary processes of photosynthesis, Primary Processes of Photosynthesis, Part 1: Principles and Apparatus, volume 8. The Royal Society of Chemistry, 5-35.

Repeta, D.J., Simpson, D.J., Jorgensen, B.B., Jannasch, H.W., 1989. Evidence for anoxygenic photosynthesis from the distribution of bacteriochlorophylls in the Black-Sea. Nature, 342, 69-72.

Reuss, N., Conley, D.J., Bianchi, T.S., 2005. Preservation conditions and the use of sediment pigments as a tool for recent ecological reconstruction in four Northern European estuaries. Marine Chemistry, 95, 283-302.

Richter, B.E., Ezzell, J.L., Knowles, D.E., Hoefler, F., Mattulat, A.K.R., Scheutwinkel, M., Waddell, D.S., Gobran, T., Khurana, V., 1997. Extraction of polychlorinated dibenzo-p-dioxins and polychlorinated dibenzofurans from environmental samples using accelerated solvent extraction (ASE). Chemosphere 34, 975-987.

Richter, B.E., Jones, B.A., Ezzell, J.L., Porter, N.L., Avdalovic, N., Pohl, C., 1996. Accelerated solvent extraction: A technique for sample preparation. Analytical Chemistry, 68, 1033-1039.

Romero-Viana, L., Keely, B.J., Camacho, A., Vicente, E., Rosa Miracle, M., 2010. Primary production in Lake La Cruz (Spain) over the last four centuries: reconstruction based on sedimentary signal of photosynthetic pigments. Journal of Paleolimnology, 434, 771-786.

Roy, S., 1987. High-performance liquid chromatographic analysis of chloro-pigments. Journal of Chromatography A, 391, 19-34.

Sane, E., Isla, E., Gremare, A., Gutt, J., Vetion, G., DeMaster, D.J., 2011. Pigments in sediments beneath recently collapsed ice shelves: The case of Larsen A and B shelves, Antarctic Peninsula. Journal of Sea Research, 65, 94-102.

Schanderl, S., Chichester, C.O., Marsh, G.L., 1962. Degradation of chlorophyll and several derivatives in acid solution. Journal of Organic Chemistry, 27, 3865-3868.

Shankle, A.M., Goericke, R., Franks, P.J.S., Levin, L.A., 2002. Chlorin distribution and degradation in sediments within and below the Arabian Sea oxygen minimum zone. Deep-Sea Research Part I-Oceanographic Research Papers, 49, 953-969.

Scheer, H., 1991. Structure and occurence of chlorophylls. In: H. Scheer (Ed.), Chlorophylls. CRC Press, Boca Raton, Florida, 3-30.

Scheer, H., 2008. Chapter 3: Chlorophylls, Primary Processes of Photosynthesis, Part 1: Principles and Apparatus, volume 8. The Royal Society of Chemistry, 101-149.

Schouten, S., Huguet, C., Hopmans, E.C., Kienhuis, M.V.M., Damste, J.S.S., 2007. Analytical methodology for TEX (86) paleothermometry by high-performance liquid chromatography/atmospheric pressure chemical ionization-mass spectrometry. Analytical Chemistry, 79, 2940-2944.

Shuman, F.R., Lorenzen, C.J., 1975. Quantitative degradation of chlorophyll by a marine herbivore. Limnology and Oceanography, 20, 580-586.

Skoog, D.A., Holler, F.J., Nieman, T.A., 1998. An Introduction to chromatographic separations., Principles of Instrumental Analysis. Harcourt Brace & Company, Florida, 674-696.

Sluijs, A., Roehl, U., Schouten, S., Brumsack, H.-J., Sangiorgi, F., Damste, J.S.S., Brinkhuis, H., 2008. Arctic late Paleocene-early Eocene paleoenvironments with special emphasis on the Paleocene-Eocene thermal maximum (Lomonosov Ridge, Integrated Ocean Drilling Program Expedition 302). Paleoceanography, 23, PA1S11.

Soma, Y., Tanaka, A., Soma, M., Kawai, T., 2001. 2.8 million years of phytoplankton history in Lake Baikal recorded by the residual photosynthetic pigments in its sediment core. Geochemical Journal, 35, 377-383.

Soma, Y., Tani, Y., Soma, M., Mitake, H., Kurihara, R., Hashomoto, S., Watanabe, T., Nakamura, T., 2007. Sedimentary steryl chlorin esters (SCEs) and other photosynthetic pigments as indicators of paleolimnological change over the last 28,000 years from the Buguldeika saddle of Lake Baikal. Journal of Paleolimnology, 37, 163-175.

Spooner, N., Keely, B.J., Maxwell, J.R., 1994. Biologically mediated defunctionalization of chlorophyll in the aquatic environment .1. Senescence decay of the diatom Phaeodactylum tricornutum. Organic Geochemistry, 21, 509-516.

Squier, A.H., Hodgson, D.A., Keely, B.J., 2002. Sedimentary pigments as markers for environmental change in an Antarctic lake. Organic Geochemistry, 33, 1655-1665.

Squier, A.H., Hodgson, D.A., Keely, B.J., 2004. Identification of bacteriophaeophytin a esterified with geranylgeraniol in an Antarctic lake sediment. Organic Geochemistry, 35, 203-207.

Squier, A.H., Hodgson, D.A., Keely, B.J., 2005. Evidence of late Quaternary environmental change in a continental east Antarctic lake from lacustrine sedimentary pigment distributions. In: Antarctic Science, 17, 361-376.

Straley, S.C., Parson, W.W., Mauzeral.Dc, Clayton, R.K., 1973. Pigment content and molar extinction coefficients of photochemical reaction centers from *Rhodopseudomonas spheroides*. Biochimica et Biophysica Acta, 305, 597-609.

Swartz, M.E., 2005. UPLC (TM): An introduction and review. Journal of Liquid Chromatography & Related Technologies, 28, 1253-1263.

Szymczak-Zyla, M., Kowalewska, G., Louda, J.W., 2008. The Influence of microorganisms on chlorophyll *a* degradation in the Marine Environment. Limnology and Oceanography, 53, 851-862.

Szymczak-Zyla, M., Kowalewska, G., Louda, J.W., 2011. Chlorophyll *a* and derivatives in recent sediments as indicators of productivity and depositional conditions. Marine Chemistry, 125, 39-48.

Talbot, H.M., Head, R.N., Harris, R.P., Maxwell, J.R., 1999a. Distribution and stability of steryl chlorin esters in copepod faecal pellets from diatom grazing. Organic Geochemistry 30, 1163-1174.

Talbot, H.M., Head, R.N., Harris, R.P., Maxwell, J.R., 1999b. Steryl esters of pyrophaeophorbide *b*: a sedimentary sink for chlorophyll *b*. Organic Geochemistry, 30, 1403-1410.

Tani, Y., Matsumoto, G.I., Soma, M., Soma, Y., Hashimoto, S., Kawai, T., 2009. Photosynthetic pigments in sediment core HDP-04 from Lake Hovsgol, Mongolia, and their implication for changes in algal productivity and lake environment for the last 1 Ma. Quaternary International, 205, 74-83.

Treibs, A., 1936. Chlorophyll and hemin derivatives in organic materials. Angewandte Chemie International Edition, 49, 682-686.

van Deemter, J.J., Zuiderweg, F.J., Klinkenberg, A., 1956. Longitudinal diffusion and resistance to mass transfer as causes of nonideality in chromatography. Chemical Engineering Science, 5, 271-289.

Van Heukelem, L., Thomas, C.S., 2001. Computer-assisted high-performance liquid chromatography method development with applications to the isolation and analysis of phytoplankton pigments. Journal of Chromatography A, 910, 31-49.

Villanueva, J., Grimalt, J.O., Dewit, R., Keely, B.J., Maxwell, J.R., 1994a. Chlorophyll and carotenoid-pigments in solar saltern microbial mats. Geochimica et Cosmochimica Acta, 58, 4703-4715.

Villanueva, J., Grimalt, J.O., Dewit, R., Keely, B.J., Maxwell, J.R., 1994b. Sources and transformations of chlorophylls and carotenoids in a monomictic sulfate-rich karstic lake environment. Organic Geochemistry, 22, 739-757.

Waldebäck, M., Rydin, E., Markides, K., 1998. Use of accelerated solvent extraction for determination of ecological important phosphorus in lake sediments. International Journal of Environmental Analytical Chemistry, 72, 257-266.

Walker, J.S., 2004a. Autoxidation reactions of chlorophyll. Ph.D. Thesis. University of York.

Walker, J.S., Keely, B.J., 2004b. Distribution and significance of chlorophyll derivatives and oxidation products during the spring phytoplankton bloom in the Celtic Sea April 2002. Organic Geochemistry, 35, 1289-1298.

Walker, J.S., Squier, A.H., Hodgson, D.A., Keely, B.J., 2002. Origin and significance of 13^2-hydroxychlorophyll derivatives in sediments. Organic Geochemistry, 33, 1667-1674.

Wang, W.T., Meng, B.J., Lu, X.X., Liu, Y., Tao, S., 2007. Extraction of polycyclic aromatic hydrocarbons and organochlorine pesticides from soils: A comparison between Soxhlet extraction, microwave-assisted extraction and accelerated solvent extraction techniques. Analytica Chimica Acta, 602, 211-222.

Watanabe, T., Hongu, A., Honda, K., Nakazato, M., Konno, M., Saitoh, S., 1984. Preparation of chlorophylls and pheophytins by isocratic liquid-chromatography. Analytical Chemistry, 56, 251-256.

Watanabe, K., Park, H.-D., Kumon, F., 2012. Historical change of phytoplankton in a eutrophic lake in Japan as determined by analysis of photosynthetic pigments in a lakebed sediment core. Environmental Earth Sciences, 66, 2293-2300.

Wilson, M.A., Airs, R.L., Atkinson, J.E., Keely, B.J., 2004. Bacterioviridins: novel sedimentary chlorins providing evidence for oxidative processes affecting palaeobacterial communities. Organic Geochemistry, 35, 199-202.

Woolley, P.S., Moir, A.J., Hester, R.E., Keely, B.J., 1998. A comparative study of the allomerization reaction of chlorophyll *a* and bacteriochlorophyll *a*. Journal of the Chemical Society-Perkin Transactions, 2, 1833-1839.

Wright, S.W., Jeffrey, S.W., Mantoura, R.F.C., Llewellyn, C.A., Bjornland, T., Repeta, D., Welschmeyer, N., 1991. Improved HPLC method for the analysis of chlorophylls and carotenoids from marine phytoplankton. Marine Ecology Progress Series, 77, 183-196.

Yacobi, Y.Z., Mantoura, R.F.C., Llewellyn, C.A., 1991. The distribution of chlorophylls, carotenoids and their breakdown products in Lake Kinneret (Israel) sediments. Freshwater Biology, 26, 1-10.

Zuloaga, O., Etxebarria, N., Fernandez, L.A., Madariaga, J.M., 1998. Comparison of accelerated solvent extraction with microwave-assisted extraction and Soxhlet. Trends in Analytical Chemistry, 7, 642-647.

Zapata, M., Ayala, A.M., Franco, J.M., Garrido, J.L., 1987. Separation of chlorophylls and their degradation products in marine phytoplankton by reversed-phase high performance liquid chromatography. Chromatographia, 23, 26-30.